PROPERTIES OF GAS MIXTURES AND LIQUID SOLUTIONS FROM INFINITE DILUTION STUDIES

By

AMOS YUDOVICH

Bachelor of Science
Technion, Israel Institute of Technology
Haifa, Israel
1959

Master of Science
Oklahoma State University
Stillwater, Oklahoma
1966

Submitted to the Faculty of the Graduate College
of the Oklahoma State University
in partial fulfillment of the requirements
for the Degree of
DOCTOR OF PHILOSOPHY
May, 1969

PROPERTIES OF GAS MIXTURES AND LIQUID SOLUTIONS

FROM INFINITE DILUTION STUDIES

Thesis Approved:

Robert T. Robinson, Jr.
Thesis Adviser

John Bluet

John H Erbar

Clarence M. Cunningham

D. D. Durham
Dean of the Graduate College

PREFACE

This thesis is concerned with the investigation of thermodynamic properties of vapor mixtures and liquid solutions at high pressures and moderate temperatures.

Two different experimental techniques were employed in this study. The "injection method" was used to obtain infinite dilution partial volumes in the carbon dioxide-methane system. A chromatographic technique was used to gather phase equilibrium (K-value) data for five solute gases at infinite dilution in the methane-n-decane system. These gases were: carbon dioxide, nitrogen, argon, ethylene and propane.

Using the data obtained by the injection method, the B-W-R equation of state was modified for predicting volumetric behavior of carbon dioxide-methane vapor mixtures at finite concentration.

Correlations were developed to predict phase behavior of the five ternary systems using the chromatographically determined K-values combined with volumetric data obtained from the injection experiment and the literature.

Sincere gratitude and appreciation are expressed to my advisor, Dr. K. C. Chao, and to Dr. R. L. Robinson who became my advisor upon Dr. Chao's departure in July 1968, for their careful guidance and perceptive comments that have directed my efforts along fruitful paths and made the development of this thesis an enjoyable experience.

The stimulating atmosphere and personal warmth generated by the Chemical Engineering faculty and my fellow graduate students went far beyond the technical content of this thesis.

The helpful comments received from Dr. C. A. Barrere, Jr., of Continental Oil Comapny are greatly appreciated.

Phillips Petroleum Company supplied the hydrocarbon chemicals for this work and donated the detector cell used in this experiment. Pan American Petroleum Corporation generously lent the sample valve used in this study.

The financial support for this research provided by the National Science Foundation and the School of Chemical Engineering is sincerely appreciated.

Finally, warmfelt gratitude is extended to my mother, Mrs. Rivka L. Yudovich, and to my brother, Malachi P. Yudovich, whose patient understanding and continued encouragement have pervaded all my work during my entire graduate studies.

TABLE OF CONTENTS

LIST OF TABLES

LIST OF FIGURES

CHAPTER I

INTRODUCTION

The study of solution theory has recently gathered considerable momentum, although its beginning can be traced back several decades. Modern analytical devices now make it possible to obtain accurate data with reasonable expenditure of time.

The thermodynamic properties of dense gas mixtures and liquid solutions at high pressures are of interest for two primary reasons. First, such properties are of direct use in the solution of engineering problems, and second, the properties of such mixtures serve to test and extend current theories of gas and liquid solutions.

A complete experimental study of two-phase systems requires analysis of the two phases separately. In two-phase systems, the vapor-liquid equilibrium constant depends on the non-ideality of the two phases. Each of these non-idealities in turn, depends on the three primary variables, temperature, pressure, and composition. The thermodynamic analysis of such systems is simplified considerably if the number of variables of the system is reduced. The "infinite dilution" approach to solutions study offers such a simplification.

The state of infinite dilution may be considered as representing a terminal condition for mixtures, just as the pure state also represents a terminal condition. There are two major advantages in studying solutions at infinite dilution. The first simplification is in the

therymodynamic equations describing the system, since concentration is discarded as a system variable. The second is that the infinite dilution condition can be used as an explicit, well defined and experimentally obtainable standard state for each constituent in the solution.

Although experimental studies on gas mixture properties at finite concentrations are reported in the literature quite abundantly, accurate data on infinitely dilute gas mixtures are scarcely found. The reliability in extrapolating finite concentration data to infinite dilution depends mainly on the accuracy of the data in the low concentration range. In most of the cases the experimental error is the greatest in this range. Thermodynamically, the infinite dilution state in a binary system is of prime importance, since the molecular interactions of the solute molecules are confined to solute-solvent interactions only. Thus, a direct and accurate measurement of partial volumes at infinite dilution, as performed in this study, is of interest.

The literature on the subject of gas-liquid chromatography (referred to in this thesis as GLC) reveals that chromatography is firmly established as a reliable and applicable technique for studying thermodynamic properties of solutions. However, it also reveals that further development and refinement of the existing techniques are needed for the study of solution containing highly volatile solutes.

To meet the objectives of the present study, the chromatographic technique was modified and extended, and a chromatographic apparatus equipped with a sensitive detecting unit was built.

The purposes of this work are:

1. To determine experimentally the partial volumetric properties of selected gas mixtures at high pressures and infinite dilution.

2. To use the mixture volumetric data at infinite dilution for modification of the Benedict-Webb-Rubin equation of state and for prediction of vapor mixture properties at finite concentrations.
3. To measure vapor-liquid equilibrium constants at infinite dilution of selected systems at high pressures using a chromatographic technique.
4. To combine the results of the chromatographic and partial volume studies for the determination of non-ideality in liquid solutions at high pressures at infinite dilution.
5. To correlate the experimental results using the Scatchard-Hildebrand and Flory-Huggins solution theories.

For the purpose of discussion, this study is divided into two parts: Gas Mixture Volumetric Properties from Infinite Dilution Study, and Liquid Solution Properties from Measurements of Vapor-Liquid Equilibrium.

For the gas mixture studies, the following systems and conditions were chosen:

Systems: 1. carbon dioxide at infinite dilution in methane.
2. methane at infinite dilution in carbon dioxide.

Conditions-Temperatures: $100^{\circ}F$ and $150^{\circ}F$.

Pressures: 100 up to 2000 psia.

For the vapor-liquid equilibrium studies, the following systems and conditions were chosen:

Systems: 1. carbon dioxide at infinite dilution in methane-n-decane system.
2. nitrogen at infinite dilution in methane-n-decane system.
3. argon at infinite dilution in methane-n-decane system.
4. ethylene at infinite dilution in methane-n-decane system.

5. propane at infinite dilution in methane-n-decane system.

Conditions-Temperatures: $10^{\circ}F$, $40^{\circ}F$, $70^{\circ}F$, $100^{\circ}F$, $125^{\circ}F$ and $150^{\circ}F$.

Pressures: up to 1750 psia.

CHAPTER II

LITERATURE SURVEY

The Partial Volume Experiment

The study of gas mixture properties at infinite dilution using the injection method is new and, therefore, little discussed in the literature.

A new method of experimental study of the volumetric properties of gas mixtures has been developed in this laboratory (34). In a recent publication, Yudovich, Robinson and Chao (105) presented the results of this study. Kate (44, 45) who followed this author using the same experimental apparatus, investigated the hydrogen sulfide-methane system.

The Gas-Liquid Chromatography Experiment

In previous years, gas chromatography has generated a great deal of interest because of its unique analytical and preparative capabilities. These unusual advantages have somewhat obscured another significant role of chromatography; the measurement of chemical and physical parameters.

The co-inventor of gas-liquid chromatography, Nobel Laureate A. J. P. Martine (62), early recognized the potential of his new analytical technique for the study of equilibrium. As early as 1955, he suggested that gas chromatography "provides perhaps the easiest of all means of studying the thermodynamics of the interactions of a volatile solute with a non-volatile solvent, and its potential value for providing this

type of data should be very great." His forecast has since been extensively implemented. Although the literature on the subject of chromatography is vast and the number of textbooks on this topic is large, the main emphasis in this section will be on the applications of chromatography to solutions study, which is the principal subject of this thesis. A number of excellent texts on the general application of chromatography are available (46, 76, 60, 23, 1, 31).

The first suggestion for using a liquid as a stationary phase fixed on solid support while another liquid served as mobile phase was made by Martin and Synge (63) in 1941 along with their famous derivation of the plate theory. It was not until 1952 that James and Martin (41) developed the chromatographic separation technique by using a gas as the mobile phase and a liquid as a stationary phase. Starting from that time, the most common non-analytical application of chromatographic techniques has been the determination of partition coefficients at infinite dilution.

Porter, Deal and Stross (80) in their pioneering work found that the chromatograph parameters such as column efficiency, column length and diameter, support size, the amount of stationary liquid and the carrier gas flow rate had no effect on the equilibrium constant.

Kwantes and Rijnders (54) also confirmed this conclusion with the restriction that the amount of stationary liquid on the packing must exceed 15% by weight to prevent absorption by the solid support upon which the liquid is impregnated. The Russian researchers Kurkchi et. al. (53) have also shown that the partition coefficient in their systems were independent of the amount of stationary phase, velocity of carrier gas, column dimensions and nature of the solid. Langer et. al. (55),

Desty et. al. (24) and Martire (66) studied solution thermodynamics using chromatography. They devised a theoretical approach for predicting the partition coefficient. These investigators compared the vapor-liquid equilibrium coefficients and activity coefficients determined from their GLC data to those determined from static data and found a very good agreement between the two. They concluded that vapor-liquid equilibrium coefficients obtained from chromatographic experiments represent true equilibrium values. The only exception to this conclusion was a case of a polar solute and a non-polar stationary solid mentioned in Kwantes et. al. work (54) and in Hardy's study (33). They found that for such systems the solid support material exerted absorption effect on the polar solute. Consequently, the partition coefficient for these systems would not be due to vapor-liquid interactions only. As mentioned before, Kwantes and Rijnders found that this problem can be solved by using a liquid load of at least 15% by weight. When the amount of stationary liquid on the solid packing exceeded 15% by weight, they noticed no absorption effects during their GLC experiments.

An unexpected phenomenon of gas-liquid interface absorption was discovered by Martin (64) when using a highly polar liquid as a stationary phase. Later, Martin (65) attributed this phenomenon to Gibbs absorption and even succeeded in predicting this type of absorption quantitatively. A further study of this problem was conducted by Martire, Pecsok and Purnell (69) using a static equilibrium apparatus. They concluded that the partition coefficient from a GLC elution experiment should be corrected only when the activity coefficient of the solute in the polar solvent exceeds the value of 10.

One of the restrictions imposed on phase equilibria study by chro-

matography in early work was that the liquid phase should be relatively non-volalite at the temperature of interest to avoid being carried off in the carrier gas stream. Keulesman (46) alleviated this restriction by proposing that the gas stream be presaturated before it enters the column. Kwantes and Rijnders (54) proposed the use of a column packed with solvent impregnated firebrick upstream of the GLC column for presaturating the carrier gas with solvent vapor in order to decrease the losses of the stationary liquid in the column.

James et. al. (42) have used successfully water at 2°C as liquid stationary phase. In addition to presaturating the carrier gas, they used a very low carrier flow rate.

Another way to minimize the amount of stationary liquid evaporation from the column is to account for the liquid losses by weighing the column before and after the experiment. If the assumption is made that the evaporation is proportional to the amount of carrier gas flowing through the column, the quantity of stationary liquid in the column can be calculated at a given time. This method was successfully used by Kurkchi and Iogansen (53), who measured the partition coefficient of acetylene in acetone at 25°C. Acetone is a considerably volatile at that temperature. These investigators obtained good agreement between the chromatographic and static data of the same system. A similar technique was used by Stalkup (93) and Koonce (50). Van Horn (99) used this method together with presaturation. This method is not practical experimentally when a series of solutes are injected successively, and not accurate when the retention times are relatively long since the quantity of the stationary liquid might change during the elution of the sample.

Littlewood, Phillips and Price (59) calculated heats of solutions from variation of retention volume with temperature. They have also established the fact that the "corrected" retention volume, $(V_R - V_G)$ is one of the critical parameters in GLC.

Porter, Deal and Stross (80) obtained equilibrium constants and calculated partial excess heat of solution using retention volume data for the systems n-heptane and 2-propanol in diisodecyle phthalate. Their data was consistent with static measurements..

Pierotti, Deal, Derr and Porter (77) extended the work of Porter et. al. to include solutes in polar solvent.

Anderson and Napier (2) studied benzene and cyclohexane in polyethylene glycol. They determined partition coefficients, heats of solutions and entropies of solutions from GLC elution data.

Wilzbach and Riez (103) used radioactively tagged samples in their GLC experiment. They showed that extensive substitution of hydrogen in organic compounds by deuterium or tritium caused significant changes in retention volumes of these compounds.

Hardy (33) obtained partition and activity coefficients for various halogenated hydrocarbons.

Rangel (82) calculated K-values for methane and propane in n-decane at pressures of 15 to 60 psia. He found the K-values in substantial agreement with values predicted from De Priester charts.

Lopez and Kobayashi (61) determined activity coefficients and heat of solutions for the C_4 hydrocarbons in furfural which were consistent with published data. They accounted for pressure drop along the GLC column.

Everett and Stoddart (28) determined activity coefficients for

for several paraffins and aromatic hydrocarbons in dinonyl phthalate by GLC. Their results agreed with the static data published by Ashworth and Everett (3).

The work so far described in this section was performed at relatively low pressures, i.e. at column pressures near atmospheric pressure. It has always been recognized that phase equilibrium data by chromatography can in principle be determined at more extreme temperature and pressure conditions.

An extensive amount of work in vapor-liquid equilibria at high pressures using GLC has been done at Rice University. An innovation in this technique is an expansion valve that is placed downstream of the chromatograph column, so that the pressure drop of the carrier gas from column pressure to atmospheric takes place after it emerges from the column. Consequently, the pressure drop along the column is negligibly small. This technique was successfully used at Rice University.

Two major problems arise in high pressure chromatography. The first one is that the solubility of the carrier gas is no longer negligible at high pressure, and consequently the solubility of the latter in the stationary liquid must be known at the system condition in order to obtain meaningful results. The second problem is that the methods for determining the column void volume such as the "air peak" or the "helium peak" methods that have been used successfully are not accurate for high pressure systems. Furthermore, the void volume itself is changing with pressure as a result of the "swelling" of the stationary phase due to absorption of carrier gas.

Stalkup and Kobayashi (95) and (96) calculated K-values from GLC data for ethane, propane, and n-butane at infinite dilution in the meth-

ane-n-decane systems at temperature of -20°F to 70°F and pressures of 20 to 2000 psia. Stalkup compared the experimental K-values favorably with NGAA (74). The K-values for the n-butane-methane-n-decane system at 40°F and 160°F agreed with static data of Sage and Lacey (87). Some inaccuracies in Stalkup's et. al. work may be attributed to two factors, the first is the inaccuracy in determining the void volume of the GLC column. This volume was determined by a direct calculation based upon the weight of solid and liquid in the column, density of the solid particles and volume of the column. The second inaccuracy occurred in determining the amount of stationary liquid losses due to evaporation. Stalkup and Kobayashi (95) also investigated the use of GLC to measure freezing points in the methane-n-decane system.

Stalkup and Deans (94) derived a relationship for the general case of an n-component carrier gas. This theory suggested the necessity of using radioactively tagged solute samples.

Koonce (50) and Koonce and Kobayashi (51) obtained K-values of methane and propane in the methane-propane-n-decane systems at temperatures of -20°F, 0°F, 40°F and 70°F and pressures up to 2000 psia. The carrier gas used in this study was a mixture of methane and propane at finite concentrations. Koonce also determined K-values of propane at infinite dilution in the same systems and conditions. K-values of propane in the propane-methane-n-heptane systems are also reported by Koonce (50). The radioactive solute samples used in these experiments were tagged with carbon 14. The K-values of propane in the propane-methane-n-decane systems determined by Koonce were satisfactorily consistent, but those for methane scattered considerably at the low pressure range. The errors in the methane K-values were attributed to in-

accuracies in evaluating the free gas volume of the chromatograph column. Comparison of Koonce's propane-methane-n-heptane data were in disagreement with Hurt (40) in the region of low propane concentrations. However, the K-values of propane at infinite dilution in the methane-n-decane system showed an excellent agreement with Stalkup (96) except at high pressures and temperatures. These deviations resulted primarily from inaccuracies in determining the GLC column free gas volume.

Martire and Polara (68), Cruickshank, Everett and Westway (20), and Barker and Hilmi (5) reported activity coefficients determined from GLC elution data, all at low pressures. Cruickshank et. al. concluded that an error of 1% to 2% in activity coefficient can be achieved by GLC experiments. An excellent paper by Cruickshank, Windsor and Young (21) reported in great detail the various techniques involved in determining activity coefficients from chromatography.

Chueh and Ziegler determined activity coefficients of benzene in diethylene glycol and n-hexane in 1,2,4-trichlorobenzene from the infinite dilution range to finite concentration. To accomplish the finite concentration, they used a gaseous mixture of solute vapor and helium gas as a carrier gas. Their data agreed with static measurements within $\pm$ 5%. The column pressure was atmospheric and the column void volume was measured by the "air peak" method.

Van Horn (99) and Van Horn and Kobayshi (100) obtained K-values for propane in the propane-methane-n-heptane systems at temperatures as low as -100^{o}F and pressures of 100 to 1000 psia by GLC. These authors determined also K-values of methane and ethane in the methane-ethane-n-heptane ternary systems, and of propane in the propane-methane-toluene systems. Van Horn used tagged solute samples in his experiment as well

as untagged samples. His reported results cover the range of infinite and finite concentration. The radioactively tagged samples were mainly used at the finite concentration range in order to obtain distinguishable solute molecules, which was required by the equations employed by this investigator. The free gas volume in the GLC column was measured by Van Horn by measuring the retention volume of tritium gas and assuming that the latter could be considered as an unretained solute; consequently, its retention volume represented the column free gas volume.

Masukawa and Kobayashi (71) and Masukawa, Alyea and Kobayashi (70) have successfully determined the free gas volumes of GLC column as a function of pressure at a fixed temperature. The free gas volume was obtained by extrapolating the series of retention volume to that of a hypothetical perfect gas.

This literature review would not be a complete one without mentioning the following two reviews. The first one is the good survey on the non-analytical uses of chromatography by Martire (67). The second one is the comprehensive review on chromatography by Kobayashi, Chappelear and Deans (48). This review covers in great detail the work done in the field of physico-chemical measurements by chromatography especially from 1952 up to this time. However, the review tends to be more informative than critical.

The conclusions that are drawn from the literature review presented in this section can be summarized in the following:

1. Equilibrium does exist between vapor and liquid in properly operated GLC columns.
2. For suitable systems, thermodynamic properties like vapor-liquid equilibrium constant, activity coefficient and heat of

vaporization can be determined via GLC.

3. The thermodynamic properties calculated from GLC elution data agree with those obtained from static methods.
4. The GLC technique for determining solute thermodynamic properties is especially suited to the case of a solute at infinite dilution.
5. To prevent absorption of a polar solute on the solid stationary phase, the liquid load on the solid should be above 15% by weight. Also, the solid support should be inert.
6. The column free volume is among the variables that effect directly the accuracy of the calculated K-values. If the solute is a light gas, an accurate value of the free volume is a necessity.
7. Stationary liquid losses from the GLC column can be minimized by saturating the carrier gas with the liquid before it enters the column.

CHAPTER III

THEORETICAL CONSIDERATIONS AND DEVELOPMENT

The development of the basic equations for reduction of experimental data to be used in this study are described in this chapter. The theoretical aspects of the experimental techniques employed during the course of this work are also discussed. The development of the correlation framework for the vapor-liquid equilibrium data is also given. The correlations developed here will be tested in Chapter VII using the experimental data.

The Partial Volume Experiment

The Injection Method

The injection method of determination of infinite dilution partial volume is based on the rigorous mathematical identity,

$$\frac{\bar{V}_2^{\infty}}{\tilde{V}_1} = \lim_{n_2 \to 0} \frac{\left(\frac{\partial P}{\partial n_2}\right)_{T_1, V_1, n_1}}{\left(\frac{\partial P}{\partial n_1}\right)_{T_1, V_1, n_2}} \tag{3-1}$$

where $\bar{V}_2$ stands for partial molal volume of component 2; $\tilde{V}_1$, molal volume of pure component 1; P is the system pressure, T is the system temperature and n is the number of moles.

Mixture Properties Related to Infinite Dilution Data

The infinite dilution partial molal volumes may be applied to the calculation of mixture molal volumes at finite concentrations. The molal volume of a mixture may be expressed in terms of the ideal mixture volume and the excess volume by

$$\tilde{V} = \tilde{V}_{ID} + \tilde{V}^E \tag{3-2}$$

The tilde sign indicates a molal quantity.

The ideal mixture volume is simply the mole fraction sum of the component volumes

$$\tilde{V}_{ID} = X_1 \tilde{V}_1 + X_2 \tilde{V}_2 \tag{3-3}$$

and

$$\tilde{V} = X_1 \tilde{V}_1 + X_2 \tilde{V}_2 + \tilde{V}^E \tag{3-4}$$

The excess volume may be conveniently related to mole fractions by an empirical series expression

$$\tilde{V}^E = X_1 X_2 [a + b(X_2 - X_1) + c(X_2 - X_1)^2 + \ldots.] \tag{3-5}$$

The coefficient a, b, c, ... depend on the temperature, pressure and the nature of the components.

The two partial volumes at the two infinite dilution conditions of a binary system at fixed temperature and pressure can be used to evaluate the coefficients a and b if terms containing c and above are discarded. The parameters a and b are related to the partial volumes by

$$a = \tfrac{1}{2}[(\bar{V}_1^{\infty} - \tilde{V}_1) + (\bar{V}_2^{\infty} - \tilde{V}_2)] \tag{3-6}$$

$$b = \tfrac{1}{2}[(\bar{V}_1^{\infty} - \tilde{V}_1) - (\bar{V}_2^{\infty} - \tilde{V}_2)] \tag{3-7}$$

Equations (3-6) and (3-7) are derived by differentiating Equation (3-2), combining with Equations (3-3) and (3-5) and taking the proper limits.

To the extent that mixture volumetric behavior is described by Equation (3-2) through (3-7), thermodynamic properties of mixtures can be derived from the infinite dilution partial volumes and the pure gas volumes. The results are illustrated as follows in terms of activities.

The activity coefficient of a mixture component is obtained by integrating the partial volumes according to

$$\ell n\gamma_i = \frac{1}{RT}\int_0^P (\bar{V}_i - \tilde{V}_i)dp \tag{3-8}$$

When the partial volumes are evaluated from Equations (3-3) through (3-7), the following relation is obtained,

$$\ell n\gamma_2 = X_1^2(\alpha + \beta X_1) \tag{3-9}$$

with

$$\alpha = \ell n \frac{\gamma_1^{\infty 2}}{\gamma_2^{\infty}} \tag{3-10}$$

$$\beta = \ell n \frac{\gamma_2^{\infty 2}}{\gamma_1^{\infty 2}} \tag{3-11}$$

The derivation of Equations (3-9) through (3-11) is given in Appendix A. The fugacity coefficient of a solute at infinite dilution in a solvent gas is readily obtained from Equation (3-8).

$$\ell n\psi_i^{\infty} = \frac{1}{RT}\int_0^P \left(\bar{V}_i^{\infty} - \frac{RT}{P}\right) dp \tag{3-12}$$

The vapor fugacity coefficient at infinite dilution can thus be obtained by integrating the experimental partial volume results according to Equation (3-12).

Equation of State Interaction Constants From Infinite Dilution Behavior

The full usefulness of equations of state for mixtures has not been achieved because of limitations in the various "combination rules" for mixtures. The usual procedure for application of an equation of state to mixtures calls for the determination of the equation constants for the best fitting of experimental data on the pure component (usually PVT data), and the combination of these constants as functions of composition to give mixture constants. The net result is that no experimental information on mixtures is needed in the application of a mixture equation of state. While this procedure has proved satisfactory for simple mixtures of similar substances at some conditions, it cannot be depended on for complex mixtures of dissimilar substances.

Wilson (102), Robinson and Jacoby (86), and Joffe and Zudkevitch (43) obtained improved representation of mixture properties through the use of empirical interaction constants in the Redlich and Kwong equation of state. Stotler and Benedict (97) introduced the use of a binary interaction constant in the Benedict-Webb-Rubin equation for the representation of phase equilibrium in nitrogen-methane mixtures. Yorizane, Yoshimura and Masuoka (104) likewise obtained substantially improved agreement in the fitting of phase equilibrium behavior in the system carbon dioxide-propylene. In both instances the binary interaction constant A_{012} was determined to fit mixture data.

In this work the Benedict-Webb-Rubin (B-W-R) equation of state was chosen to illustrate the use of infinite dilution partial volumetric data for the development of the interaction constants. The B-W-R equation is selected as it is suitably realistic and not unreasonably complex:

$$P = RT\rho + (B_o RT - A_o - C_o/T^2)\rho^2 + (bRT - a)\rho^3$$

$$+ a\alpha\rho^6 + (c\rho^3/T^2)(1 + \gamma\rho^2)\exp(-\gamma\rho^2) \qquad (3\text{-}13)$$

The constants in Equation (3-13) can be combined according to either of the following two rules. For A_o, B_o, C_o, and γ, the rule is illustrated by

$$A_o = \sum\sum_{ij} x_i x_j A_{o\,ij} \qquad (3\text{-}14)$$

with

$$A_{oij} = (A_{oi}A_{oj})^{1/2} \qquad (3\text{-}15)$$

The rule for a, b, c and α is illustrated by

$$a = \sum\sum\sum_{ijk} x_i x_j x_k a_{ijk} \qquad (3\text{-}16)$$

with

$$a_{ijk} = (a_i a_j a_k)^{1/3} \qquad (3\text{-}17)$$

Equation (3-15) or (3-16) is not used for an interaction constant when it is determined to fit mixture data.

If Equation (3-1) is evaluated in terms of the B-W-R equation of state the following relationship is obtained,

$$\frac{\bar{V}_2^{\infty}}{\bar{V}_1} = \frac{\begin{array}{l} RT\rho + 2(B_{o12}RT - A_{o12} - C_{o12}/T^2)\rho_1^2 \\ + 3(b_{112}RT - a_{112})\rho_1^3 + 3(a_{112}\alpha_1 + a_1\alpha_{112})\rho_1^6 \\ + (3c_{112}\rho_1^3/T^2)(1 + \gamma_1\rho_1^2)\exp(-\gamma_1\rho_1^2) \\ - (2c_1\gamma_1\gamma_{12}\rho_1^7/T^2)\exp(-\gamma_1\rho_1^2) \end{array}}{\begin{array}{l} RT\rho_1 + 2(B_{o1}RT - A_{o1} - C_{o1}/T^2)\rho_1^2 \\ + 3(b_1RT - a_1)\rho_1^3 + 6\alpha_1 a_1\rho_1^6 \\ + 3(c_1\rho_1^3/T^2)(1 + \gamma_1\rho_1^2)\exp(-\gamma_1\rho_1^2) \\ - (2\gamma_1^2 c_1\rho_1^7/T^2)\exp(-\gamma_1\rho_1^2) \end{array}} \qquad (3\text{-}18)$$

Equation (3-18) relates infinite dilution partial volume data to B-W-R equation constants.

The denominator on the right hand side of Equation (3-18) contains only constants of the pure solvent gas; these are presumed known. The interaction constants appear in Equation (3-18) in a form that makes their evaluation relatively easy to carry out. When experiemental partial volumes at infinite dilution become available over wide ranges of temperature and pressure, several of the interaction constants can be simultaneously determined.

The Gas-Liquid Chromatography Experiment

The Basic Chromatographic Equations

Martin and Synge (63) were the first to derive the basic chromatographic equation Their derivation, which was based on theoretical plate theory, was later verified by Glueckauf (32). Van Deemter, Zuiderweg and Klinkenberg (98) derived the same equation using the statistical distribution approach. This equation has been used in one form or another by all the investigators mentioned in the second part of Chapter II. A detailed discussion on the GLC basic equation is given by Keulemans (46), Littlewood (60), and Dal Nogare and Juvet (23).

A rather simple derivation of the basic chromatographic equation is discussed by Pecsar and Martin (107). A modified version of this derivation is presented here. The equation is then rearranged to fit the systems studied in this thesis.

The partition coefficient k_i is defined by

$$k_i = \frac{\text{conc. of comp. i in the liquid phase}}{\text{conc. of comp. i in the vapor phase}} \qquad (3\text{-}19)$$

The assumptions involved in this derivation are:

1. Sample size is infinitely small.
2. Constant partition coefficient k throughout the column.
3. Negligible pressure drop along the column.
4. Negligible change in the amount of liquid in the column during solute elution.
5. Mixing and diffusion effects are negligible.
6. No interaction between solute and solid support in the column.
7. Instantaneous equilibrium of solute sample exists between the vapor phase (carrier gas), and the liquid phase (stationary liquid).

According to the definition of k_i in Equation (3-19),

$$k_i = \frac{(n_{L_i}/V_L)}{(n_{v_i}/V_G)} = \frac{x_i \rho_L}{y_i \rho_G} = \frac{1}{K_i} \frac{\rho_L}{\rho_G} \tag{3-20}$$

The retention volume of component i, V_{R_i}, is defined by

$$V_{Ri} = f t_{R_i} \tag{3-21}$$

where f is the carrier gas flow rate. From Equation (3-21),

$$t_{Ri} = \frac{V_{R_i}}{f} \tag{3-22}$$

The total number of moles of i contained in the sample pulse that travels through the column, n_i, is divided into two parts, n_{G_i}, the part of the pulse that is contained in the gas phase, and n_{L_i}, the part of the pulse contained in the liquid phase; therefore,

$$n_i = n_{G_i} + n_{L_i} \tag{3-23}$$

The average linear velocity of the solute gas is defined by

$$u_i = \frac{L}{t_{R_i}} \tag{3-24}$$

where L is the length of the chromatograph column. Substituting t_{R_i} from Eq. (3-22),

$$u_i = \frac{f}{V_{R_i}/L} \tag{3-25}$$

Similarly, the average linear velocity of the carrier gas will be

$$u_G = \frac{f}{V_G/L} \tag{3-26}$$

The velocity u_i is the effective linear velocity of i. It is the velocity of propagation of the impulse through the column. The average linear velocity u_i may be therefore expressed as the ave age velocity of i moving in the gas phase and in the liquid phase, i.e.,

$$u_i = \frac{n_{G_i} u_{G_i} + n_{L_i} u_{L_i}}{n_i} \tag{3-27}$$

but

$$u_{L_i} = 0 \tag{3-28}$$

and

$$u_{G_i} = u_G = \frac{f}{V_G/L} \tag{3-29}$$

Substituting Eqs. (3-28) and (3-29) into Eq. (3-27)

$$u_i = \frac{n_{G_i}}{n_i}\left(\frac{f}{V_G/L}\right) \tag{3-30}$$

Substituting Eq. (3-23) into Eq. (3-30) and dividing through by V_G

$$u_i = \frac{n_{G_i}/V_G}{(n_{G_i}/V_G) + (n_{L_i}/V_L)(V_L/V_G)} \cdot \left(\frac{f}{V_G/L}\right) \tag{3-31}$$

Substituting n_{L_i}/V_L from Eq. (3-20)

$$u_i = \frac{n_{G_i}/V_G}{(n_{G_i}/V_G) + \left(k_i \frac{n_{G_i}}{V_G}\right)\left(\frac{V_L}{V_G}\right)} \cdot \left(\frac{f}{V_G/L}\right) = \frac{1}{V_G + k_i V_L} \cdot \frac{f}{1/L}$$

$$= \frac{V_R}{V_G + k_i V_L} \cdot \frac{f}{V_{R_i}/L} \qquad (3\text{-}32)$$

Substituting u_i from Eq. (3-25) into Eq. (3-32) and rearranging,

$$V_{R_i} = V_G + k_i V_L \qquad (3\text{-}33)$$

Since $k_i = \frac{1}{K_i}\frac{\rho_L}{\rho_G}$ (Eq. (3-20))

$$V_{R_i} = V_G + \frac{1}{K_i}\frac{\rho_L}{\rho_G} V_L$$

or

$$K_i = \frac{\left(\frac{\rho_L}{\rho_G}\right) V_L}{V_{R_i} - V_G} \qquad (3\text{-}34)$$

The vapor-liquid equilibrium constant, K_i, is expressed by Eq. (3-34) in terms of GLC elution parameters.

Equation (3-34) can be modified to make it more convenient to use with GLC experimental data.

Define the following variables:

$V_L \rho_L = W_L \equiv$ moles of stationary liquid and carrier gas solution.

$W_L^o \equiv$ moles of pure stationary liquid.

$x_1 \equiv$ mole fraction of carrier gas in the liquid phase.

The number of moles of pure liquid in the stationary liquid phase, W_L^o, is $W_L^o = (1 - x_1)\rho_L V_L$ moles of pure liquid. Therefore,

$$\rho_L V_L = \frac{W_L^o}{1 - x_1} \tag{3-35}$$

Substituting $\rho_L V_L$ from Eq. (3-35) into Eq. (3-34)

$$K_i = \frac{W_L^o}{(1 - x_1)\rho_G (V_{R_i} - V_G)} \tag{3-36}$$

where

K_i - vapor liquid equilibrium constant of solute i

W_L^o - moles of pure stationary liquid in GLC column

x_1 - mole fraction of carrier gas in the liquid phase

ρ_G - density of the carrier gas

V_{R_i} - retention volume of solute i

V_G - free gas volume, or volume of gas phase inside the GLC column.

If the flow rate of the carrier gas is measured at ambient conditions, like in the present experiment, the retention volume V_{R_i}, in Eq. (3-36), should be converted to column conditions by the following relation:

$$V_{R_i} = t_{R_i} f_a \left(\frac{P_a}{P}\right)\left(\frac{T}{T_a}\right) Z_G \tag{3-37}$$

where

f_a - the carrier gas flow rate at temperature T_a and pressure P_a

Z_G - compressibility factor of the carrier gas at column conditions, i.e., at temperature T and pressure P

t_{R_i} - retention time of solute i.

The retention time is the time lapse between the injection of the sample and the detection of the elution peak on the recorder chart.

Equations (3-36) and (3-37) were used for obtaining K-values for the various systems in this work. Equation (3-36) can be easily modified for the case of a carrier gas containing a mixture of gases.

Determination of the Void Volume in the Chromatograph Column

The determination of void volume, or free gas volume V_G in the GLC column is essential for calculating K-value as can be seen from Eq. (3-36).

Previous investigators (93, 21, 50, 99) have indicated a lack of precision in estimating the volume of the gas phase in the column.

The most known and used methods for estimating gas phase volume in a GLC column are the "geometric method" and the "marker gas" method. In the first method, the void volume is determined by subtracting the volume of the stationary solid and liquid phases from the interior volume of the column. In the second method, the retention volume of a gas which is assumed to be virtually insoluble in the particular stationary liquid phase is taken to be the void volume in the column. The gases usually used as "markers" or "unretained" gases are helium, hydrogen, nitrogen or air. Many of the investigators mentioned in Chapter II have used one of those techniques. Koonce (50) used a different method; he estimated V_G by measuring the retention time of radioactively tagged methane in methane-n-decane system. Then he calculated V_G from an equation similar to Eq. (3-36) knowing the K-value for methane in the same system from another source.

The errors that stem from the geometric method are due to the intrinsical difficulties in calculating precisely the volume of the solid and liquid stationary phases.

In the second method, the errors arise from the assumption that the "marker" gas is not retained by the liquid in the column; this assumption is specially inaccurate for systems at high pressures.

The reliability of Koonce's method depends upon the accuracy of the K-values used. The problems involved in this technique is that it is necessary to determine the response time of the detector and electronic system.

It is evident from Eq. (3-36) that the K-value is dependent directly upon the value $(V_{R_i} - V_G)$. Consequently, when K-values for highly retained (heavy) components are measured, the accuracy in evaluating V_G is not essential, since for heavy components $V_{R_i} \gg V_G$. However, for the study of volalite solutes, an extremely accurate knowledge of V_G is required.

The assumption of "unretained component" that may be acceptable at low pressures might lead to a considerable error in high pressure systems, or when the solute is a light gas.

In the rest of this section, a method for estimating free gas volume of a column is developed.

Pierotti (78, 79) determined the Henry's law constant of a "hard-sphere" gas in a given solvent by plotting the logarithm of the Henry's law constant of real gases in a given solvent as a function of the polarizability of the gas and extrapolating to zero polarizability. A smooth curve is defined by the noble gases, thus a precise extrapolation is possible. The section of the curve defined by helium, neon,

and argon is usually a straight line for simple solvents (89, 57). The extrapolation of the curve to zero polarizability yields a finite, non-zero volue of solubility even though the polarizability term is zero. This solubility is designated as "solubility of a hard-sphere gas." The solubility of a hard-sphere gas will differ from solvent to solvent.

Lin (58) obtained results similar to Pierotti's by extrapolating the solubilities of a number of real gases in different solvents versus their polarizabilities; the solubility data were taken from literature sources (57). The shape of the curves observed by Lin were generally similar to those obtained by Pierotti (78, 79).

A method for determination of free gas volume, V_G, based on the above works may be developed as follows:

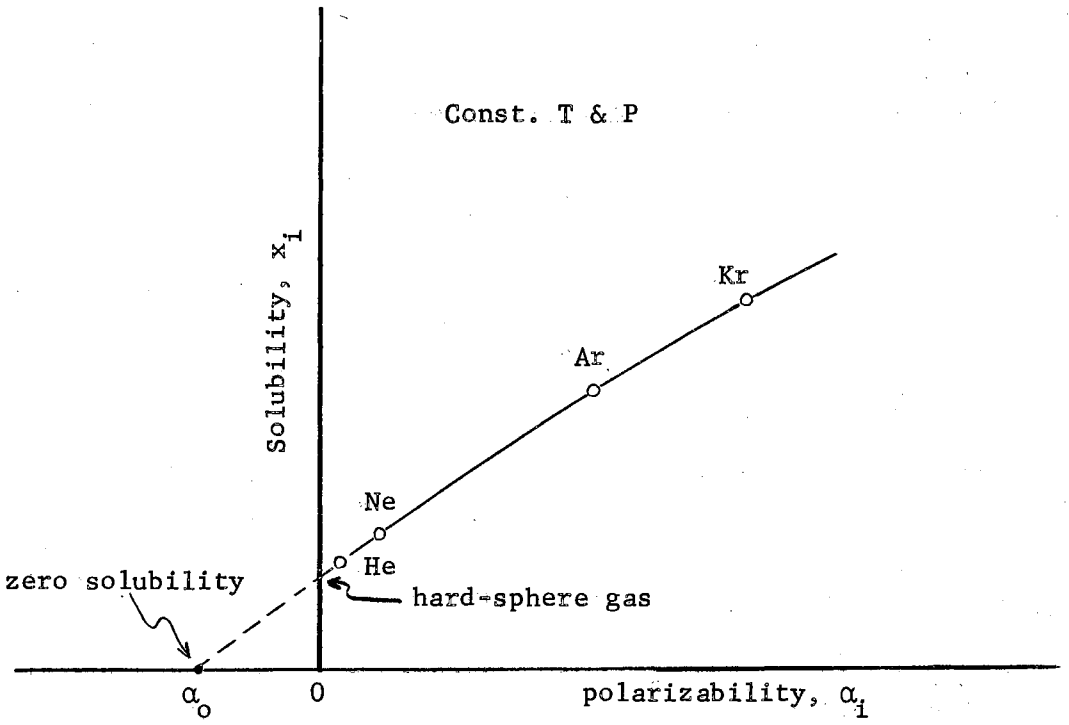

Figure 1. Solubility of Solute Gases as a Function of Their Polarizability

Figure 1 shows an extrapolation scheme to obtain the polarizability, α_o, of a fictitious solute gas whose solubility in a given solvent at specified temperature and pressure is equal to zero.

The following expression, obtained from Eq. (3-36),

$$\frac{x_i}{y_i} = \frac{(1 - x_1)\rho_G(V_{R_i} - V_G)}{W_L^o} \tag{3-37}$$

shows that when a "zero-solubility" solute is injected into a chromatograph column, its retention volume V_{R_i}, is equal to the free gas volume in the column, V_G, since according to Eq. (3-37)

$$V_{R_i} \to V_G \text{ when } \frac{x_i}{y_i} \to 0 \quad (K_i \to \infty)$$

Consider an experiment in which the gases shown in Figure 1 are injected into a chromatograph column containing a fixed solvent as a stationary liquid at specified temperature and pressure conditions, and the retention volume, V_{R_i}, is plotted as a function of the polarizability. If this plot is extrapolated to α_o previously obtained from Figure 1, the value of V_{R_i} at α_o will be equal to V_G, since the fictitious gas for which $\alpha = \alpha_o$ is insoluble at the given system. However, the liquid solubilities of He, Ne, Ar, Kr, etc. are not always available and are rarely available for high pressure systems. Therefore, the extrapolation scheme shown in Figure 1 cannot be performed in most cases of interest. On the other hand, the principle of the extrapolation to "zero-solubility" gas demonstrated in Figure 1 can be applied to the chromatography experiment, as described in the following.

Consider a series of plots of V_{R_i} as a function of α_i, each at a different fixed pressure. Each plot should cross $\alpha = \alpha_o$ at $V_{R_i} = V_G$.

In general, the resultant set of V_G values will be a function of pressure. The change in V_G with column pressure is due to expansion of the stationary liquid phase, caused by solubility changes of the carrier gas with pressure.

If the expansion of the column tubing due to pressure is neglected, the total column volume remains constant as pressure increases. Therefore, the sum of the free-gas volume and the liquid volume must be constant. Thus for any column pressure P, and reference pressure, P_o, $(P > P_o)$

$$(V_L)_P + (V_G)_P = (V_L)_{P_o} + (V_G)_{P_o} = \text{Constant}$$

or

$$(V_G)_{P_o} - (V_G)_P = (V_L)_P - (V_L)_{P_o} = (\Delta V_L)_P \tag{3-38}$$

and therefore,

$$(V_G)_{O_o} = (V_G)_P + (\Delta V_L)_P$$

where $(\Delta V_L)_{P_o}$ is the change in the stationary liquid solution volume. This volume change, $(\Delta V_L)_P$, can be calculated at any column pressure, P, if volumetric data on the carrier gas-solvent binary system are available.

The value of $(V_G)_P + (\Delta V_L)_P$ may be determined as

$$\lim_{\alpha \to \alpha_o} (V_{R_i} + \Delta V_L)_P = (V_G)_P + (\Delta V_L)_P = (V_G)_{P_o} \tag{3-39}$$

Thus a plot such as shown in Figure 2 should show a series of isobaric lines with a common intersection at the point $[(V_G)_{P_o}, \alpha_o]$. With $(V_G)_{P_o}$ known, $(V_G)_P$ may be calculated from the following relation,

$$(V_G)_P = (V_G)_{P_o} - (\Delta V_L)_P$$

The extrapolation scheme represented in Figure 2 circumvents the need for knowing the value of α_o.

Validity of the above method rests on the postulated existence of a fictitious insoluble component characterized by a fixed polarizability, α_o. Results of the present study indicate that this postulate can be used for obtaining the chromatograph column free-gas volume. An intersection point, $[(V_G)_{P_o}, \alpha_o]$, was obtained when experimental retention volumes were plotted according to Figure 2.

Development of a General Framework for Correlation of Activity Coefficients in Liquid Solutions at High Pressures

Conventions for Activity Coefficients

The chemical potential for a component in solution is defined by,

$$\mu_i = \mu_i^1 + RT\ell n\gamma_i x_i \qquad (3\text{-}40)$$

where μ_i^1 is to be taken as a function of temperature and pressure only. The activity coefficient γ_i may be a function of temperature, pressure and composition. Both γ_i and μ_i^1 in Eq. (3-40) need to be defined. By specifying the concentration x_i under which γ_i becomes equal to unity, both of those quantities are defined. For the purpose of this definition, it is convenient to choose either of two conventions. These conventions are based on the fact that a component i of a real solution is normally found to approach ideal behavior in the following two cases,

$$\text{as } x_i \to 1 \text{ and as } x_i \to 0.$$

The "symmetric convention" is defined by the limiting condition $\gamma_i \to 1$ as $x_i \to 1$ for all component in solution. Under these conditions, μ_i is

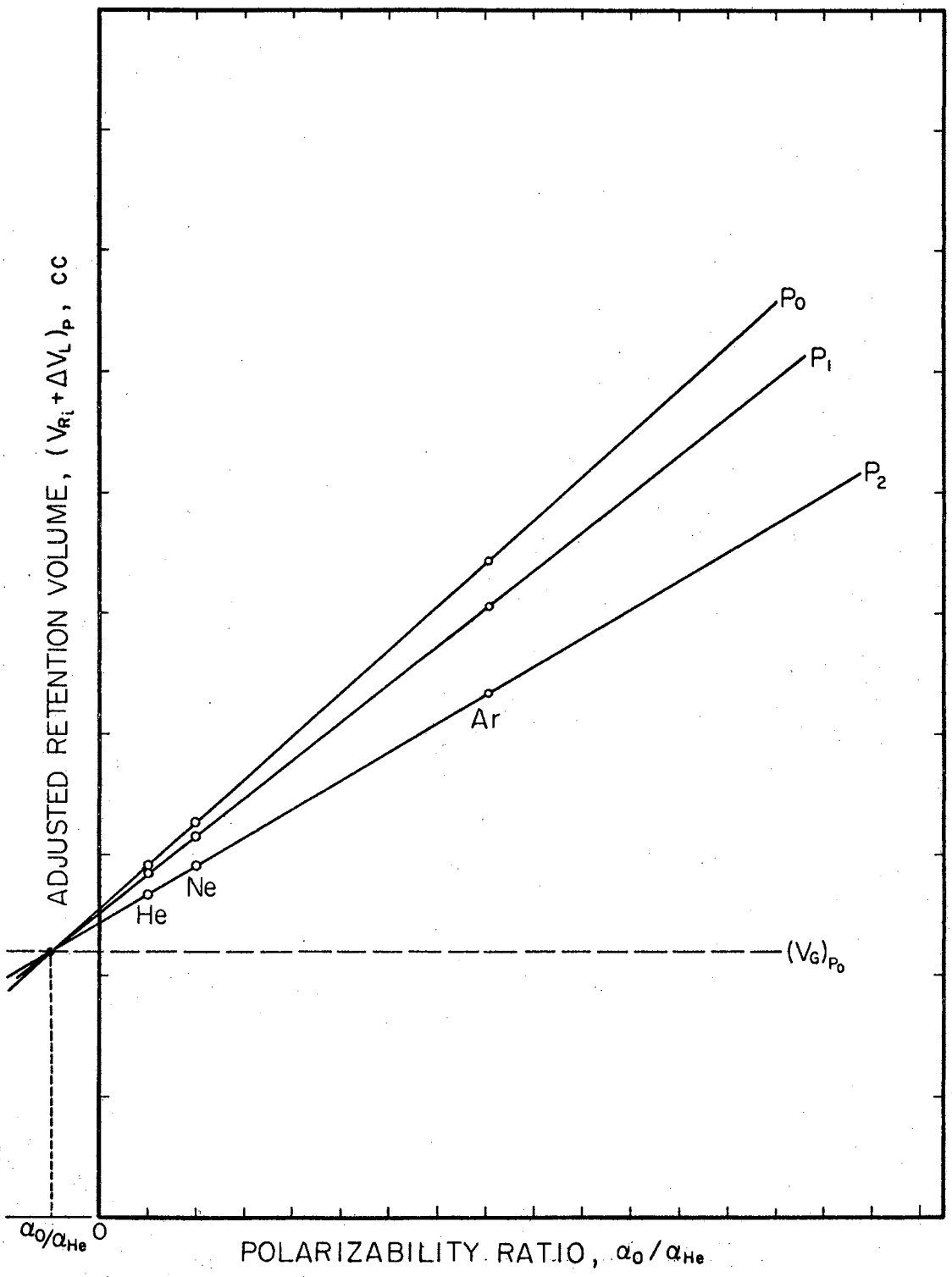

Figure 2. Determination of Chromatograph Column Void Volume

equal to the chemical potential of the pure substance at the solution temperature and pressure, as can be seen from Eq. (3-40). This convention is referred to as "symmetric" since it is symmetric in all of the components.

The "unsymmetric convention" is defined by the following limiting conditions,

$$\text{for solute(s):} \quad \gamma_i \to 1 \text{ as } x_i \to 0, \text{ or as } x_s \to 1$$

$$\text{for solvent:} \quad \gamma_s \to 1 \text{ as } x_s \to 1$$

Here the solvent activity coefficient is defined according to the symmetric convention. On the other hand, the activity coefficients of the solutes are taken as approaching unity at infinite dilution. Therefore, μ_i^1 in Eq. (3-40) is the chemical potential of the solute in a hypothetical liquid state corresponding to the extrapolation from infinite dilution to $x_i = 1$ along Henry's law line. This convention is called "unsymmetric" since the reference states the solvent and that of the solute are defined differently, or unsymmetrically.

The Derivation of the Unsymmetric Activity Coefficient. The chemical potential at constant temperature in the differential form is expressed by,

$$d\mu_i = RTd\ell nf_i \tag{3-41}$$

Integrating at constant temperature from a certain standard state of component i (this standard state is yet to be specified),

$$\mu_i = \mu_i^1 + RT\ell n \frac{f_i}{f_i^o} \tag{3-42}$$

where f_i^o is the standard state fugacity of component i. The activity

coefficient of component i in solution is defined according to

$$\gamma_i = \frac{f_i}{x_i f_i^o} \tag{3-43}$$

and

$$\gamma_i x_i = \frac{f_i}{f_i^o} \tag{3-44}$$

Equation (3-40) was obtained by substituting Eq. (3-44) into Eq. (3-42). Also from Eq. (3-43)

$$\frac{f_i}{x_i} = f_i^o \gamma_i \tag{3-45}$$

By definition of Henry's law constant,

$$H_i = \lim_{x_i \to 0} \frac{f_i}{x_i} \tag{3-46}$$

therefore,

$$\lim_{x_i \to 0} \frac{f_i}{x_i} = \lim_{x_i \to 0} f_i^o \gamma_i \tag{3-47}$$

at standard state $\gamma_i = 1$, therefore,

$$\lim_{x_i \to 0} \left(\frac{f_i}{x_i}\right) = f_i^o \tag{3-48}$$

or,

$$H_i = f_i^o \tag{3-49}$$

From Eqs. (3-44) and (3-49),

$$\gamma_i^* = \frac{f_i}{x_i H_i} \tag{3-50}$$

The asterisk in Eq. (3-50) is used to emphasize that the activity coefficient is in the unsymmetric convention. The activity coefficient for the solvent is given by the symmetric convention,

$$\gamma_s = \frac{f_s}{x_s f_s^o} \tag{3-51}$$

Equation (3-50) satisfies the requirement,

$$\gamma_i^* \to 1 \text{ as } x_s \to 1$$

and Eq. (3-51) satisfies the condition $\gamma_s \to 1$ as $x_s \to 1$.

Thermodynamically, the choice of standard state for a solution constituent is arbitrary; the only two restrictions are that it must be at solution temperature and at fixed composition. Both of the activity conventions mentioned above comply with these restrictions.

The activity coefficient in the unsymmetric convention can be obtained from the symmetric activity coefficient by normalizing the latter. For example, consider the binary system consisting of a solute 2, and a solvent 1,

$$\gamma_2^* = \frac{\gamma_2}{\gamma_2^\infty} \tag{3-52}$$

where

$$\gamma_2^\infty = \lim_{x_2 \to o} \gamma_2 \tag{3-53}$$

from Eq. (3-52),

$$\ell n\gamma_2^* = \ell n\gamma_2 - \ell n\gamma_2^\infty \tag{3-54}$$

For multicomponent system, the unsymmetric activity coefficient will be,

$$\ell n\gamma_i^* = \ell n\gamma_i - \lim_{x_s \to 1} \ell n\gamma_i \tag{3-55}$$

where s is always the heaviest component in the system and referred to as the solvent. Note that according to Eq. (3-46)

$$H_2 = \lim_{x_2 \to 0} \frac{f_2}{x_2} = \lim_{x_s \to 1} \frac{f_2}{x_2} \qquad (3\text{-}56)$$

binary system — multicomponent system

It is entirely a matter of convenience which one of the conventions is adopted.

The symmetric activity coefficient has some advantages. The most important is that the activity coefficient relates solution properties to a pure-component property. Thus, only pure substance data are needed to evaluate the standard-state properties. Furthermore, pure material data are more available than solution data and can be extrapolated and generalized more successfully.

However, the major weakness of the activity coefficient in the symmetric form arises when the standard state is physically unattainable. This situation is encountered for the light components in the system. When the solution temperature is above the critical temperature of one of the components one has to hypothesize a component at a pure liquid state in a region where it cannot exist as pure liquid at any pressure.

There is no unique standard state fugacity for a noncondensable, supercritical component in the symmetric convention. The hypothetical pure-liquid fugacities obtained from vapor-liquid equilibria of that component in various solvents may differ considerably from each other (81, 14, 18).

The advantage of the activity coefficient in the unsymmetric convention is that it is explicitly defined. The disadvantages are that the standard-state of each component depends not only on its properties, but on the properties of the solvent as well.

A comprehensive discussion of the use of unsymmetric activity coefficients in high pressure systems has been given by Prausnitz (81).

The numerical value of the activity coefficient for a component in a particular solution depends on the convention chosen; therefore, the convention used should be clearly defined.

Correlation for Activity Coefficient

A common method for analyzing equilibrium data involves separating the equilibrium parameters into several factors and assuming that each factor depends solely upon one thermodynamic variable, either extensive or intensive. Each part is referred to as "contribution" such as pressure contribution, concentration contribution, etc.

A similar type of analysis is used in this section to correlate the activity coefficients for the various systems.

Activity Coefficient from Regular Solution Theory. The literature abounds with correlations for activity coefficients of liquid solutions. In particular, the Scatchard-Hildebrand regular solution theory (36) is very commonly used. This theory was successfully used by Chao and Seader (12) to correlate vapor liquid equilibrium data.

The activity coefficient of a solute k in a multicomponent system at constant temperature and pressure is derived from Scatchard's regular solution theory (90, 91) and is given below:

$$\ell n\gamma_k = \frac{V_k}{RT}\left[a_{kk} - 2\sum_j \Phi_j a_{kj} + \sum\sum_{ij} \Phi_i \Phi_j a_{ij}\right] \qquad (3\text{-}57)$$

where a_{ij} is the cohesive energy density, a_{ij} is related to A_{ij}, the exchange energy density by

$$A_{ij} = a_{ii} - 2a_{ij} + a_{jj} \tag{3-58}$$

The detailed derivation of Eq. (3-57) is given in Appendix B.

From Eq. (3-57), taking the limit $x_s \rightarrow 1$,

$$\lim_{x_s \rightarrow 1} \ln\gamma_k = \frac{V_k}{RT}\left[a_{kk} - 2a_{ks} + a_{ss}\right] \tag{3-59}$$

The activity coefficient of component k in the unsymmetric convention in a multicomponent system, according to equations (3-55), (3-57), and (3-59), is

$$\ln(\gamma_k^*)_{SH} = \frac{V_k}{RT}\left[-2\sum_j \Phi_j a_{kj} + \sum\sum_{ij} \Phi_i \Phi_j a_{ij} + 2a_{ks} - a_{ss}\right] \tag{3-60}$$

The subscript SH on the left side of Eq. (3-60) indicates that the activity coefficient is based on the Scatchard-Hildebrand theory.

For a binary system, Eq. (3-60) converges to Eq. (3-61) by setting i,j = 1,2, k = 2, and s = 1,

$$\ln(\gamma_2^*)_{SH} = \frac{V_2 (\Phi_1^2 - 1) A_{12}}{RT} \tag{3-61}$$

compared with the well known symmetric activity coefficient (36)

$$\ln\gamma_2 = \frac{V_2 \Phi_1^2 A_{12}}{RT} \tag{3-62}$$

Scatchard (90) assumed that the interaction between unlike molecules is given by the geometric mean of the interaction between the like molecules,

$$a_{ij} = (a_{ii} a_{jj})^{\frac{1}{2}} \tag{3-63}$$

Scott (92) has pointed out that a small deviation from the geometric mean assumption might have a large effect on the solubility.

Hildebrand and Scott (37) have shown that the geometric mean assumption is only justified if the ionization potential and collision diameter of unlike molecules are equal.

Eckert and Prausnitz (27), have suggested a modification of the relationship given by Eq. (3-63), introducing a correction constant, ℓ_{ij}, characteristic of interaction between unlike molecules, i.e.,

$$a_{ij} = (1 - \ell_{ij})(a_{ii}a_{jj})^{\frac{1}{2}} \tag{3-64}$$

Chuch and Prausnitz (15, 16) have used a similar approach, but they have introduced a correction to the geometric mean for critical temperatures of solutions, the correction factor being evaluated from experimental data on binary systems.

$$T_{c_{12}} = (1 - k_{12})(T_{c_1} T_{c_2})^{\frac{1}{2}} \tag{3-65}$$

Cheung and Zander (13) have suggested that ℓ_{12} in Eq. (3-64) and k_{12} in Eq. (3-65) will be essentially numerically equal if the collision diameters of the two unlike molecules do not differ too widely.

Chuch and Prausnitz (15) and Cheung and Zander (13) found that k_{12} and ℓ_{12} are to a good approximation independent of temperature, density, and composition.

Equation (3-64) can be expressed as

$$a_{ij} = \alpha_{ij}(a_{ii}a_{jj})^{\frac{1}{2}} \tag{3-66}$$

or using the solubility parameters

$$a_{ij} = \alpha_{ij}\delta_i\delta_j \tag{3-67}$$

where $\alpha_{ij} = 1 - \ell_{ij}$, the parameter α_{ij} is the correction factor of the mean square rule.

Activity Coefficient from Flory-Huggins Theory. Kohn (49) has shown that the Flory-Huggins version of the regular solution theory (29, 30, 38, 39) appears to be a more reliable approach for correlating vapor-liquid, vapor-liquid-liquid, and vapor-liquid-solid data than Scatchard's original regular solution theory (90, 91).

Cheung and Zander (13) have shown that solubility data of carbon dioxide and hydrogen sulfide in hydrocarbons can be adequately represented by a solubility equation containing the Flory-Huggins term in addition to the Scatchard-Hildebrand term.

A number of investigators (13, 49, 11, 10, 35) had previously observed that the addition of Flory-Huggins term to the Scatchard-Hildebrand equation resulted in improving the solubility equation in most cases where there was a great difference in size between unlike molecules. Based on the findings and observations of the investigators quoted above, the Flory-Huggins activity coefficient was included in the present correlation work.

The derivation of the unsymmetric activity coefficient based on Flory-Huggins theory is outlined below.

The partial entropy of mixing of a component k in a multicomponent solution at constant temperature and pressure is give by Flory-Huggins theory (36) as,

$$\overline{\Delta S}_k = -R\left[\ell n\Phi_k + \sum_i \Phi_i\left(1 - \frac{V_k}{V_i}\right)\right] \qquad (3\text{-}68)$$

The excess partial entropy is therefore,

$$\overline{\Delta S}_k^E = -R\left[\ell n\Phi_k + \sum_i \Phi_i\left(1 - \frac{V_k}{V_i}\right)\right] - (-R\ell n\ x_k) \qquad (3\text{-}69)$$

Rearranging Eq. (3-69)

$$\overline{\Delta S}_k^E = -R\left[\ell n\left(\frac{V_k}{\sum_i x_i V_i}\right) + \sum_i \Phi_i\left(1 - \frac{V_k}{V_i}\right)\right] \tag{3-70}$$

according to the Flory-Huggins theory $\overline{\Delta H}^E = 0$ and therefore the activity coefficient is related to the excess partial free energy by

$$RT\ell n(\gamma_k)_{FH} = \overline{\Delta G}_K^E = -T\overline{\Delta S}_k^E \tag{3-71}$$

The subscript FH on the left side of Eq. (3-71) indicates that the derivation of the activity coefficient is based on the Flory-Huggins theory.

Combining Eq. (3-70) and Eq. (3-71),

$$\ell n(\gamma_k)_{FH} = \ell n\left(\frac{V_k}{\sum_i x_i V_i}\right) + \sum_i \Phi_i\left(1 - \frac{V_k}{V_i}\right) \tag{3-72}$$

taking the limit $x_s \to 1$

$$\lim_{x_s \to 1} \ell n(\gamma_k)_{FH} = \ell n \frac{V_k}{V_s} + \left(1 - \frac{V_k}{V_s}\right) \tag{3-73}$$

according to Eqs. (3-73) and (3-55)

$$\ell n(\gamma_k^*)_{FH} = \ell n\left(\frac{V_s}{\sum_i x_i V_i}\right) + \sum_i \Phi_i \left(1 - \frac{V_k}{V_i}\right) - \left(1 - \frac{V_k}{V_s}\right) \tag{3-74}$$

Equation (3-74) expresses the Flory-Huggins activity coefficient in the unsymmetric convention for the general case of a multicomponent solution.

For a binary system, Eq. (3-74) converges to Eq. (3-75) by setting $i = 1,2$, $k = 2$ and $s = 1$,

$$\ell n(\gamma_2^*)_{FH} = \ell n \frac{V_1}{V_m} - \Phi_2\left(1 - \frac{V_2}{V_1}\right) \tag{3-75}$$

where V_m is the molar volume of the solution.

The Combined Activity Coefficient. The activity coefficient is assumed to be composed of two terms, namely, the one derived from Scatchard-Hildebrand theory, and the second from the Flory-Huggins theory as shown by Eq. (3-76),

$$\ell n(\gamma_k^*)_o = \ell n(\gamma_k^*)_{SH} + \ell n(\gamma_k^*)_{FH} \tag{3-76}$$

The subscript o on the left side of Eq. (3-76) is to indicate that the activity coefficient as expressed by Scatchard-Hildebrand and Flory-Huggins theories is applicable only at constant pressure and temperature.

The unsymmetric activity coefficient for a multicomponent system is obtained by combining equations (3-60) and (3-74)

$$\ell n(\gamma_k^*)_o = \frac{V_k}{RT}\left[-2\sum_j^n \Phi_j a_{kj} + \sum_{ij}^{nn}\Phi_i\Phi_j a_{ij} + 2a_{ks} - a_{ss}\right]$$

$$+ \ell n\left(\frac{V_s}{\sum_i^n x_i V_i}\right) + \sum_i^n \Phi_i\left(1 - \frac{V_k}{V_i}\right) - \left(1 - \frac{V_k}{V_s}\right) \tag{3-77}$$

Solving Eq. (3-77) for a binary system,

$$\ell n(\gamma_2^*)_o = \frac{V_2(\Phi_1^2 - 1)A_{12}}{RT} + \ell n\frac{V_1}{V_m} - \Phi_2\left(1 - \frac{V_2}{V_1}\right) \tag{3-78}$$

Activity Coefficient from GLC Data. A method for determining activity coefficients from chromatographic measurements is outlined below.

The vapor-liquid equilibrium constant is defined by

$$K_i = \frac{y_i}{x_i} \tag{3-79}$$

or by

$$K_i = \frac{f_{L_i}/x_i}{f_{v_i}/y_i} \tag{3-80}$$

Multiplying by system pressure, P,

$$K_i = \frac{f_{Li}/x_i P}{f_{vi}/y_i P} = \frac{f_{Li}/x_i P}{\psi_i} \tag{3-81}$$

where ψ_i is the vapor phase fugacity coefficient. From Eq. (3-81) it follows that,

$$\frac{f_{L_i}}{x_i} = K_i \psi_i P \tag{3-82}$$

The standard state liquid fugacity f^o_{Li}, is defined as Henry's law constant, i.e.,

$$f^o_{L_i} = H_i = \lim_{x_s \to 1} \frac{f_{L_i}}{x_i} \tag{3-83}$$

Therefore, by definition of standard state of component i,

$$f^o_{L_i} = \lim_{x_s \to 1} (K_i \psi_i P) \tag{3-84}$$

also, at constant temperature, while pressure may change with x_i,

$$\gamma^*_i = \frac{f_{L_i}}{x_i f^o_{L_i}} \tag{3-85}$$

Combining Eq. (3-82) and Eq. (3-85),

$$\gamma^*_i = \frac{K_i \psi_i P}{f^o_{L_i}} \tag{3-86}$$

For a solute "2" at infinite dilution, Eq. (3-82) becomes

$$\left(\frac{f_{L_2}}{x_2}\right)^\infty = K_2^\infty \psi_2^\infty P \tag{3-87}$$

and the activity coefficient of solute 2 at infinite dilution in the methane-n-decane system is readily obtained from Eq. (3-86)

$$\gamma_2^{*\infty} = \frac{K_2^{\infty}\psi_2^{\infty}P}{f^{o}_{L_2}} \tag{3-88}$$

where,

$$f^{o}_{L_2} = \lim_{x_s \to 1} (K_2^{\infty}\psi_2^{\infty}P) \tag{3-89}$$

The standard state liquid fugacity, $f^{o}_{L_i}$, is determined by extrapolating Eq. (3-89) graphically as demonstrated in Figure 3.

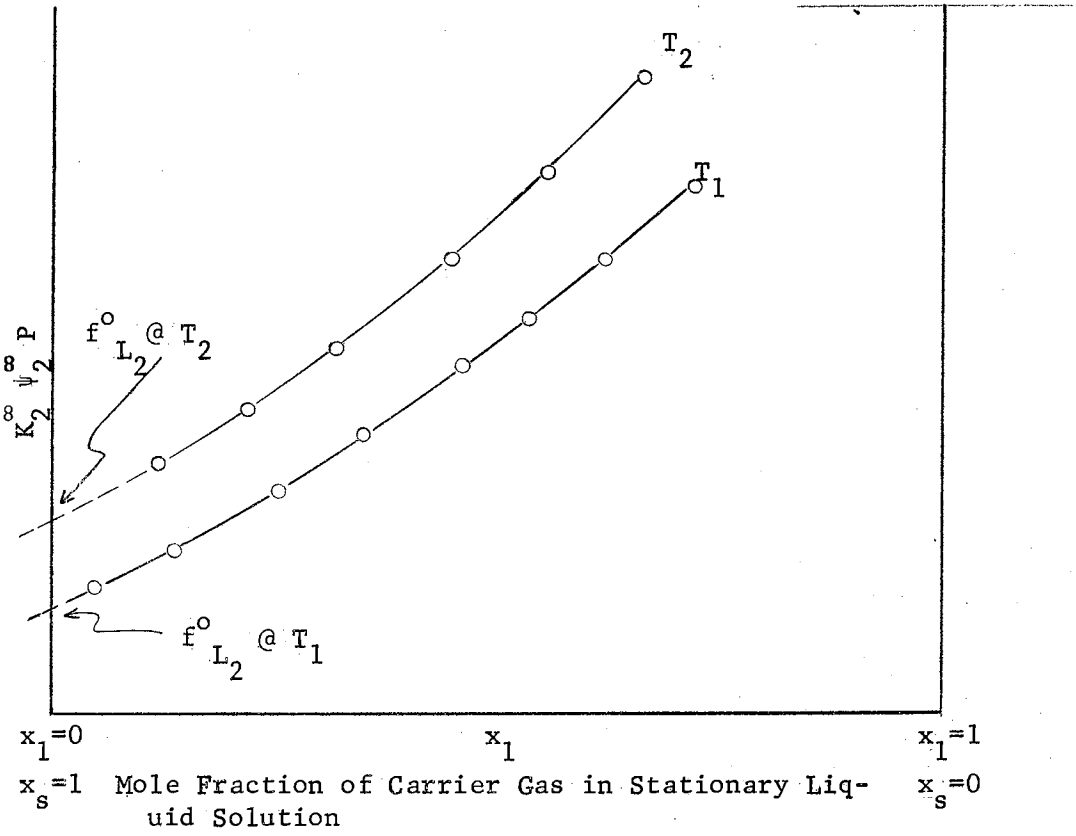

Figure 3. Standard State Liquid Fugacity by Extrapolating Experimental GLC Data

The standard state liquid fugacity, f^{o}_{Li}, as determined by the extrapolation shown in Figure 3 is evaluated at the vapor pressure of pure solvent at the system temperature. This standard state fugacity can be adjusted to zero pressure at the system temperature by the following rigorous relation,

$$(f^{o}_{L_2})_{P=0} = (f^{o}_{L_2})_{P=P_{vp}} \exp\left(\frac{1}{RT}\int_{o}^{P_{vp}} \bar{V}^{\infty}_{L_2} dP\right) \tag{3-90}$$

where P_{vp} is the vapor pressure of the solvent at temperature T.

The pressure correction for $f^{o}_{L_2}$ shown in Eq. (3-90) provides the same reference pressure, in this case, zero pressure, for the standard fugacity at all system temperatures. The choice of the reference pressure is entirely arbitrary; zero pressure is usually chosen as reference pressure for convenience.

The solvent is always chosen as the heaviest component in the system, if the solvent has low vapor pressures at solution temperatures, than $P_{vp} \cong 0$. Therefore, the pressure correction is negligibly small and Eq. (3-90) becomes

$$(f^{o}_{L_2})_{P=0} \cong (f^{o}_{L_2})_{P=P_{vp}} \tag{3-91}$$

If the solvent vapor pressure at solution temperature is not negligibly small, the standard state fugacity, $f^{o}_{L_2}$, would be at the vapor pressure of the solvent at the system temperature.

Having obtained $f^{o}_{L_2}$ by extrapolating the combined chromatographical and partial volume data, the unsymmetric activity coefficient is determined from Eq. (3-86).

The Correlation for Pressure Dependent Activity Coefficient

Prausnitz (81), Orentlicher and Prausnitz (75), Chueh, Muirbrook and Prausnitz (14), and Chueh and Prausnitz (18) have studied high pressure vapor-liquid equilibria using pressure-dependent unsymmetric activity coefficients.

The unsymmetric activity coefficient γ_k^* can be expressed in terms of a pressure-independent activity coefficient $(\gamma_k^*)_o$ and a term involving the partial volume in the liquid phase as shown by Eq. (3-92)

$$\ell n\gamma_k^* = \ell n(\gamma_k^*)_o + \frac{1}{RT}\int_{P_{vp}}^{P} \bar{V}_{L_k}\, dP \tag{3-92}$$

where P_{vp}, the vapor pressure of the solvent (the heaviest component in the system), is arbitrarily chosen as the reference pressure.

Substituting for $\ell n(\gamma_k^*)_o$ from Eq. (3-77)

$$\ell n\gamma_k^* = \frac{V_k}{RT}\left[-2\sum_j^n \Phi_j a_{kj} + \sum_{ij}^{nn}\Phi_i\Phi_j a_{ij} + 2a_{ks} - a_{ss}\right]$$

$$+ \ell n\left(\frac{V_s}{\sum_i^n x_i V_i}\right) + \sum_i^n \Phi_i\left(1 - \frac{V_k}{V_i}\right) - \left(1 - \frac{V_k}{V_s}\right) + \frac{1}{RT}\int_{P_{vp}}^{P} \bar{V}_{L_k}\, dP \tag{3-93}$$

Equation (3-93) represents the model for activity coefficient of component k in a multicomponent system as a function of temperature, pressure and composition.

The activity coefficient for a binary solution is obtained from the general correlation, i.e., from Eq. (3-93)

$$\ell n\left(\frac{K_2\psi_2 P}{f^o_{L_2}}\right) = \frac{V_2}{RT}(\Phi_1^2 - 1)(a_{11} + a_{22} - 2a_{12}) + \ell n\frac{V_1}{V_m}$$

$$- \Phi_2\left(1 - \frac{V_2}{V_1}\right) + \frac{1}{RT}\int_{P_{vp}}^{P} \bar{V}_{L_2}\, dP \tag{3-94}$$

CHAPTER IV

EXPERIMENTAL APPARATUS

During the course of this study, experimental measurements were made on infinite dilution partial volumes in the carbon dioxide-methane systems and on the vapor liquid equilibrium constants of a number of solute gases at infinite dilution in the methane-n-decane systems. Two experimental apparatus were employed to obtain the data. The first included an apparatus for measuring the change in pressure of a gaseous system with increase of the number of moles at constant volume. The second apparatus consisted of a specially designed chromatographic system for measuring phase equilibria.

A detailed description of the experimental systems is given in this chapter.

The Partial Volume Experiment

The objective of the apparatus was to obtain experimentally the quantity $(\partial P/\partial n_j)_{T,V,n_k}$ by the injection method according to Eq. (3-2).

The apparatus used in this work is identical to that described previously (34) except for the following changes:

1. A ball valve was installed between the burette and the main vessel. The straight channel in the ball valve makes it unlikely that any small quantity of gas will be trapped as it could in the needle-type valve which was used previously.

2. A Leeds & Northrup K-3 potentiometer was used for the measurement of the output emf of the differential pressure transducer to a precision of $\pm$ 0.2μv.
3. The temperature control was improved by introducing a constant temperature coolant bath instead of using tap water for cooling. The tap water temperature can often vary as much as 10^{o}F; this temperature variation previously caused fluctuations in the thermostat.
4. A vacuum pump was connected to the mercury line, thus insuring that no gas will get trapped inside the mercury pump piston.
5. A Texas Instrument low pressure quartz tube gauge was installed for the measurement of the burette pressure. The quartz tube element was rated for 100 psia full range. The accuracy of this instrument is such that the low pressure measurements are no longer a limiting factor in the accuracy of the experimental results. A schematic diagram of the experimental apparatus is shown in Figure 4.

The Gas-Liquid Chromatography Experiment

The objective of the chromatographic apparatus was to facilitate measurement of solute gases in ternary systems.

A schematic diagram of the experimental apparatus is shown in Figure 5.

General Description of the Apparatus

The apparatus consisted of a chromatograph, constant temperature bath, high pressure tubing and fitting system and auxiliary equipment.

The apparatus was mounted on an angle iron frame. The overall di-

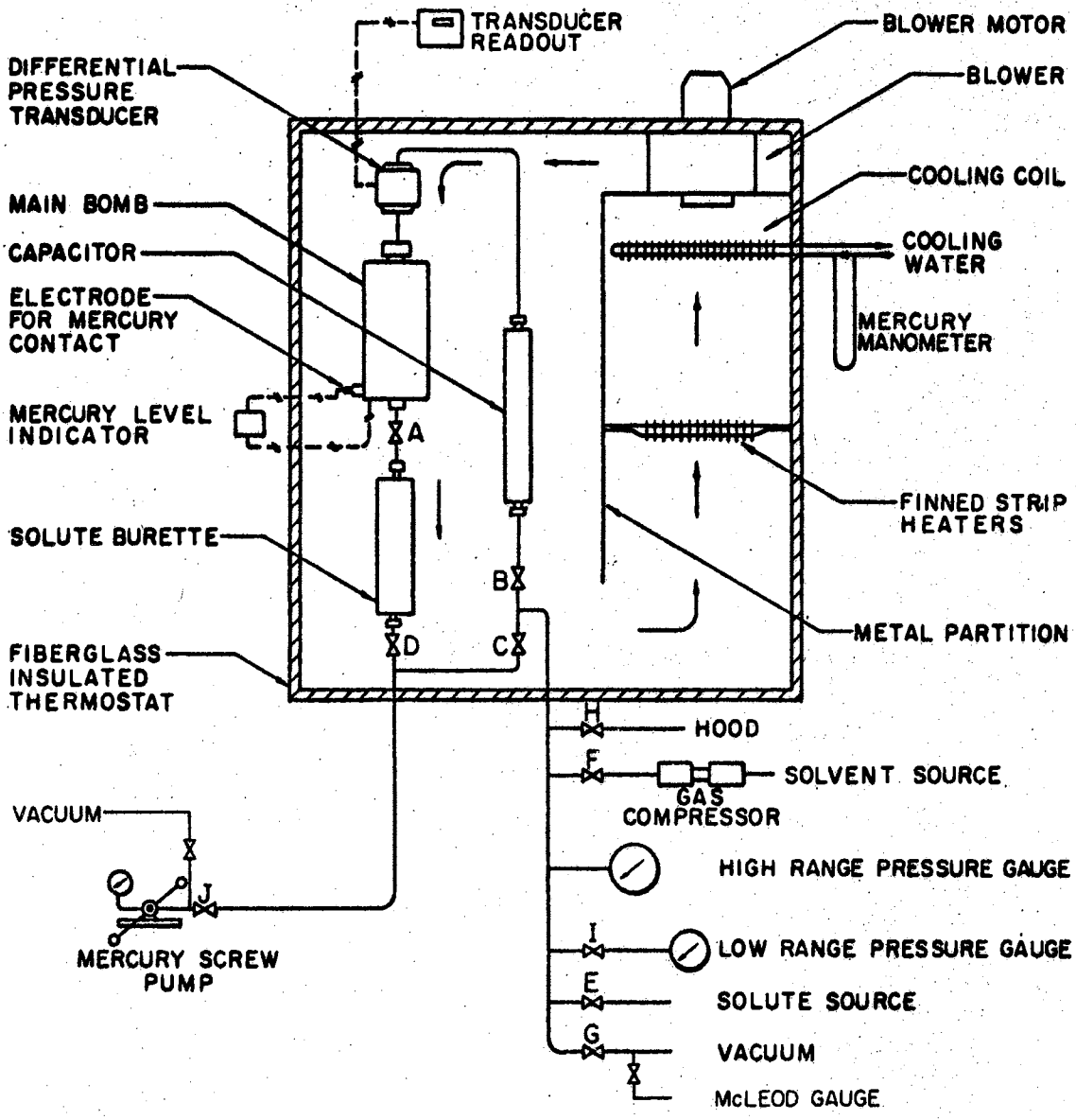

Figure 4. Equipment for Measurement of Partial Volume at Infinite Dilution

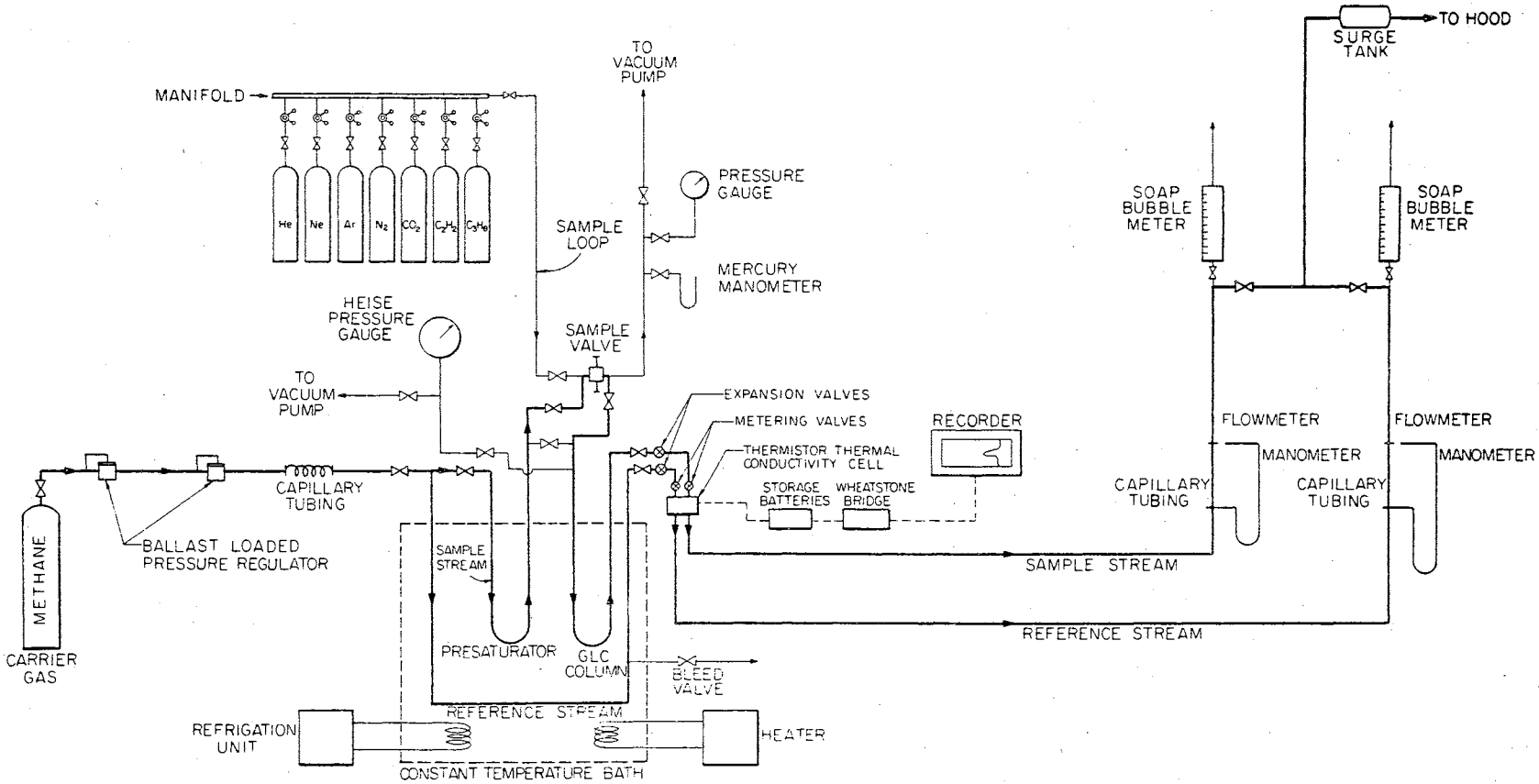

Figure 5. Schematic Diagram of the Chromatographic Apparatus

mensions of the frame were length: 7'6", width: 2'2", height: 5'8". Plywood platforms of different widths were used for the main construction. Most of the fixed components such as valves, flow control and temperature control units, pressure gauges and stirrers were mounted thereon. The refrigeration unit, the coolant tank, the coolant circulation pump, gas cylinders and the recorder unit were placed on the floor or metal shelves adjacent to the main apparatus.

The insulated constant temperature bath was placed in a wooden box and mounted on a metal platform. The bath could be raised and lowered by a manual hoist. The chromatograph column, presaturator, coolant coil, stirrer, heaters, temperature control probe and the thermocouple were suspended from the wooden platform installed directly above the bath, so that the bath could be lowered and raised freely. The connecting tubing was mostly 1/8 inch stainless steel tubing. Also 1/4 inch stainless steel tubings, 1/8 inch and 1/4 inch copper tubings were used.

The Chromatograph Column and Presaturator

The chromatograph columns were made from 1/4 inch OD and 5/32 inch ID copper tubing. Originally, 1/4 inch stainless steel tubing was to be used for this purpose. However, a column made from stainless steel of the required length was found to weigh over 100 grams which was above the weight range of the analytic balance that was used for weighing the column. Since accuracy in weighing the columns was of prime importance, the use of a wider-range less accurate balance might increase the experimental error considerably. The maximum pressure specification for the 1/4 inch copper tubing is 1900 psi with a safety factor of 5. This copper tubing was previously pressure tested at 5000 psi and a room tem-

perature by the Research and Development Laboratory of the College of Engineering and also tested at 1850 psi and 160°F by this investigator.

Since the system pressure could never exceed 1900 psi, it was felt that the use of this type of tubing is well within the safety limits.

The chromatograph column packing was acid washed, 30/60 mesh size firebrick (Varian Aerograph, Catalog No. 82-0128), impregnated with pure n-decane. The liquid load of the stationary phase was about 30% by weight.

The presaturator, the function of which was to saturate the carrier gas with n-decane before it entered the chromatograph column, was made of 1/4 inch OD, 0.049 inch wall thickness stainless steel tubing. The presaturator lengths varied from 35 to 50 inches, depending upon the system temperatures.

The presaturator column was packed with packing identical to that in the chromatograph column.

The Chromatograph Detector

The chromatograph was equipped with a highly sensitive thermal conductivity thermistor cell. The detector cell was designed for high sensitivity gas analysis and for rapid rate of response using two matched thermistors as sensing elements.

The glass coated thermistors had a nominal resistance (at 25°C) of 30,000 ohm each, (manufactured by Victor Engineering Corp., Catalog No. AX1243); each pair of thermistors was matched by the manufacturer. The 0.285 mm bead diameter thermistors were located directly in the gas flow path.

The thermal conductivity cell block was made from 304 stainless

steel and was fabricated by the Research and Development Shop, Phillips Petroleum Company, Bartlesville, Oklahoma.

The drawing of the detector cell is shown in Figure 6. The high sensitivity and rapid response of the thermistor are attributed to its very small volume, and the highly sensitive thermistors located in a through-flow path. The detector cell internal volume is 0.012 cc.

In operation one of the two thermistors senses the carrier stream containing the sample, and the second senses the reference gas stream.

The detector cell was tightly fastened to a thermostated aluminum block by two bolts. The aluminum block was heated by a 30 watt Chromlox cartridge heater supplied by E. L. Wiegand Company (Catalog No. C-202). The thermostated aluminum block is shown in Figure 6. The constant-temperature block was placed in a 7" x 5 1/4" x 4 1/8" galvanized metal box. Pellet-type insulation was fitted between the block and the box walls, (Zonolite, moisture-repellant insulation). The detector was connected to the system by 1/16" OD stainless steel tubing.

Sample Valve for High Pressure Injection

The solute sample was injected into the high pressure carrier gas by a sample valve.

The sample valve was specially designed for high pressure operation. This valve has a sweep-out configuration when it is open to inject the sample. This is accomplished by having the 1/8" tubing by-pass, through which the carrier gas normally flows; the by-pass has much higher flow resistance than the sample cavity between the two valve stems. The volume of the sample cavity is 0.05 cc.

The sample valve was fabricated by Pan American Petroleum Corp.,

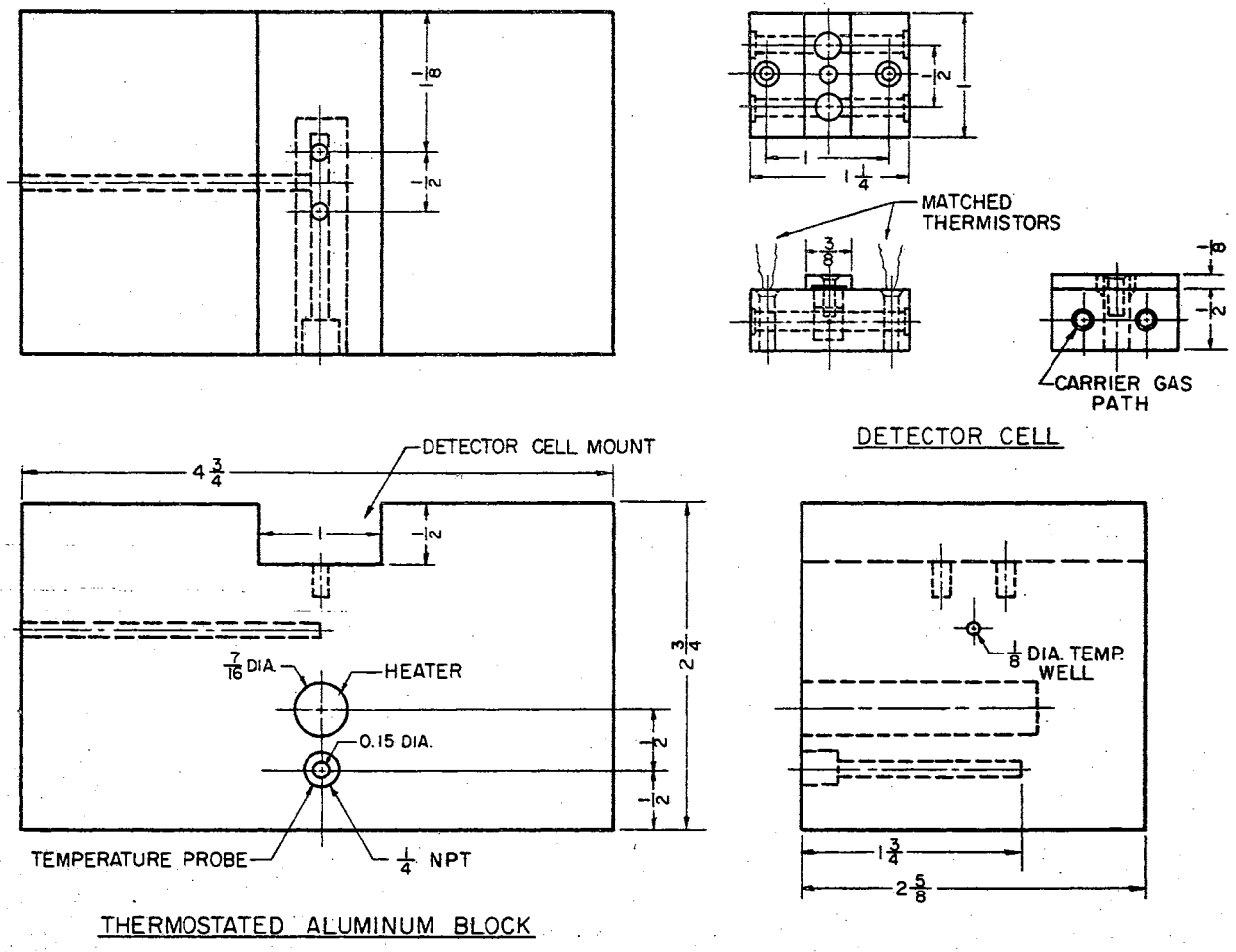

Figure 6. Chromatograph Detector and Detector Thermostated Block

Tulsa, Oklahoma.

The 1/4 inch valve stems and stem fittings were obtained from Autoclave Engineering Company. The valve was charged with sample gas by trapping the gas inside the sample cavity at the desired pressure. The sample loop and the sample cavity were evacuated by a Duo Seal vacuum pump, Model 18185A, manufactured by Welch Scientific Company.

Temperature Control and Measurement

During the course of this experiment, temperature was controlled independently in two different locations; the constant-temperature bath and the detector cell.

The chromatograph column, the presaturator and the reference-side dry column were immersed in the thermostated bath. The bath was a stainless steel, 8.5 inches ID and 18.5 inches deep Dewar cylinder filled with ethylene glycol-water solution. The bath insulation was made of Styrofoam block, in which a cylindrical hole was cut to fit the bath dimensions. Heat was removed from the bath by a 1/3 HP Blue M refrigeration unit (Model: PCC 24A), temperature range of -23°C to ambient. The refrigeration unit was equipped with a temperature control system for maintaining a constant temperature within $\pm$ 0.15 °C. The refrigerator cooling coil was immersed in a well insulated, 12 in. diameter, 26 in. high Pyrex glass cylinder, containing ethylene glycol-water coolant solution. The coolant was continuously stirred by a Lightning Model "F" mixer.

The coolant was circulated through a 1/4 inch copper tubing cooling coil immersed in the bath. The coolant circulation pump was a single stage centrifugal pump driven by a 1/8 HP electrical motor, manufactured

by Eastern Industries, Inc. (Model: DH-11). The pump was connected to the motor by an extended shaft to allow for thermal insulation when pumping cold fluid. The coolant flow rate was adjusted by a valve in the coolant line.

Heat to the bath was supplied by several 250 and 500 watt immersion heaters. The number of heaters used depended on the system temperature. One of the heaters was connected to an 8 amp Powerstat for heat input regulation. The bath fluid was continuously stirred to minimize temperature gradients within the bath. The stirrer shaft held two 2 1/4-inch propellers, 6 inches apart. The stirrer was drived by a 35 watt, 1600 RPM electrical motor supplied by Precision Scientific Company; the motor was connected to a Powerstat for speed adjustment.

The bath temperature was controlled with a Model 1053A Thermotrol temperature controller supplied by Hallikainen Instrument Company. A platinum resistance temperature sensor was used as a sensing probe. The Model 104N96AA temperature probe was supplied by Rosemount Engineering Company.

The temperature of the bath was measured by a calibrated copper-constantan thermocouple which was placed in the middle of the U-shaped GLC column.

The detector unit was heated by a 30 watt 3/8 x 1 9/16 inch Chromlox cartridge heater (Catalog No. C-202). The cartridge heater was placed inside a hole drilled into the aluminum block to which the detector was afixed. The temperature of the detector was controlled by a separate Thermotrol temperature controlled identical to the one used for the thermostated bath. The temperature probe employed for the detector cell was Rosemount Model 104AK temperature sensing probe. The tempera-

ture probe was inserted inside a small hole drilled in the aluminum block for this purpose. The detector unit temperature was measured by a copper constantan thermocouple placed in a temperature well inside the block, (see Figure 6).

The two thermocouples were connected through a selector switch to a Leeds & Northrup potentiometer, Catalog No. 8687. The potentiometer measured the output electromotive force of the thermocouples to a precision of 0.001 mv. The calibration of the thermocouples is given in Appendix C. The ambient temperature was measured by a certified calibrated mercury thermometer.

Pressure and Flow Rate, Control and Measurement

The gases used were contained in high pressure cylinders equipped with two-stage Matheson regulators of different output pressure ranges.

The pressure of the system was measured at the GLC column inlet with a Heise bourdon tube pressure gauge. The pressure gauge was calibrated at the factory; the calibration was checked in this laboratory with a Ruska dead weight gauge. The pressure range of the gauge was 0-2500 psi, with 2 psi subdivision. The pressure could be recorded with a precision of 1 psi.

The system pressure was controlled by two ballast-loaded pressure regulators. The first stage of the pressure control was a high precision Hoke, Model 521B20 ballast-loaded pressure regulator. The second control stage was a Mity-Mite, Model 94 ballast-loaded regulator, manufactured by Grove Regulator Company. Both regulators were upstream of the column and were connected in series. The reason for using two regulators was to eliminate flow-rate drift during the sample elution, since changes

in flow rate during the sample elution could not be tolerated. The use of two regulators in series often caused short-term pressure fluctuation (relative to the retention time). To overcome this problem, a 15 inch capillary tubing was inserted between the second regulator outlet and the system. The resultant high resistance to flow damped the pressure fluctuations.

The main gas stream was split into two streams, the carrier gas stream or the sample stream, and the reference stream. A column filled with dry solid support was introduced into the reference gas line in order to balance the extra resistance to flow caused by the GLC column and presaturator in the carrier gas line.

The flow rate was controlled by two metering valves. The valves, Whitey micrometer flow control valves, had 0.020 inch orifices and very slightly tapered stems for precise control of small flow rates. The valves were equipped with vernier micrometer handles to permit precise and repeatable flow control setting. The gas flow rate was measured by a 50 cc soap bubble flow meter, the volume of which had been previously calibrated by mercury. The timer used for measuring flow rates was a Model K 15110 electrical stop-clock manufactured by A. W. Haydon Company. The precision of this timer was 0.01 second. The reference gas flow rate was carefully controlled, but an accurate measurement of the latter was not essential.

Flow rates were monitored using two orifice meters equipped with glass manometers containing iodine-dyed triethylene glycol. The manometers were observed by a cathetometer fitted with a telescope, manufactured by Gaerter Scientific Corp. The gas streams were diverted from the soap bubble meters to the orifice meters by two 3-way glass stop-

cocks.

Tygon tubing connected the gas line to a one-gallon surge tank before being discharged into a vented laboratory hood. The surge tank was introduced in order to eliminate the small fluctuation in flow caused by the hood fan.

The pressure in the sample loop, i.e., the pressure at which the gas sample was trapped, was measured by mercury manometer.

Atmospheric pressure was measured by a barometer.

Electronic Components and Circuits

The output signal from the detector was fed into a Minneapolis-Honeywell recorder for a visual representation of the chromatogram. The recorder had 1 mv full scale deflection. A modified F & M Wheatstone bridge was used in the chromatograph circuit. The ratio between the resistances of the bridge arms was altered to be compatible with the two 30,000 ohm thermistors and to achieve maximum sensitivity and stability of the bridge output.

The current for the Wheatstone bridge was supplied by two 12-volt storage batteries. Storage batteries were chosen because of their current stability and because they are rugged and economical. The batteries were recharged every two weeks for optimum performance.

The milliameter in series with each thermistor measured the current through the thermistor. A high impedence voltmeter, (Triplet Model 850, Electronic volt-meter) was used to measure the voltage across each thermistor. The power dissipation of a thermistor was calculated from measurements of the current and voltage drop. The maximum power rating for the thermistor used was 14 mw at 25^{o}C and decreased linearly to zero

at 200 ^{o}C.

All electronic components were grounded according to ASTM specifications and all electrical lines were elctrically shielded.

Filter capacitors (0.25 MF, 150 vdc) were connected between the recorder terminal and the ground in order to protect the recorder from AC stray voltage.

Chemicals

The chemicals used in this study were: helium, neon, nitrogen, argon, carbon dioxide, methane, ethylene, propane, n-butane and n-decane.

The specification for these chemicals and the suppliers are listed below.

Material	Min. purity Mole %	Grade	Supplier
Helium	99.995	high purity	Airco
Neon	99.995	research	Matheson Co.
Nitrogen	99.7	bone dry	Airco
Argon	99.998	purified	Matheson Co.
Carbon Dioxide	99.8	bone dry	Matheson Co.
Methane	99.05	instrument	Phillips Petroleum Co.
Ethylene	99.99	research	Phillips Petroleum Co.
Propane	99.97	research	Phillips Petroleum Co.
N-butane	99.93	research	Phillips Petroleum Co.
N-decane	99	pure	Phillips Petroleum Co.

CHAPTER V

EXPERIMENTAL PROCEDURE

The Partial Volume Experiment

The basic equation for calculating partial volumes at infinite dilution using the injection method is given by Eq. (3-1). The derivative in Eq. (3-1) can be expressed by

$$\left(\frac{\partial P}{\partial n_j}\right)_{T,V,n_k} = \lim_{\Delta n_j \to o} \left(\frac{\Delta P}{\Delta n_j}\right)_{T,V,n_k} \tag{5-1}$$

The expression on the right hand side of Eq. (5-1) is related to experimentally observed quantities by

$$\left(\frac{\Delta P}{\Delta n_j}\right)_{T,V,n_k} = \frac{ke_i}{\frac{V}{RT}\sum_i \left(\frac{\pi_i}{Z_i}\right)} \tag{5-2}$$

where e_i is the pressure transducer output resulting from the i's injection of Δn moles of gas j; π_i is the injection pressure, i.e., the pressure in the gas burette; k is the transducer sensitivity, Z_i is the compressibility factor of the injected gas at pressure π_i and temperature T. The pressure transducer sensitivity k, in Eq. (5-2) is common to both derivatives in Eq. (3-1); it is, therefore, cancelled upon substitution. This cancellation eliminates the necessity of carrying out tedious calibrations of the pressure transducer to determine the value of k for each temperature and pressure condition.

A preliminary experiment described in the next chapter established

that the response of the pressure transducer to successive injections is linear in the differential pressure range employed during the experiment. This means that the transducer output due to injection of a gas sample can be taken as an average of two or more successive injections of this gas.

The injections were started with the use of low pressure solvent gas in the gas burette, (see Figure 4). Two injections of each gas were made in a regular run, (n = 2 in Eq. (5-2)). First the denominator of Eq. (3-1) was evaluated according to Eq. (5-2). The gas burette was then filled two successive times with solute gas. The latter results were used in Eq. (5-2) for the evaluation of the numerator of Eq. (3-1). The system pressure differed from the initial filling pressure of the main pressure vessel by the differential pressure developed as a result of the successive injections up to the end of the solvent gas injection.

The experimental procedure used by Hensel (34) was modified. The most significant modifications were made to eliminate gas from being trapped inside the valves and the mercury pump cylinder, to improve temperature control, to measure the pressure of the solute gas more accurately and to improve mixing of solute and solvent gases. For detailed description of the experimental procedure the reader is referred to Kate (44).

The Gas-Liquid Chromatography Experiment

The basic equations for determining K-values from chromatography elution data are given by Eq. (3-36) and Eq. (3-37),

$$K_i = \frac{W_L^{\,o}}{(1-x_1)\,\rho_G (V_{R_i} - V_G)} \qquad (3\text{-}36)$$

and

$$V_{R_i} = t_{R_i} f_a \left(\frac{P_a}{P}\right)\left(\frac{T}{T_a}\right) Z_G \qquad (3\text{-}37)$$

Of the experimental parameters in these equations, the following were determined experimentally in the present study:

- P - system pressure
- T - system temperature
- W_i - total moles of pure liquid contained in the GLC column
- f_a - flow rate of the carrier gas
- t_{R_i} - retention time of solute i
- T_a - ambient temperature
- P_a - ambient pressure

The value of the parameters ρ_G, x_1 and Z_G were obtained from literature sources.

The experimental procedure and techniques used to obtain the parameters listed above are described below.

General

All the tubing, valves and fittings used in the experimental apparatus had been thoroughly washed in a Sonogen ultra sonic cleaner containing cleanser solution and by acetone solvent to remove traces of oil and grease.

All the lines had been flushed by flowing carrier gas through them for a few hours.

All joints were sealed tightly and the system was pressure tested.

Preparation of Column Support

A pre-weighed amount of firebrick solid support was mixed with pure

n-decane in a beaker by a glass rod until a homogeneous slurry was formed. The slurry was allowed to stay for a hour or more in a sealed desiccator, the slurry being mixed from time to time. The excess liquid was then boiled off under vacuum, using a vacuum pump connected to the desiccator.

The vacuum pump was disconnected frequently and the slurry was stirred and weighed. This procedure was repeated until a liquid load of 27-30% by weight was obtained. The wet support was then tightly sealed into bottles.

Preparation of the Column and Presaturator

The Column: As can be seen from Eq. (3-36), any error in determining W_L^o will result in an error in the calculated K-value; therefore, extreme care was taken in preparing the GLC column.

To make the column, 1/4 inch copper tubing was cut to the proper length, thoroughly washed with acetone and dried. The column was then equipped with fittings and rubber caps on both sides and weighed along with a small amount of glass wool that was later used for plugging the column ends. The column was then rewashed, redried and reweighed until two successive weights agreed within 0.1 mg. After that, one end of the column was plugged by part of the pre-weighed glass wool and capped with the rubber cap. The column then was fastened to a laboratory stand and filled with the packing material using a small glass funnel connected to the column by plastic tubing.

During the packing of the column small portions of the material were placed in a small pre-weighed weighing bottle and tightly sealed. These samples were to represent the packing material used for the column. An electrical vibrator was employed to ensure uniformity in packing.

After the column was full, its other end was plugged with the remainder of the glass wool, capped with the rubber cap, bent into a U-shape and weighed. The difference between full and tare weights of the column determined the weight of the packing.

The weighing bottle containing the sample of the wet packing material sample was weighed and then the liquid decane was boiled off under vacuum for about 8 hours in a desiccator containing silica gel until two successive weights of the dry solid agreed within 0.1 mg. The weight was not corrected for bouyancy since this correction proved negligible.

The weight fraction (wet basis) of liquid was calculated by the following relation:

$$\text{wt. fraction of liquid} = \frac{\text{(wet solid wt.)} - \text{(dry solid wt.)}}{\text{(wet solid wt.)} - \text{(empty weighing bottle)}}$$

The number of moles of liquid in the column was calculated by,

$$W_L^o = \frac{[\text{(wt. of packed column)} - \text{(wt. of empty column)}]\text{(wt. fraction of liquid)}}{\text{(molecular wt. of liquid)}}$$

After the packed column was weighed, the two rubber caps were removed and placed in a sealed bottle, and the column was immediately connected to the system by Swagelok union fittings. The length of the column varied from 15 to 18 inches.

The Presaturator: The function of the presaturator is to saturate the carrier with the stationary liquid before it enters the column, thus minimizing the losses of the stationary liquid. Column bleeding is even troublesome in analytical chromatography where it causes an irregular baseline shifting. But in vapor-liquid equilibrium chromatography, the column bleeding would not only cause experimental difficulties, but will also cause an error in the calculated K-value as is evident from Eq.

(3-36). Furthermore, it is more practical experimentally to change the presaturator during an experimental run than to change the chromatograph column.

The presaturator was prepared using the same procedure used for the GLC column with the exception that the exact amount of liquid load of the packing was not determined.

A preliminary experiment was conducted to determine the number of presaturators to be used for each isotherm to ensure that no liquid evaporated from the GLC column. The test run was performed at 160°F, which was 10°F above the maximum temperature used in this experiment. Methane carrier gas was flowing through a 50 inch long presaturator and 17 inch long column for nine hours at a flow rate of about 55 ml/min. The liquid losses in the column were found to be negligible.

Based upon this experiment the following procedure for replacing of the presaturators was adopted:

Isotherm-°F	presaturator length-inch	number of presaturator per isotherm
150	50	4
125	50	3
100	45	3
70	45	3
40	40	3
10	40	2

The chromatograph column was sealed off from the rest of the system during the replacement of the presaturator.

After an isotherm was concluded, the GLC column was disconnected from the system and the two ends of the column were immediately sealed using the rubber caps that had been originally used for capping the column. The column was thoroughly washed with acetone, dried, and weighed several times until two successive weighings agreed within 0.1 mg. The final column weight was compared with the original weight. A change in column weight greater than 0.1 mg was attributed to a change in liquid content in the column. Experimental runs were disregarded when the change in weight exceeded 0.1 mg.

Temperature Control and Measurement

The temperatures measured during the course of this experiment were: system temperature, detector cell temperature and ambient temperature. The temperatures controlled were the former two.

The system temperature was maintained at the desired value by the Hallikainen proportional temperature control within $\pm$ 0.04 ^{o}F and was measured by a copper constantan thermocouple.

The temperature of the detector cell was set to a value slightly higher than that of the system. It was also controlled by a Hallikainen unit and measured by a copper constantan thermocouple.

A good indication of temperature stability was the stability of the chromatograph base line. However, the base line was more sensitive to fluctuation in the detector cell temperature than that of the GLC column.

Pressure Control and Measurement

The pressure of the system was measured at the inlet to the chromatograph column. The pressure was reduced to essentially atmospheric pressure by expansion of the carrier gas through a needle valve at the column outlet. The highest system pressure was 1750 psia and the lowest was 100 psia.

Pressure drop along the column was negligible, (e.g. Stalkup (93) reported a pressure drop of 0.3 psi at column pressure of 41.3 psia using a column of smaller diameter and four times the length of those used in the present study).

The accuracy of the Heise gauge was 0.1% of full scale (2500 psi).

The system pressure and the reference gas pressure were reduced to atmospheric before entering the detector by a Ruska micrometer needle valve and Nupro needle valve respectively. The pressure at the detector was essentially atmospheric. The atmospheric pressure was measured by a barometer to the nearest 0.1 mm Hg.

Flow Rate Control and Measurement

The special characteristics of the detector cell, such as its very small volume, the through-flow configuration and the small, highly sensitive thermistors increased the chromatograph sensing capability. However, these features of the detector also augment the sensitivity of the chromatograph to other experimental variables, the most problematic of these being the flow rate.

The flow rates were determined by measuring the time for a soap film to travel between two reference marks on the bubble meter.

Only the carrier gas flow rate was accurately measured and recorded.

The reference gas stream flow was kept as close as possible to that of the carrier, but was not recorded since its value did not enter any of the calculations. Both flows were kept constant for each pressure. Higher flow rates were used for higher pressures, but the increase in flow rate was not proportional to the increase in pressure. The flows ranged from 30 ml/min to 130 ml/min at ambient conditions.

The carrier gas flow rate measurement took place during the solute elution, i.e., between solute injection and the appearance of solute peak on the recorder chart. For solutes with long retention time two or three measurements were taken depending upon the retention time.

The expansion valves and the metering valves were slightly heated by a heating tape to prevent the n-decane from condensing inside the metering valve as a result of the carrier gas expansion. Otherwise n-decane condensate accumulated inside the metering valves and caused periodic deflection of the recorder pen resulting from the disturbance to flow.

The stability of the detector output signal when no solute injection took place served as a criteria for steady-state conditions of the chromatographic system.

Sample Trapping and Injection

The solute gases were stored under pressure in cylinders equipped with pressure regulators and connected to the sample manifold. The outlet of the sample manifold was connected to the inlet of the sample loop. The latter contained the sample valve and was connected to a vacuum pump and a mercury manometer.

The procedure for trapping a sample involved the following steps:

1. Evacuating the sample loop.
2. Flushing the sample loop twice by filling it with the solute gas to be injected at a pressure of about 30 psia and re-evacuating.
3. Charging the solute gas into the sample loop at the desired pressure. The charging pressures varied from 2 inches of mercury for the lowest system pressure up to 32 inches of mercury for the highest system pressure.
4. Trapping the solute gas inside the sample cavity by sealing the cavity off from the sample loop after the desired pressure of solute was established. The sample cavity was sealed by tightening two of the four stems of the sample valve.
5. Injecting the solute sample into the high pressure carrier gas stream by rapidly opening the two sample auxiliary valves and thus connecting the sample cavity to the carrier gas line.

Each solute was injected twice for each of the system pressures.

Evaluation of Optimum Thermistor Response

One of the methods for evaluating optimum thermistor response involves plotting the power dissipation in the thermistor versus response (9). The power dissipation of a thermistor is equal to the product of the current through it and the voltage drop across the thermistor.

The following experiment was conducted to establish the thermistor optimum power for a maximum response. The bridge voltage was set to a low value after methane gas was flowing through the column at a constant flow rate. The voltage across the thermistor was measured by placing a high impedence voltmeter across the thermistor. The current was determined by a millimeter connected in series with the thermistor. A helium

sample was then injected into the carrier gas and the height of the resulting peak was recorded. The bridge voltage was then slightly increased and the measurements discussed above were repeated using the same amount of sample, until the thermistor power reached the maximum power rating (14 mw at 25 ^{o}C).

The optimum bridge voltage was determined by plotting the peak height against power dissipation.

The results of this experiment are shown in Appendix D.

Retention Time Measurement

The time lapse between the sample injection into the carrier gas and the visual detection of the elution peak on the recorder chart was taken as the retention time. The response time of the electronic system and the detector cell had no effect on the calculated K-values since it cancelled out, as can be seen from the term $(V_{R_i} - V_G)$ in Eq. (3-36).

The retention time was measured by an electrical stop-clock with subdivision of 1/100 of a second and a cycle of one minute. An auxiliary stop-clock was also used for retention times over one minute.

A series of tests performed in this laboratory indicated that the reaction time of a trained observer, i.e., the time lapse between seeing the elution peak on the recorder chart and pressing the clock switch, varied between $\pm$ 0.02 seconds to $\pm$ 0.04 seconds providing the observer was well aware of and expected the type of occurrence he was supposed to observe.

CHAPTER VI

EXPERIMENTAL RESULTS

In this chapter, the experimental results obtained during the course of this work are presented in tabulated and graphical forms. Appendix G contains the measured data from which the results reported here were obtained. The accuracy of the data is assessed in Chapter VII. The experimental results presented in this chapter are also analyzed, discussed and correlated in Chapter VII.

The Partial Volume Experiment

A preliminary experiment was performed in the partial volume equipment in which a larger than usual number of solute as well as solvent injections was carried out in order to observe the response of the system. Methane was charged into the main vessel at an initial filling pressure of 1000±2 psia, and a temperature of 100°F. Seven injections of methane were followed by nine injections of carbon dioxide. The emf values observed after the successive injections are shown in Figure 7.

Table I shows the volume ratios, $\bar{V}_2^{\infty}/\tilde{V}_1$, and partial compressibility factors, $\bar{\mathcal{Z}}^{\infty}$, at conditions of infinite dilution of carbon dioxide in methane at 100° and 150°F. Table II shows the volume ratios, $\bar{V}_2^{\infty}/\tilde{V}_1$, and partial compressibility factors, $\bar{\mathcal{Z}}^{\infty}$, at conditions of infinite dilution of methane in carbon dioxide at 150°F. The compressibility factors

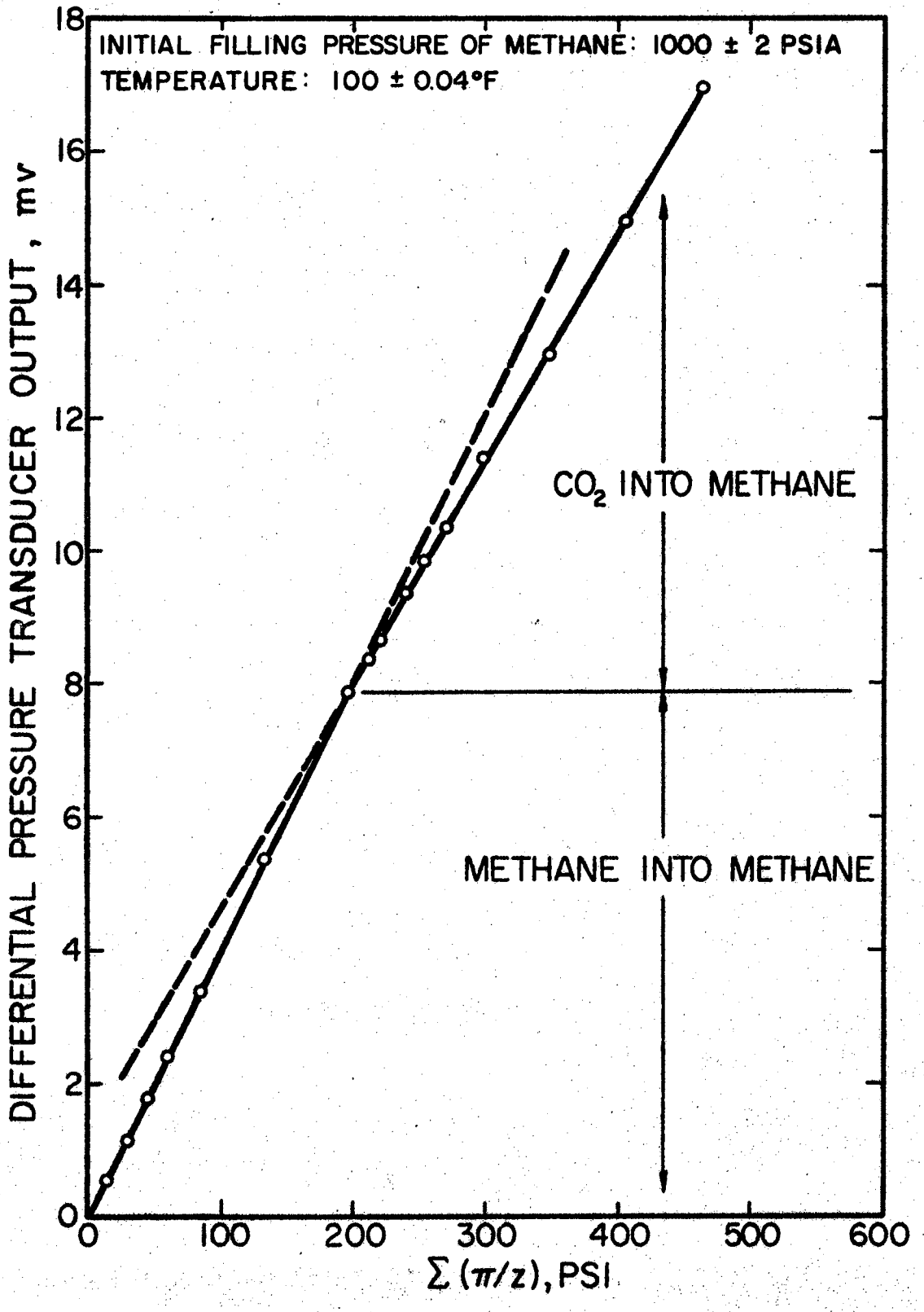

Figure 7. Response of the System to Successive Injections

TABLE I

INFINITE DILUTION PARTIAL VOLUMES OF
CARBON DIOXIDE (2) IN METHANE (1)

Temp. °F	Pressure, psia	$\bar{V}_2^\infty/\tilde{V}_1$	$\bar{Z}_2^\infty$
100±0.04	252	0.960	0.940
	495	0.913	0.868
	767	0.861	0.795
	1040	0.816	0.738
	1280	0.786	0.698
	1501	0.755	0.657
	2005	0.708	0.604
150±0.04	266	0.988	0.970
	518	0.966	0.933
	736	0.945	0.903
	1025	0.917	0.853
	1511	0.851	0.781
	1997	0.786	0.711

TABLE II

INFINITE DILUTION PARTIAL VOLUMES OF
METHANE (2) IN CARBON DIOXIDE (1)
AT 150 ± 0.04°F

Pressure, psia	$\overline{V}_2^\infty/\tilde{V}_1$	$\overline{Z}_2^\infty$
265	1.116	1.052
506	1.221	1.102
1019	1.642	1.215
1512	2.266	1.326
1811	2.785	1.375
1997	3.128	1.433

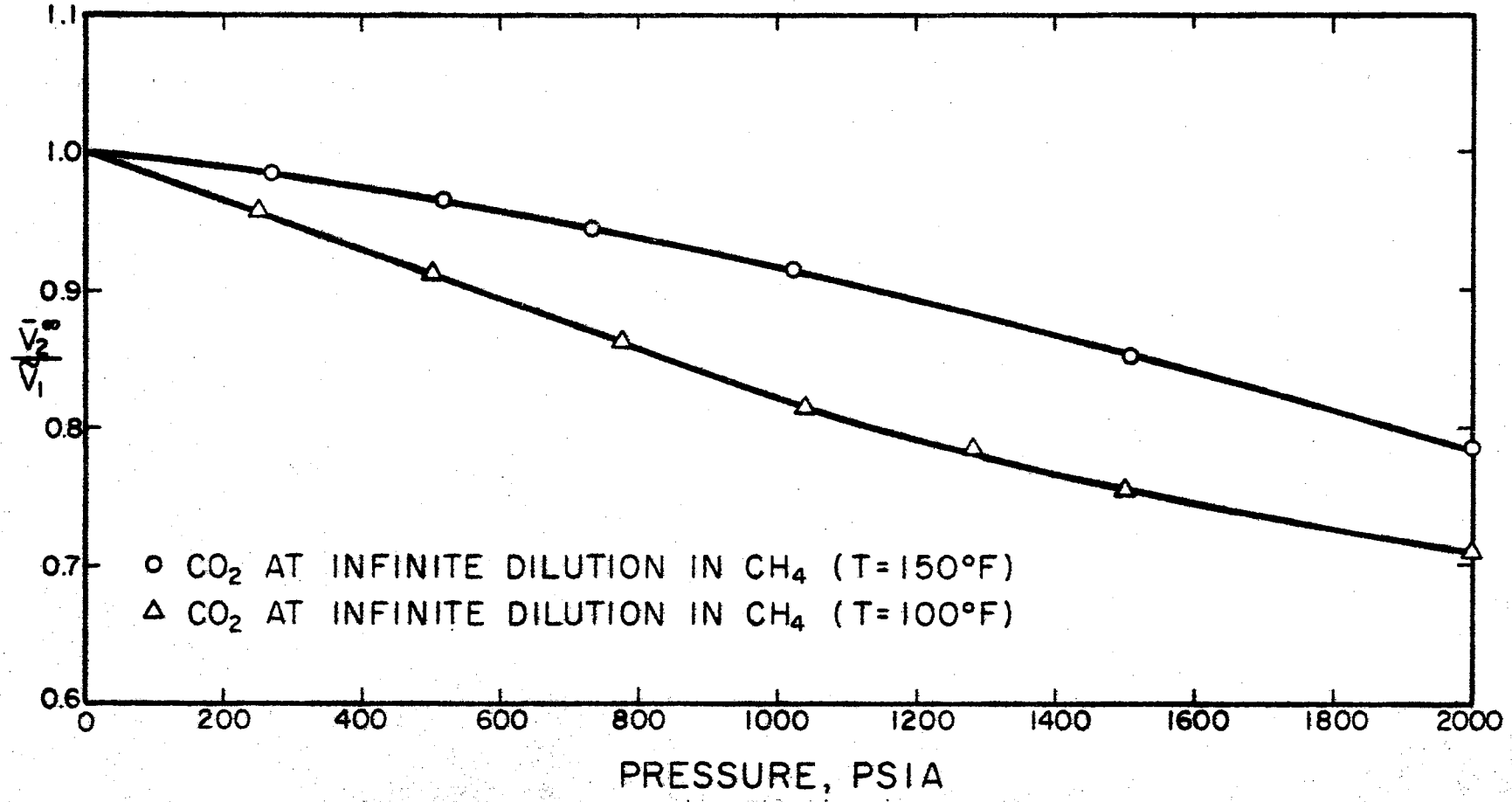

Figure 8. Volume Ratios of Carbon Dioxide at Infinite Dilution in Methane

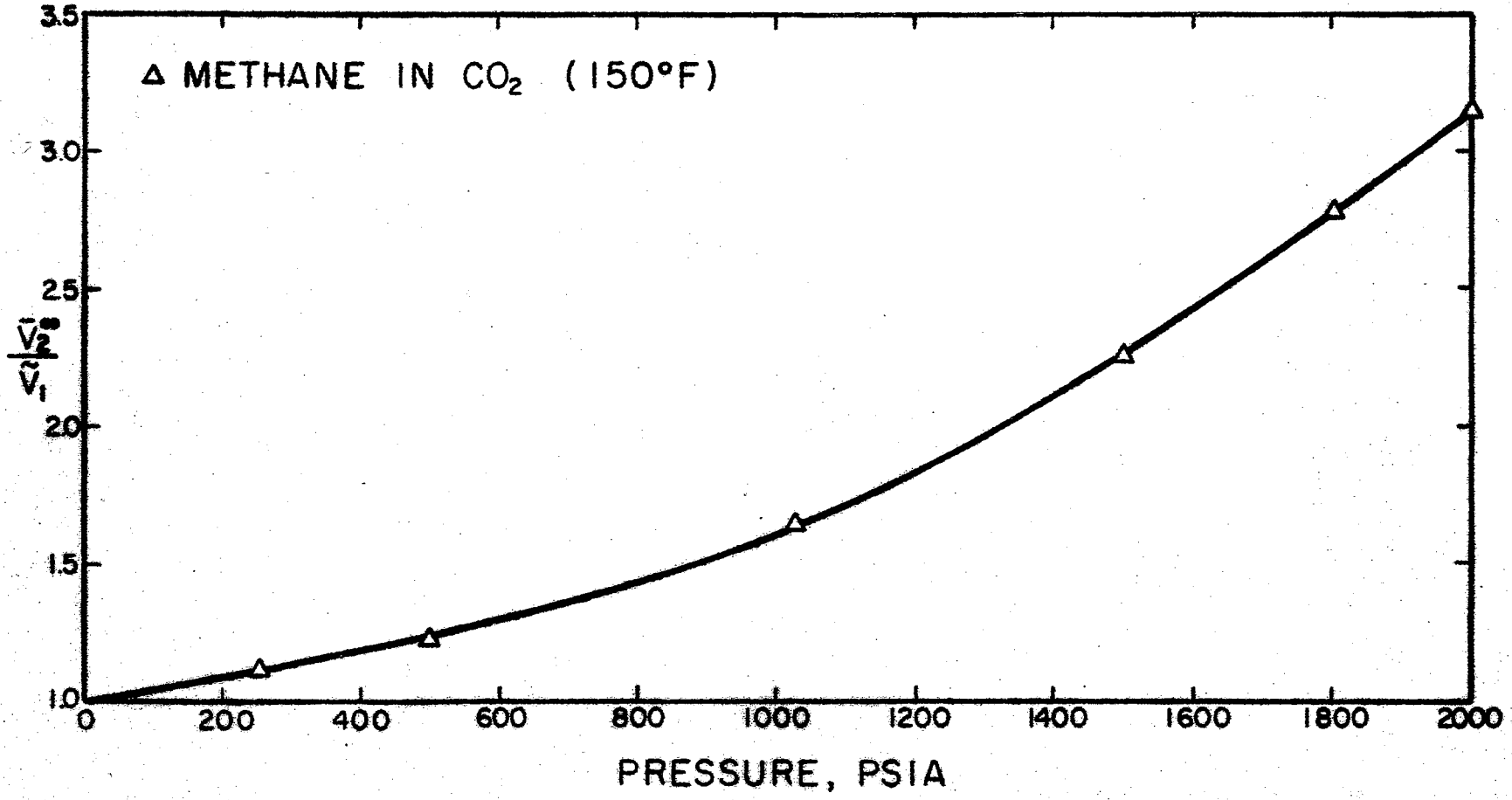

Figure 9. Volume Ratios of Methane at Infinite Dilution in Carbon Dioxide

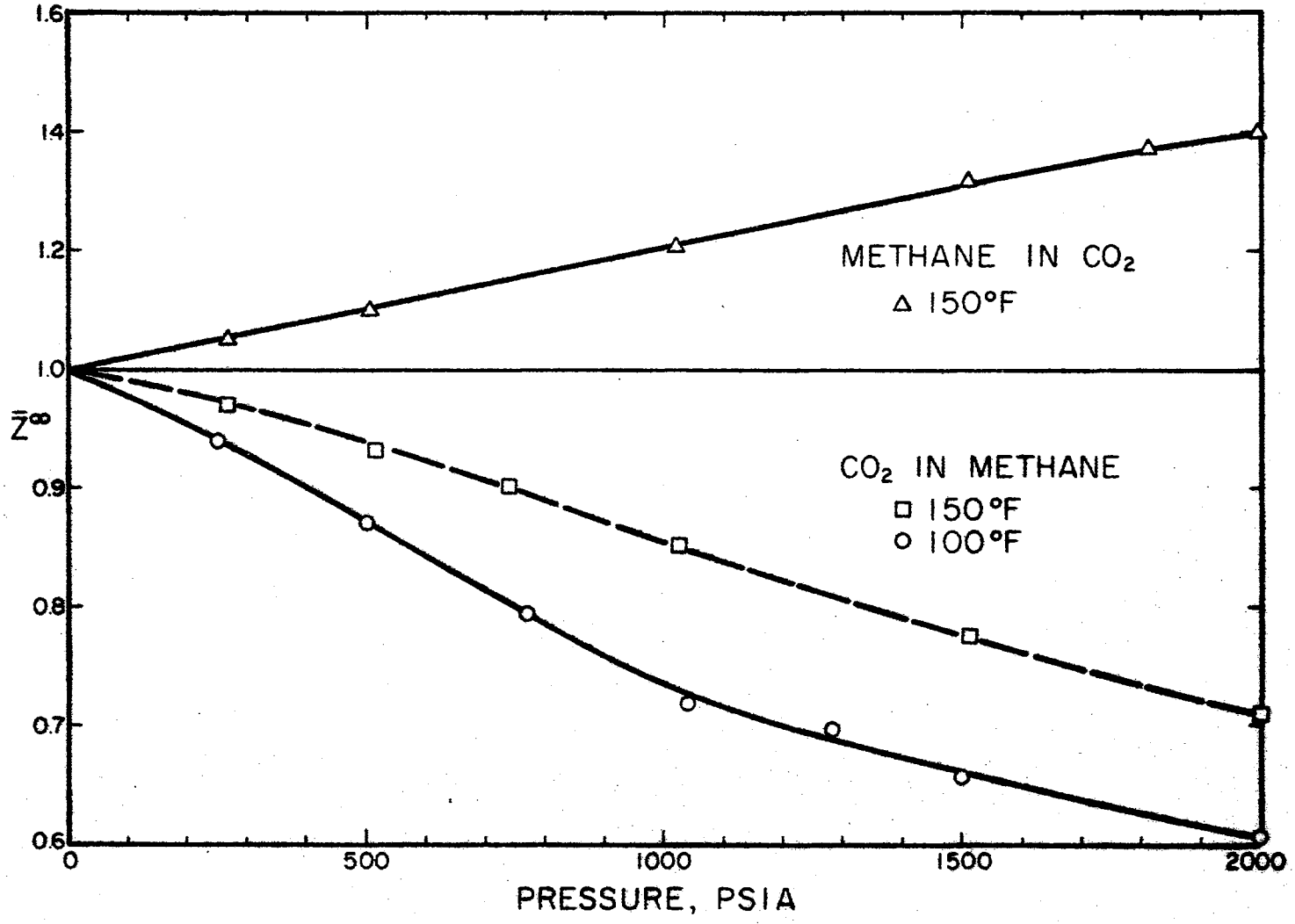

Figure 10. Partial Compressibility Factors at Infinite Dilution

at infinite dilution were calculated from the experimental volume ratio data using pure component molal volumes available in the literature (87,88). The experimental results tabulated in Tables I and II are illustrated in Figures 8, 9, and 10.

The Gas-Liquid Chromatography Experiment

A preliminary experiment was performed as a check of the reliability of the chromatographic apparatus and procedure employed; K-values of n-butane at infinite dilution in the methane-n-decane system were determined chromatographically at 160°F and compared with literature values (87) determined by classical methods. The results of this experiment are shown in Table III.

TABLE III

K-VALUES OF N-BUTANE AT INFINITE DILUTION IN THE METHANE N-DECANE SYSTEM AT 160°F

	K-Values		
Pressure, psia	Sage and Lacey (87)	This Work	% Deviation
300	*0.2815	0.279	0.90
400	0.2725	0.270	0.93
600	0.2450	0.242	1.24
800	0.2315	0.230	0.65
1000	0.2260	0.224	0.89
		Absolute Average % Deviation:	0.92

*Extrapolated by this author

% Deviation = $(K_{SL} - K_{exp.}) \cdot 100/K_{exp.}$

The experimental K-values of five systems are listed in Table IV through Table VIII. Each table presents vapor-liquid equilibrium constants of a solute at infinite dilution in the methane-n-decane system at six isotherms and pressures from 100 up to 1750 psia. The five solutes are:

carbon dioxide - Table IV

nitrogen - Table V

argon - Table VI

ethylene - Table VII

propane - Table VIII

The K-values were calculated from chromatographic elution data via Eq. (3-36). Densities of methane gas and solubility of methane in n-decane were obtained from literature sources (6, 52, 83, 87, 101). In addition to the retention volumes of the five solutes listed above, the retention volumes of two other solute gases, namely, helium and neon, were recorded at each pressure and temperature. The free gas volume in the GLC column, V_G, at a given pressure and temperature condition was determined by extrapolating the retention volumes of helium, neon and argon according to the extrapolation scheme discussed in section B of Chapter III. The extrapolation was performed numerically using a least square fitting technique.

In Figures 11 through 16 the K-values tabulated in Tables IV through VIII are plotted isothermally for the five ternary systems.

Figures 17 through 22 show plots of K-values as a function of reciprocal temperature at different isobars.

TABLE IV

K-VALUES OF CARBON DIOXIDE AT INFINITE DILUTION IN THE METHANE-N-DECANE SYSTEM

Pressure, psia	Temperature 10°F	40°F	70°F	100°F	125°F	150°F
100	7.252	9.563	11.92	14.51	16.95	19.21
200	3.781	4.819	6.064	7.271	8.539	9.841
300	2.602	3.322	4.123	4.933	5.725	6.431
400	2.106	2.648	3.210	3.837	4.308	4.791
500	1.781	2.157	2.645	---	3.556	3.985
600	1.524	1.906	2.318	2.691	3.035	3.257
700	1.361	1.717	2.052	---	2.651	2.885
800	1.263	1.581	1.874	2.146	2.352	2.525
1000	1.084	1.351	1.601	1.835	1.975	2.123
1250	0.933	1.204	1.385	1.522	1.687	1.801
1500	0.862	1.162	1.274	1.379	1.481	1.584
1750	0.818	1.123	1.218	1.289	1.373	1.475

TABLE V

K-VALUES OF NITROGEN AT INFINITE DILUTION IN THE METHANE-N-DECANE SYSTEM

Pressure, psia	Temperature 10°F	40°F	70°F	100°F	125°F	150°F
100	67.52	76.26	86.34	95.58	91.70	80.23
200	32.86	38.08	43.03	47.32	45.31	40.11
300	21.54	24.46	27.50	32.33	29.67	26.43
400	15.26	17.60	21.63	23.43	20.63	18.55
500	11.75	14.49	15.79	---	16.35	15.74
600	10.38	11.90	13.06	14.74	14.43	13.24
700	8.807	9.502	11.65	---	11.57	10.43
800	7.301	8.247	9.828	11.42	10.36	8.802
1000	5.813	6.326	7.701	8.303	7.609	7.448
1250	4.453	5.304	5.654	6.625	6.188	5.413
1500	3.835	4.306	4.579	5.556	4.701	4.561
1750	3.047	3.389	3.950	4.647	4.248	3.885

TABLE VI

K-VALUES OF ARGON AT INFINITE DILUTION IN THE METHANE-N-DECANE SYSTEM

Pressure, psia	Temperature 10°F	40°F	70°F	100°F	125°F	150°F
100	57.34	65.63	73.68	82.10	88.79	96.31
200	28.01	32.19	36.26	40.33	43.72	47.80
300	18.90	20.52	23.75	27.03	28.58	30.05
400	14.53	15.84	17.22	19.53	21.49	23.06
500	11.36	12.16	13.55	---	16.48	17.81
600	9.140	10.48	11.08	12.26	13.76	14.53
700	7.947	8.608	9.615	---	11.40	12.14
800	6.877	7.401	8.457	9.045	10.11	10.77
1000	5.632	5.828	6.481	7.201	7.625	8.203
1250	4.325	4.609	5.242	5.522	5.988	6.384
1500	3.520	3.909	4.195	4.622	4.806	5.249
1750	2.477	3.304	3.500	3.747	4.119	4.387

TABLE VII

K-VALUES OF ETHYLENE AT INFINITE DILUTION IN THE METHANE-N-DECANE SYSTEM

Pressure, psia	Temperature 10°F	40°F	70°F	100°F	125°F	150°F
100	3.543	4.825	6.330	8.207	9.804	11.55
200	2.030	2.601	3.330	4.206	4.953	5.635
300	1.474	1.843	2.301	2.848	3.258	3.694
400	1.196	1.484	1.810	2.184	2.506	2.792
500	1.022	1.250	1.501	---	1.975	2.228
600	0.894	1.101	1.305	1.524	1.720	1.906
700	0.814	0.985	1.156	---	1.515	1.644
800	0.756	0.906	1.032	1.213	1.348	1.432
1000	0.661	0.797	0.894	1.037	1.130	1.207
1250	0.601	0.713	0.788	0.896	0.973	1.021
1500	0.569	0.660	0.730	0.811	0.871	0.906
1750	0.561	0.636	0.699	0.761	0.813	0.845

TABLE VIII

K-VALUES OF PROPANE AT INFINITE DILUTION IN THE METHANE-N-DECANE SYSTEM

Pressure, psia	Temperature 10°F	40°F	70°F	100°F	125°F	150°F
100	0.495	0.791	1.179	1.715	2.254	2.852
200	0.273	0.426	0.626	0.869	1.134	1.390
300	0.208	0.307	0.452	0.634	0.811	1.022
400	0.175	0.258	0.373	0.523	0.658	0.802
500	0.166	0.226	0.332	---	0.551	0.674
600	0.152	0.207	0.292	0.394	0.483	0.600
700	0.151	0.196	0.277	---	0.439	0.551
800	0.151	0.193	0.255	0.333	0.403	0.486
1000	0.155	0.192	0.245	0.306	0.367	0.431
1250	0.165	0.194	0.241	0.291	0.350	0.395
1500	0.177	0.203	0.248	0.288	0.341	0.383
1750	0.195	0.214	0.251	0.290	0.339	0.377

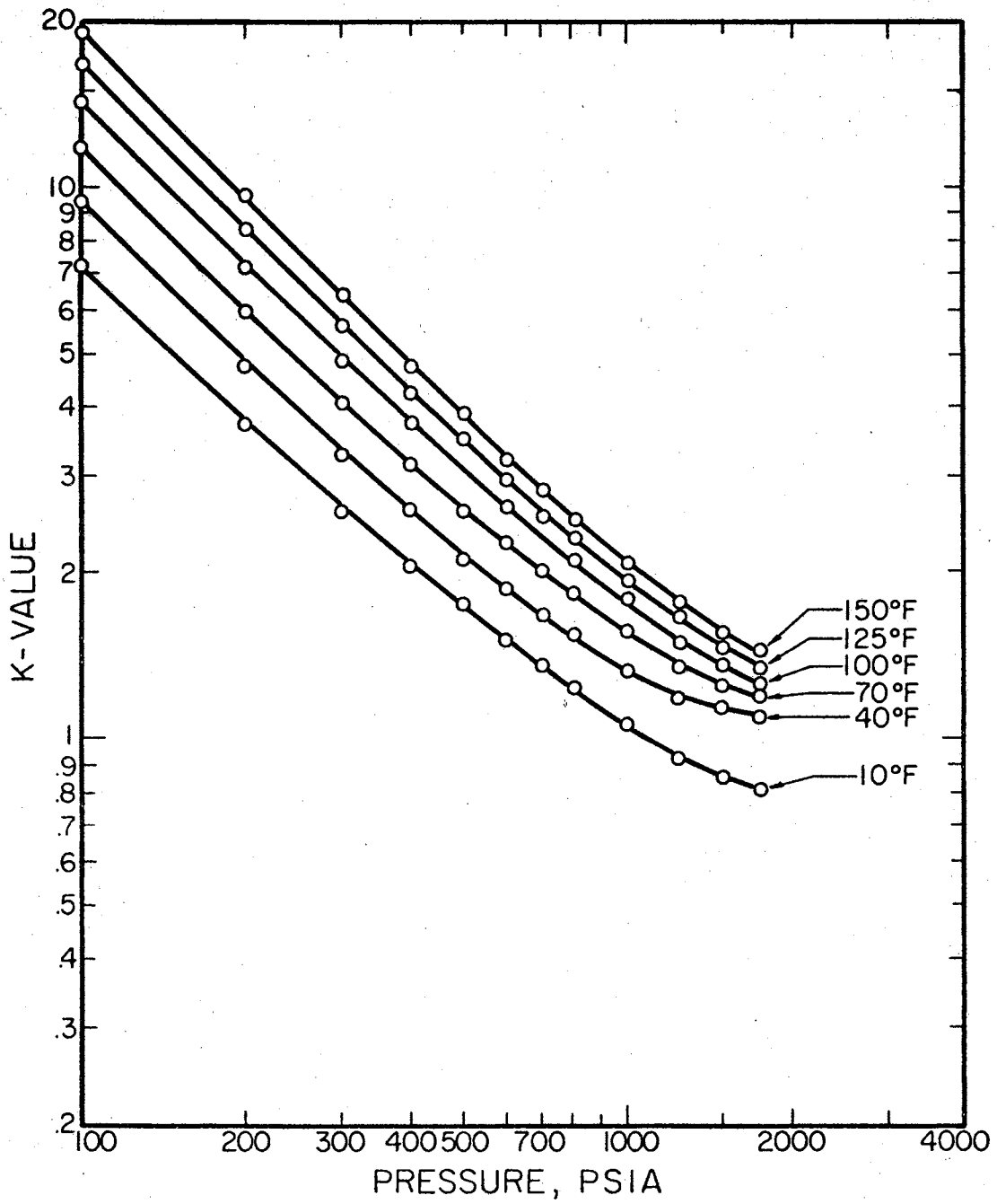

Figure 11. K-Values for Carbon Dioxide at Infinite Dilution in the Methane-n-Decane System

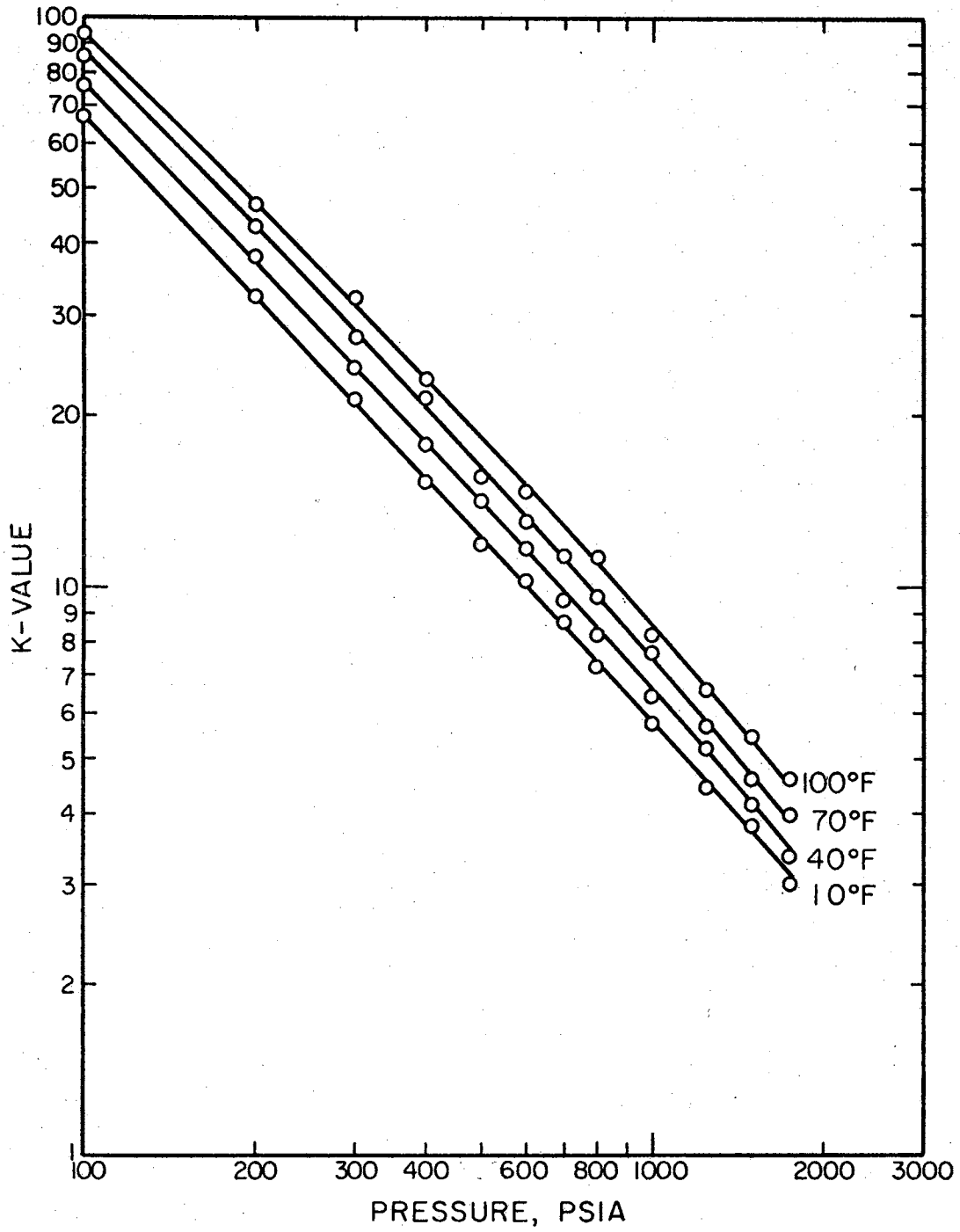

Figure 12. K-Values for Nitrogen at Infinite Dilution in the Mechane-n-Decane System

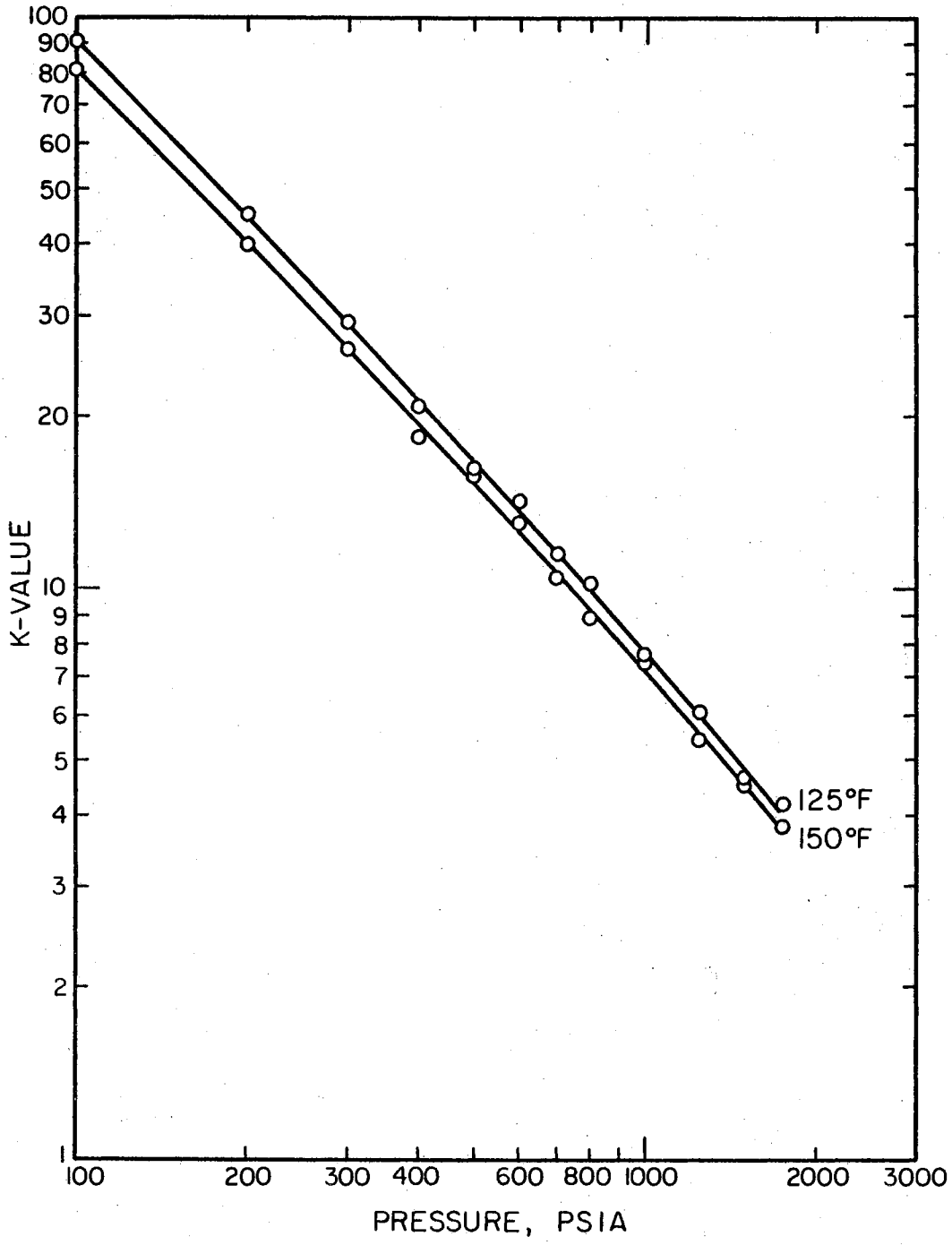

Figure 13. K-Values for Nitrogen at Infinite Dilution in the Methane-n-Decane System, High Temperature Range

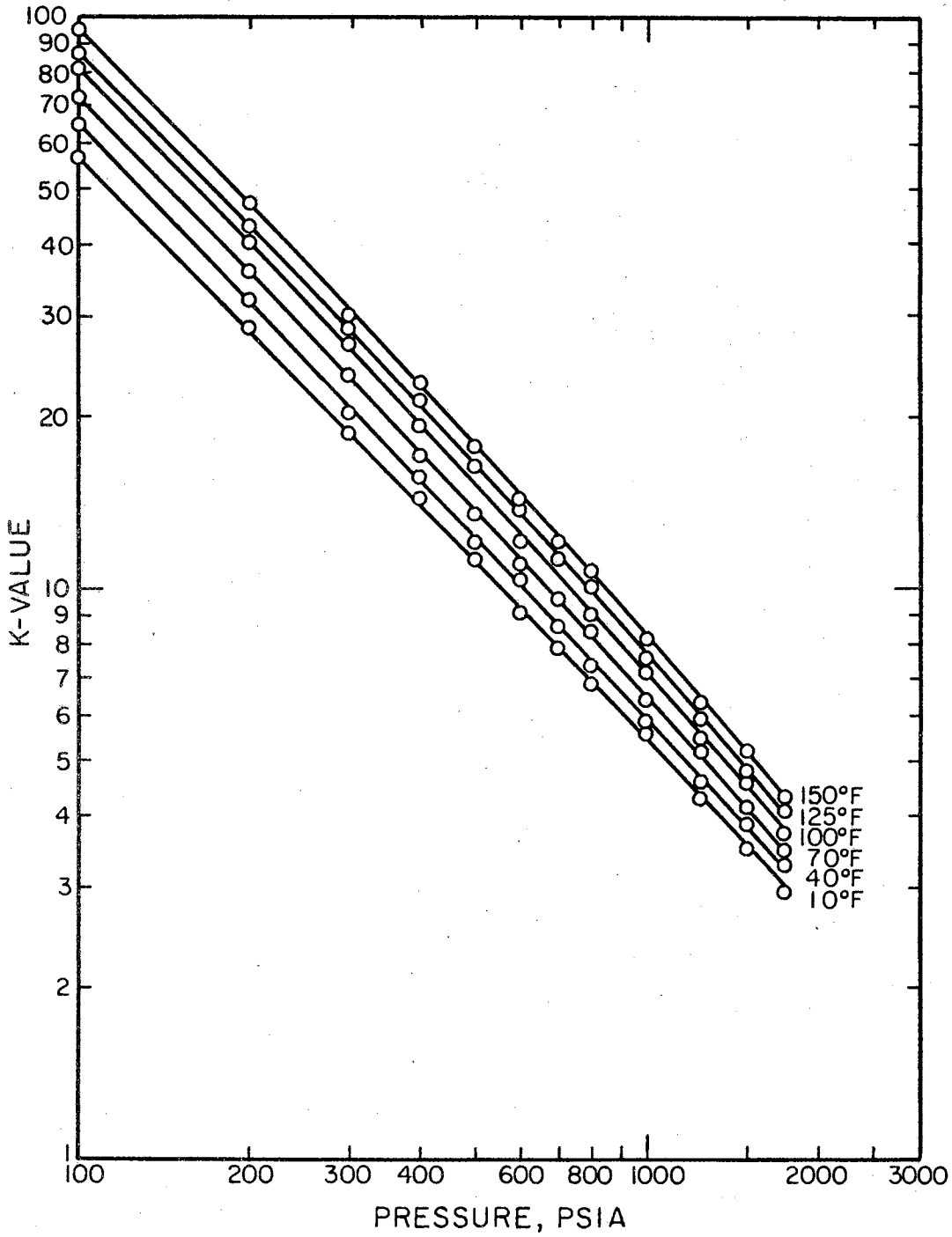

Figure 14. K-Values for Argon at Infinite Dilution in the Methane-n-Decane System

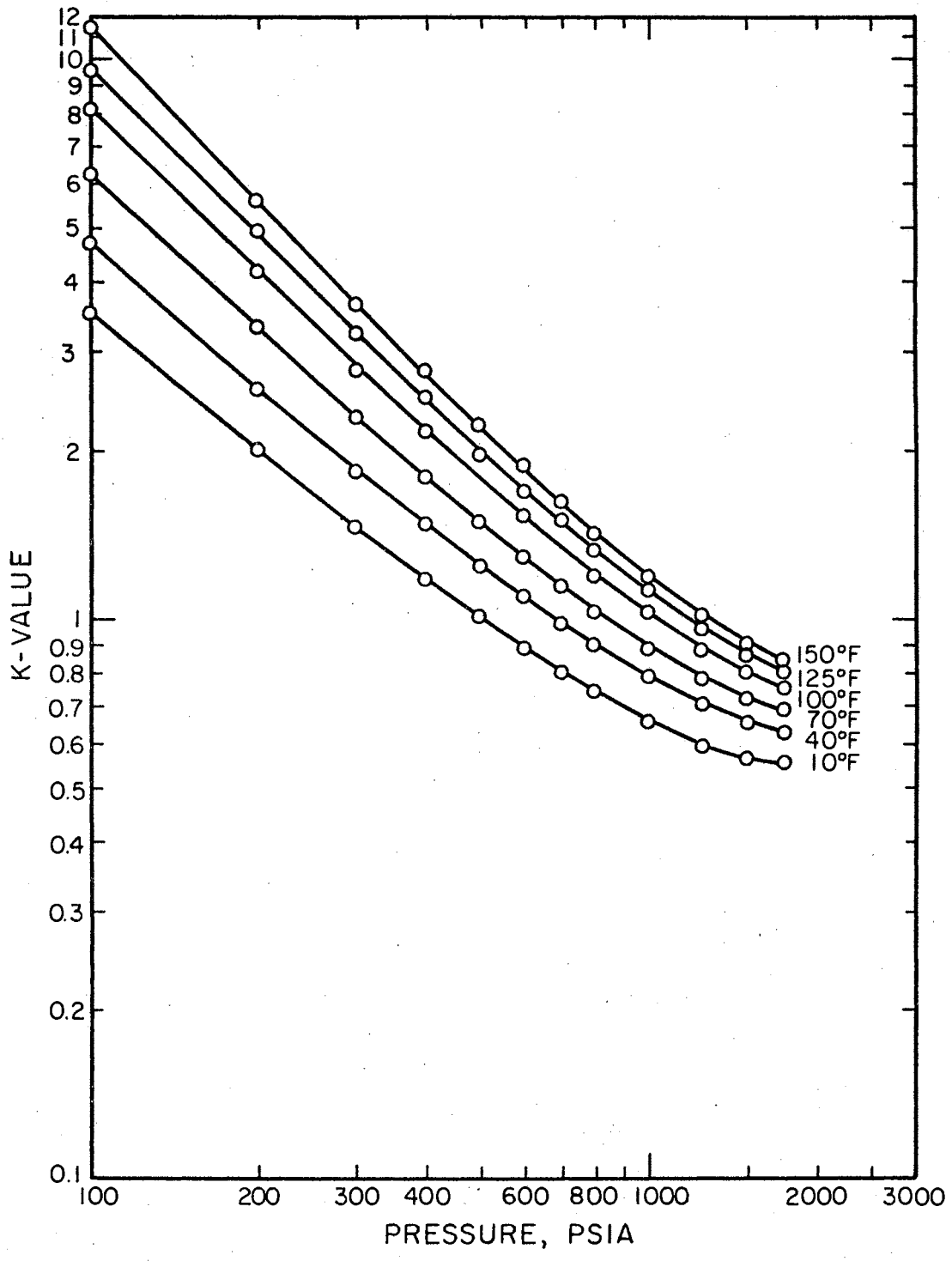

Figure 15. K-Values for Ethylene at Infinite Dilution in the Methane-n-Decane System

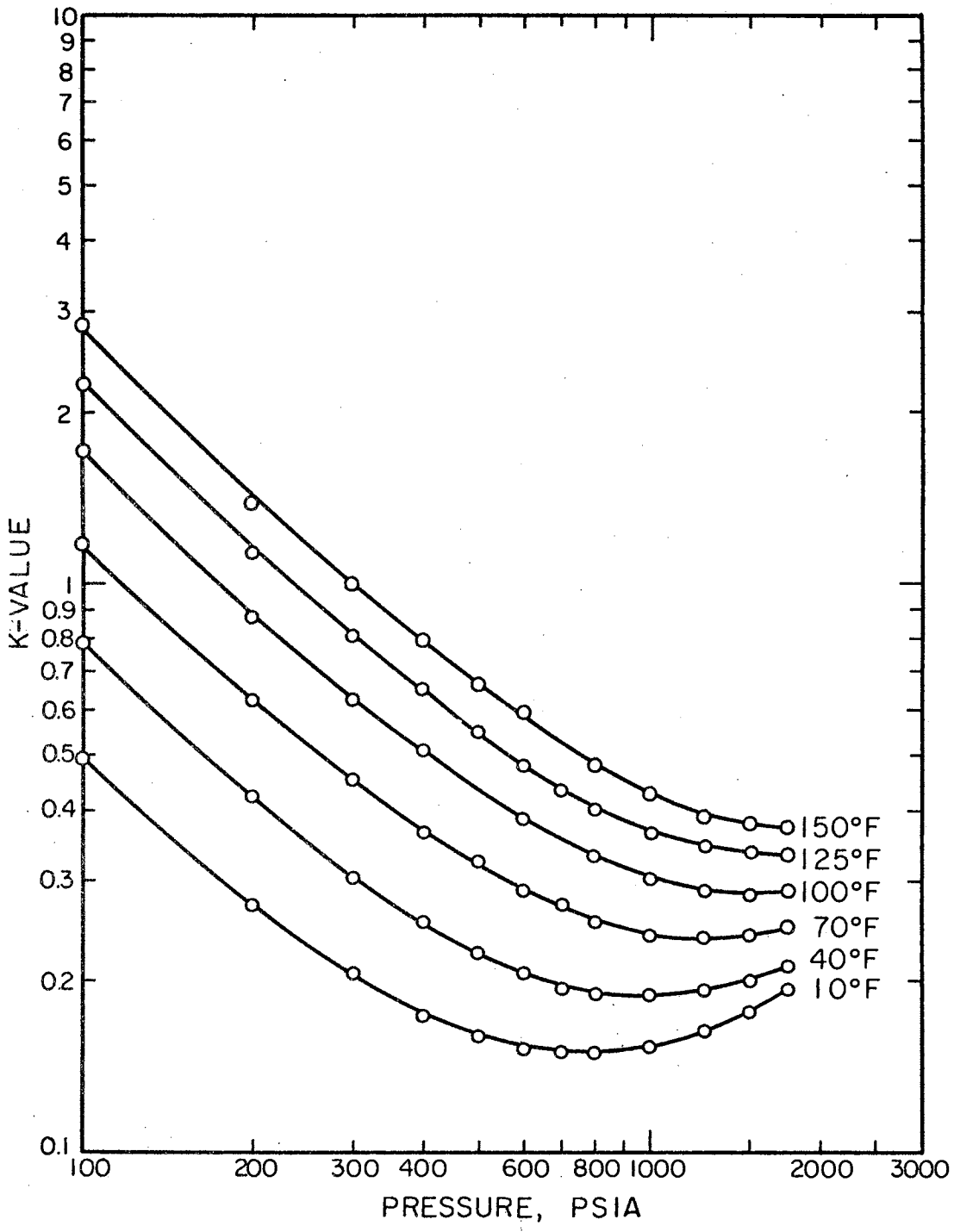

Figure 16. K-Values for Propane at Infinite Dilution in the Methane-n-Decane System

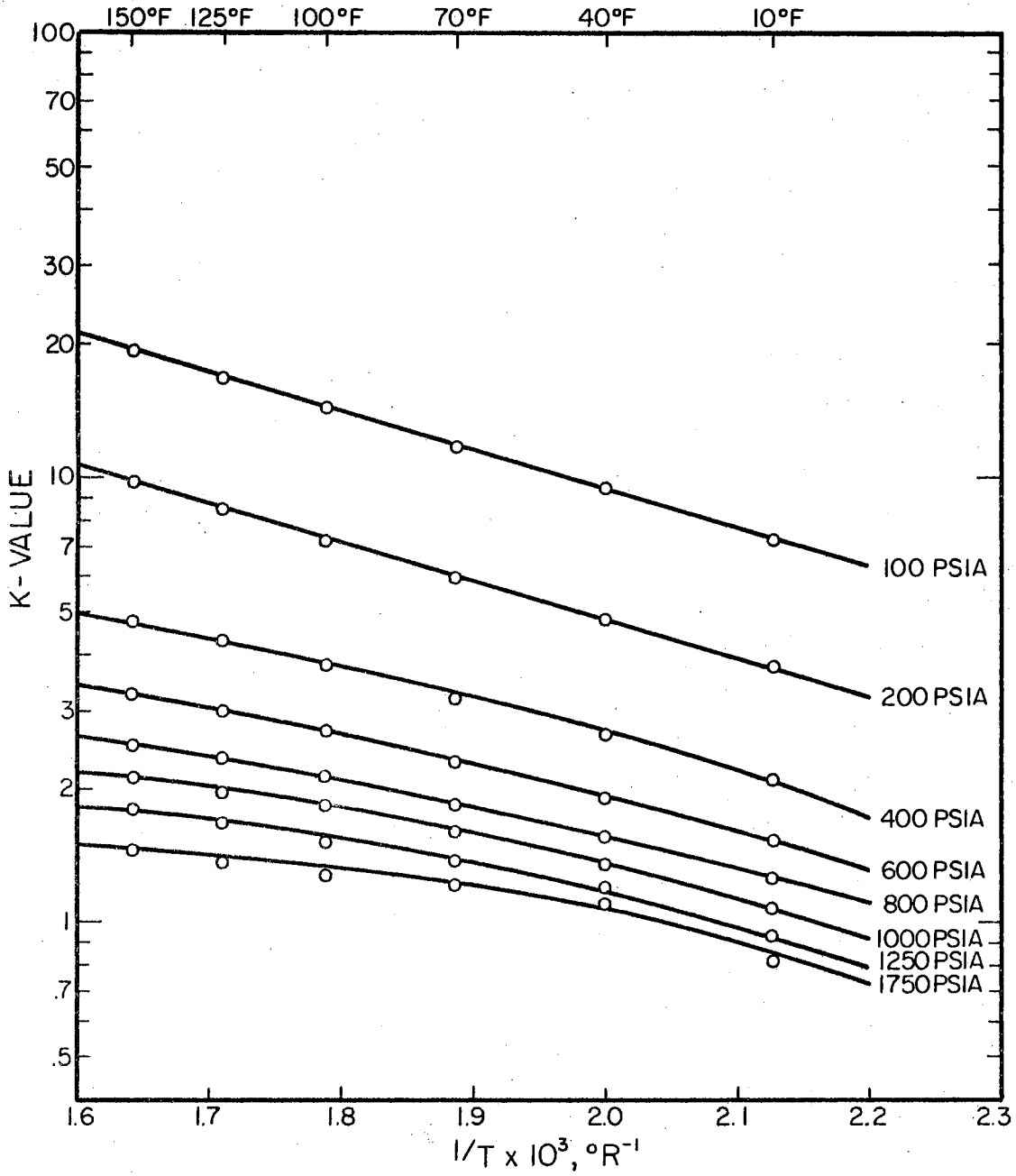

Figure 17. K-Values for Carbon Dioxide at Infinite Dilution in the Methane-n-Decane System as a Function of Reciprocal Temperature

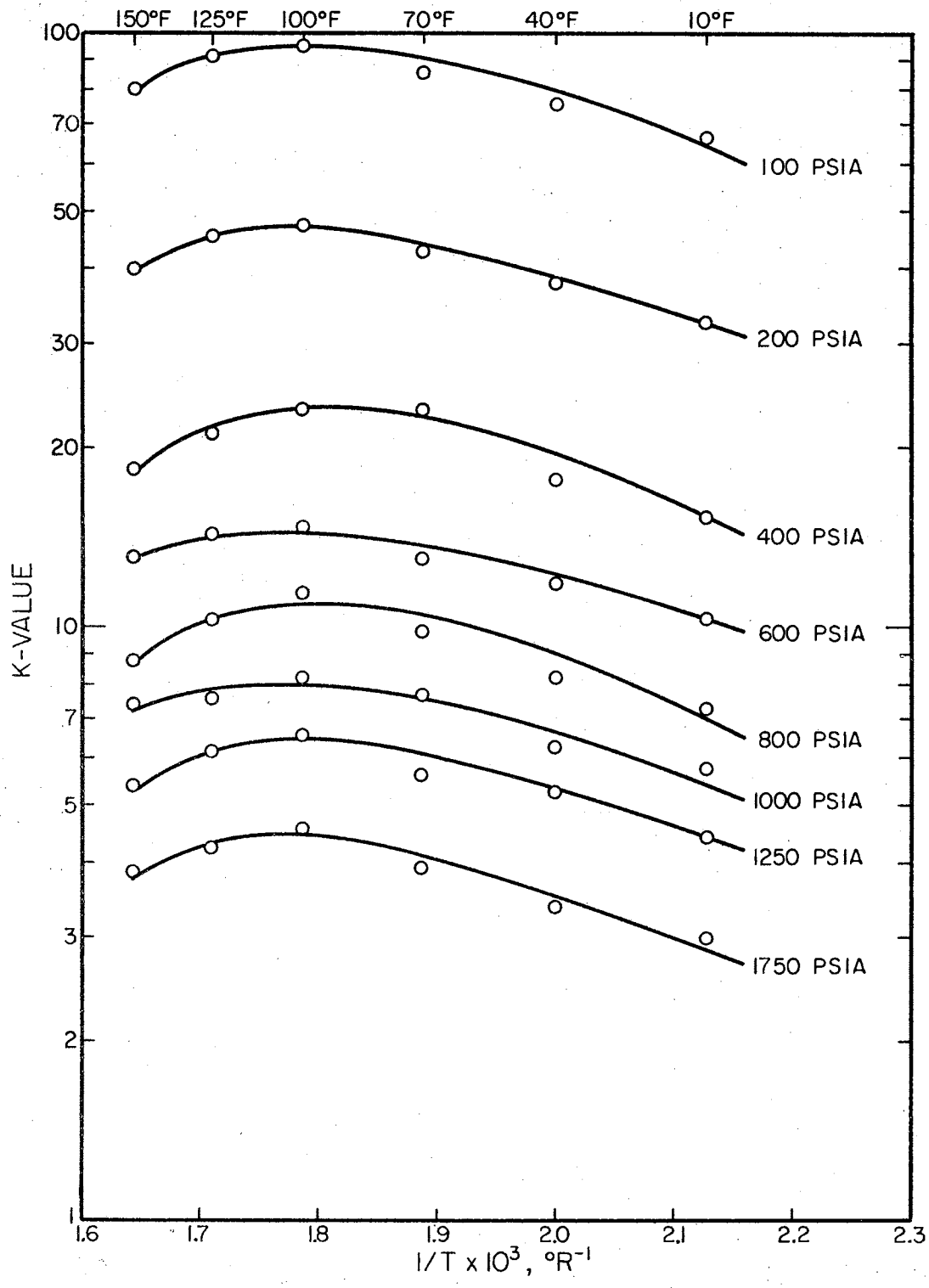

Figure 18. K-Values for Nitrogen at Infinite Dilution in the Methane-n-Decane System as a Function of Reciprocal Temperature

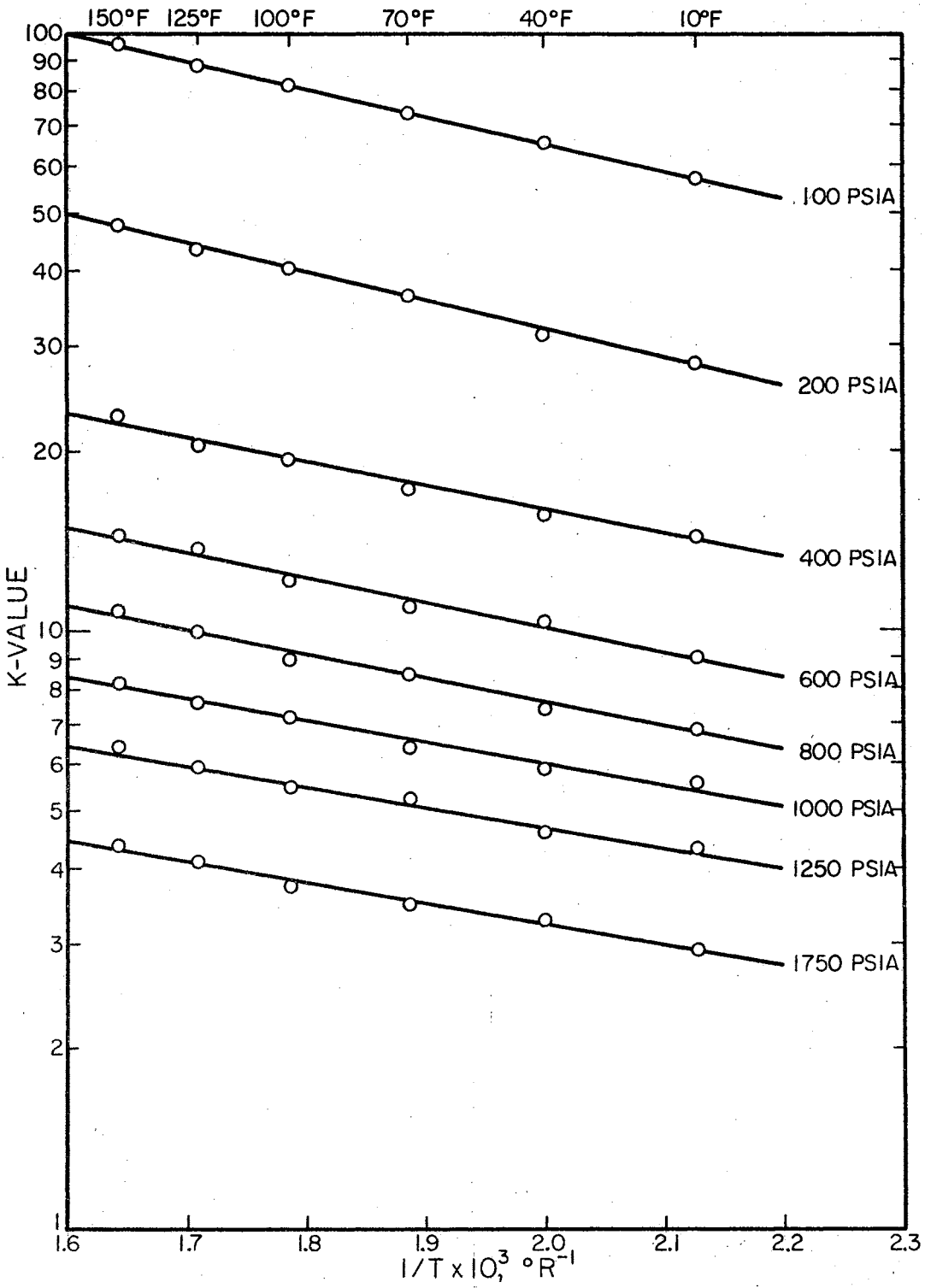

Figure 19. K-Values for Argon at Infinite Dilution in the Methane-n-Decane System as a Function of Reciprocal Temperature

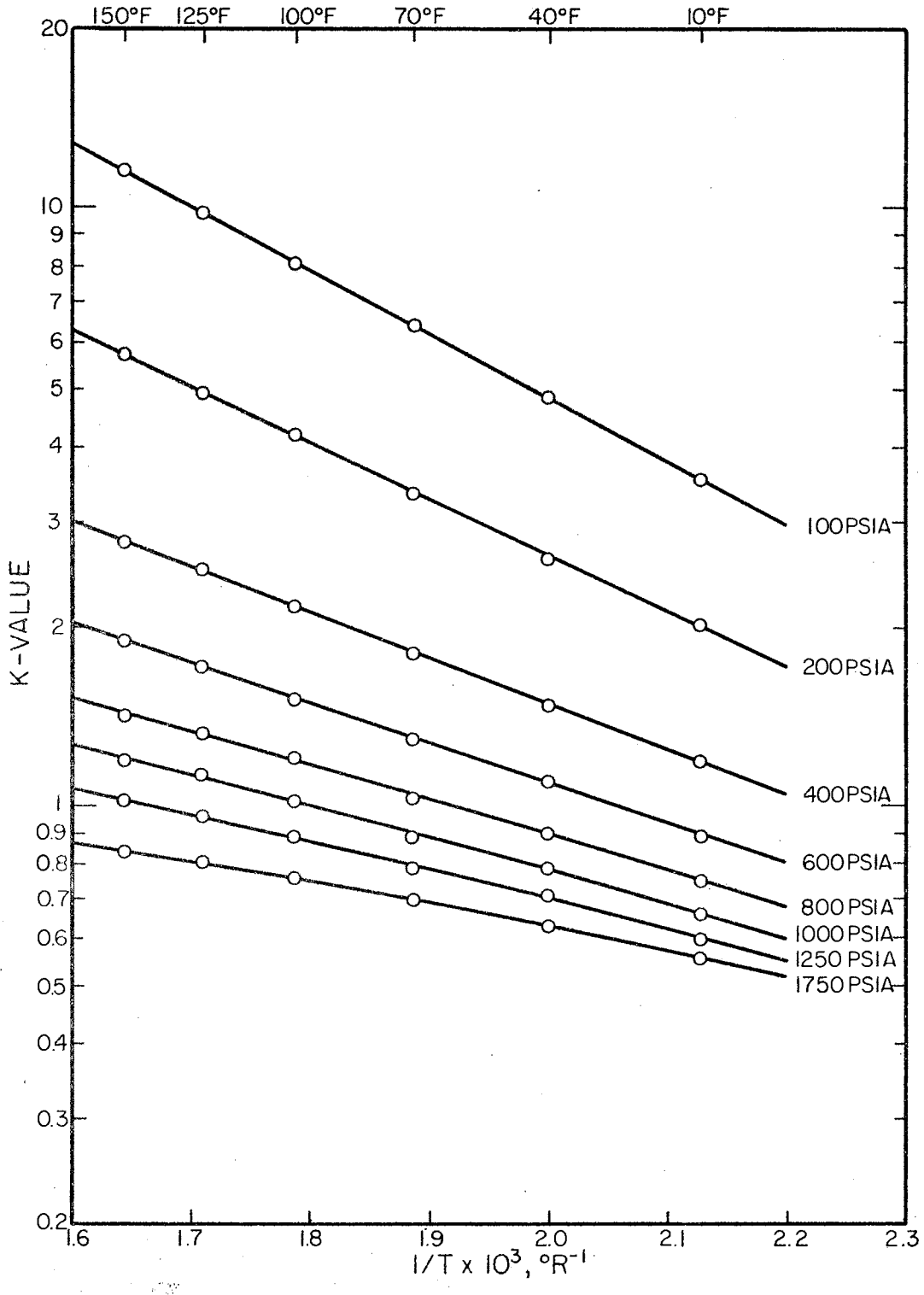

Figure 20. K-Values for Ethylene at Infinite Dilution in the Methane-n-Decane System as a Function of Reciprocal Temperature

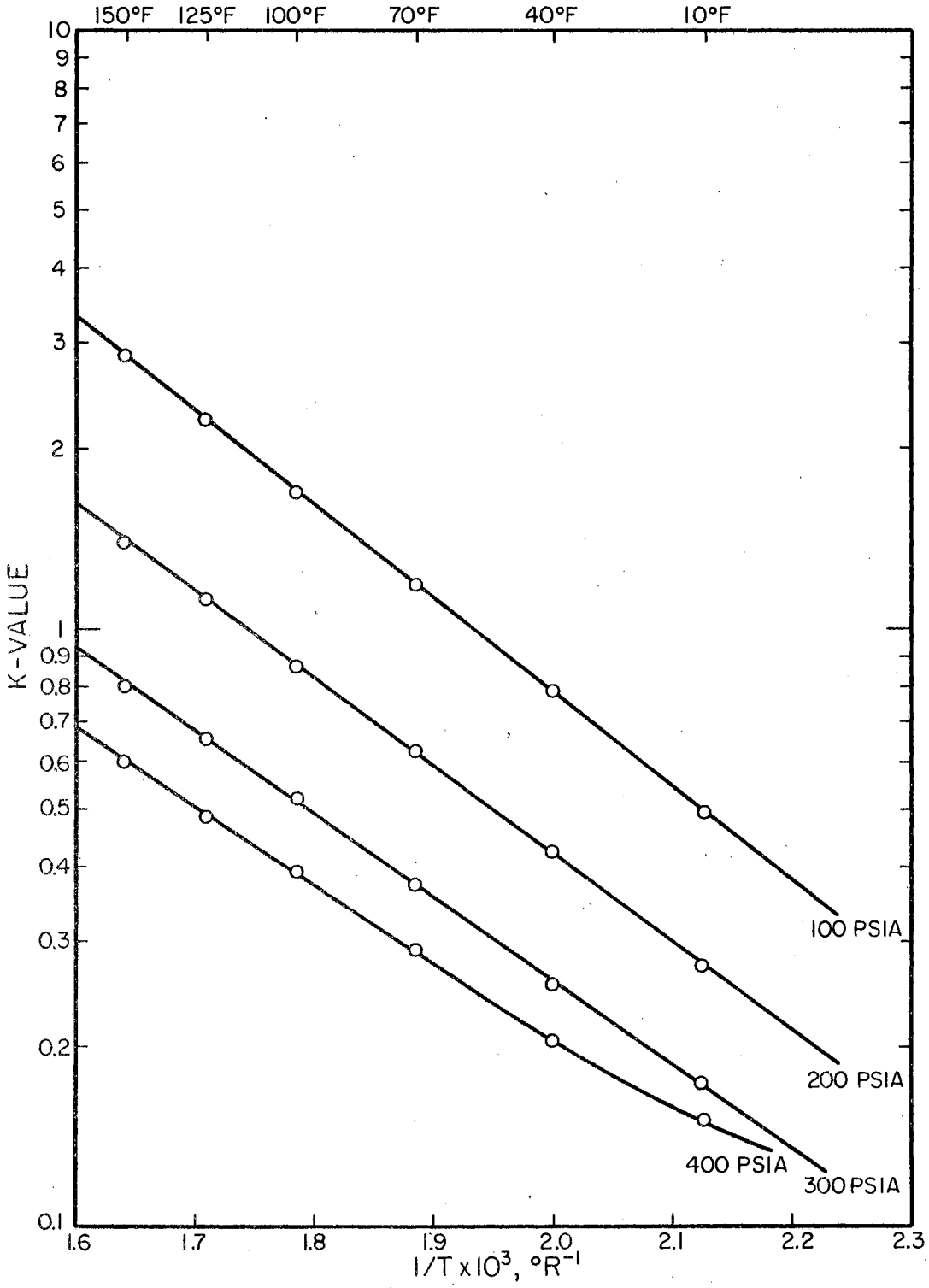

Figure 21. K-Values for Propane at Infinite Dilution in the Methane-n-Decane System as a Function of Reciprocal Temperature

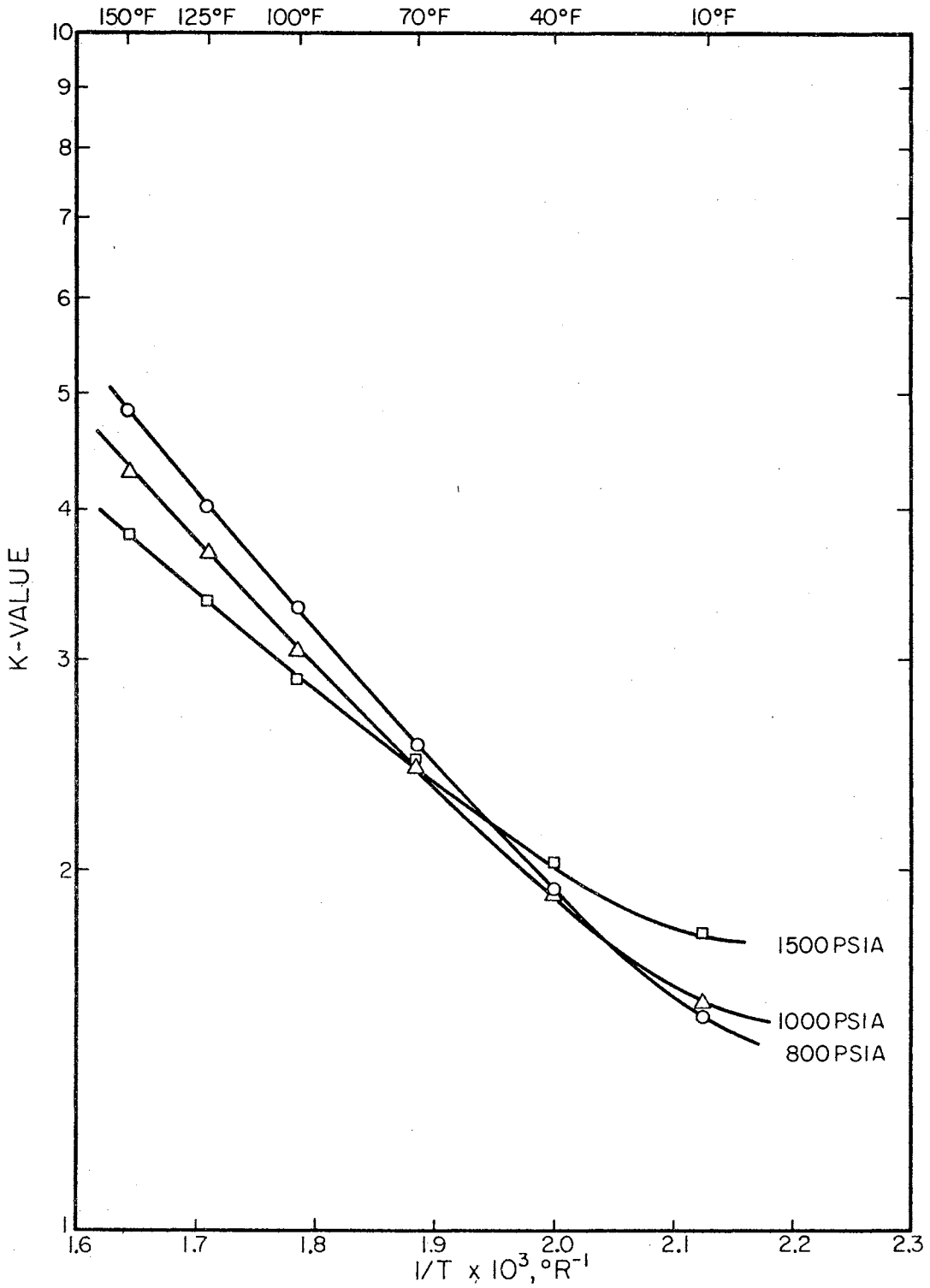

Figure 22. K-Values for Propane at Infinite Dilution in the Methane-n-Decane System as a Function of Reciprocal Temperature, High Pressure Range

CHAPTER VII

DISCUSSION OF RESULTS

In this chapter the experimental results obtained during this study are examined, analyzed and correlated.

The chromatographic vapor-liquid equilibrium data are combined with the partial volume data to determine the thermodynamic properties of liquid mixtures at high pressures.

The correlation framework developed in Chapter III is tested, using data from this experiment as well as from the literature. The general correlation for determining activity coefficient in liquid solutions at high pressures is applied for ternary systems.

The Partial Volume Experiment

Error Analysis

The accuracy of determination of the quotients of Eq. (3-2) was largely controlled by the accuracy of the strain gauge differential pressure transducer. The instrument used was a Consolidated Electrodynamics Corporation type 4-351-0005. Its hysterisis amounted to about 0.02 psi, corresponding to a relative accuracy of about 0.2% in the usual differential pressures developed with the injections. The transducer response was linear to within the error of the measurement as can be seen from Figure 7. There was also an appreciable error associated with the total pressure measurement. The relative accuracy of pressure reading at 2000

psia was about 0.1% and about 1% at 200 psia. Temperature was controlled within $\pm$ 0.04°F. The uncertainty in determining the pressure of the injected gas was $\pm$ 0.005 psi which made the relative error in injection pressures negligible. The precision of the Leeds and Northrup K-3 potentiometer was 0.0002 mv. The estimated maximum error in the volume ratio $\overline{V}_2^{\infty}/\tilde{V}_1$, calculated from the above mentioned uncertainties amounted to 0.6% (see Appendix E).

Prediction of Mixture Volumetric Behavior at Finite Concentration from Infinite Dilution Data

Mixture volumetric behavior predicted by Eqs. (3-3) through (3-7) is compared with literature experimental data (84) in Figure 23 at 150°F and pressures of 500, 1000, 1500 and 1750 psia for the methane-carbon dioxide gaseous mixture. The interpolation formula was based on the two sets of infinite dilution data, namely, infinite dilution partial volumes of carbon dioxide in methane and of methane in carbon dioxide. The agreement between the interpolated data and the experimental data is good.

Modification of B-W-R Equation of State Using Infinite Dilution Data

Eq. (3-18) relates infinite dilution partial volume data to B-W-R equation constants. The denominator on the right hand side of Eq. (3-18) contains only constants of the pure solvent gas (methane). The constants of methane have been determined by Douslin and co-workers (26) and were used in this study.

Experimental values of the volume ratio, $\overline{V}_2^{\infty}/\tilde{V}_1^{o}$, were used to calculate A_{012} by a least square method. All other interaction constants

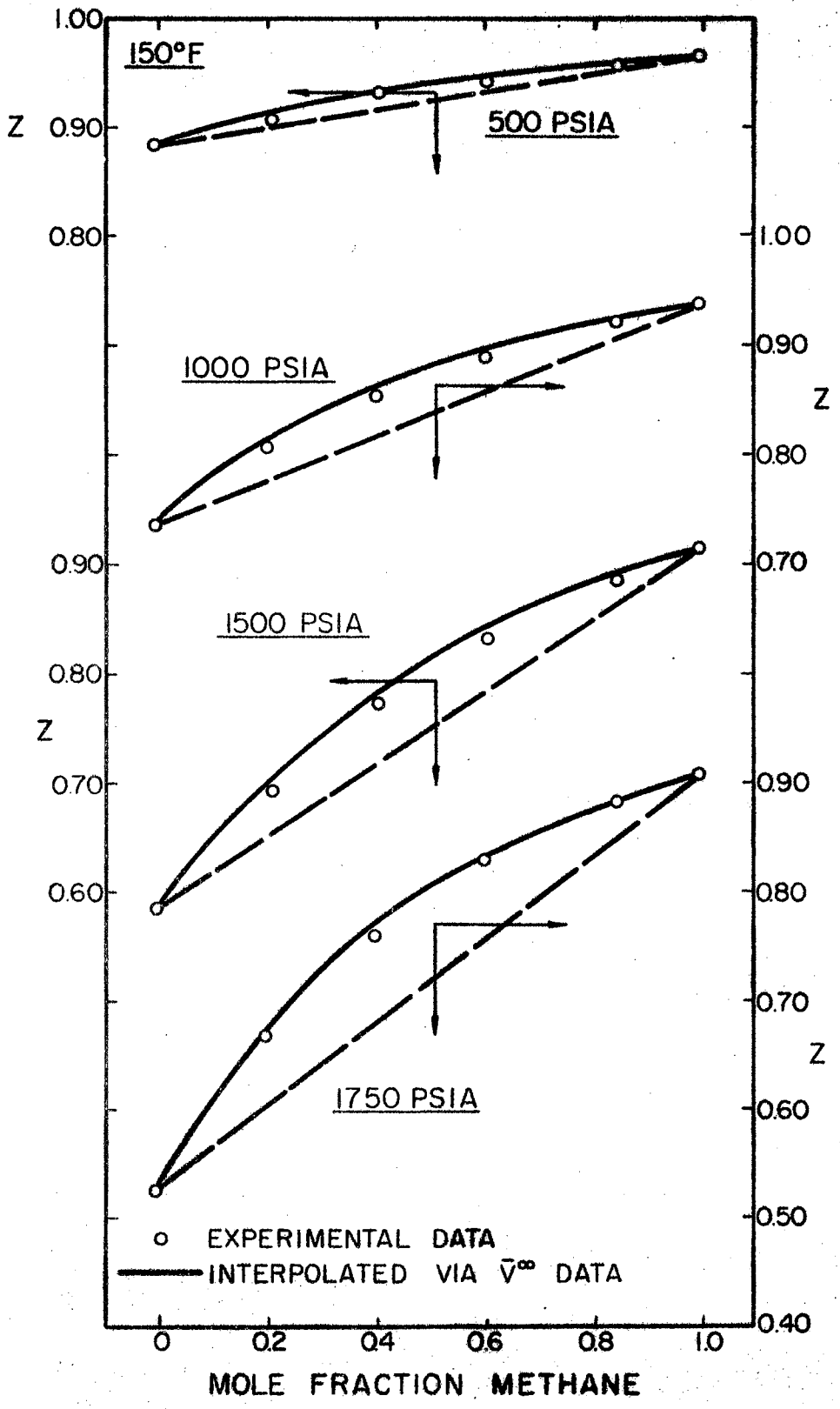

Figure 23. Volumetric Behavior Interpolated from Infinite Dilution Data at 150°F

were calculated from Eqs. (3-15) and (3-17). The result is given by,

$$A_{012} = 0.9534\ (A_{01}A_{02})^{\frac{1}{2}} \tag{7-1}$$

Figure 24 shows the fit to the data along with predictions by the usual combination rules. The BWR constants for carbon dioxide were taken from the literature (22).

The experimentally based A_{012} value was used with the B-W-R equation to predict the volumetric behavior of carbon dioxide-methane mixtures at finite concentrations. Figures 25 through 27 show comparisons of these predictions, along with those based on the usual combination rules, with the data of Reamer et. al. (84). The comparisons illustrate the improved fit resulting from the experimentally determined A_{012}. The improvement apparently extends to temperature and pressure conditions outside the range covered by the infinite dilution data, as Figures 25 through 27 demonstrate.

The largest deviation between experimental data and predictions by the B-W-R equation (modified and unmodified) in Figures 25 and 27 often occurred in the range of pure carbon dioxide and high concentrations of carbon dioxide. These deviations are largely due to the failure of the B-W-R equation to predict accurately the volumetric behavior of pure carbon dioxide using the constants of Douslin et. al. (26).

The Gas-Liquid Chromatography Experiment

Error Analysis

Eq. (3-36) shows that the accuracy of a measured K-value depends directly on the value $(V_{R_i} - V_G)$. For highly retained solutes this value will be larger; on the other hand, it will be smaller for the less re-

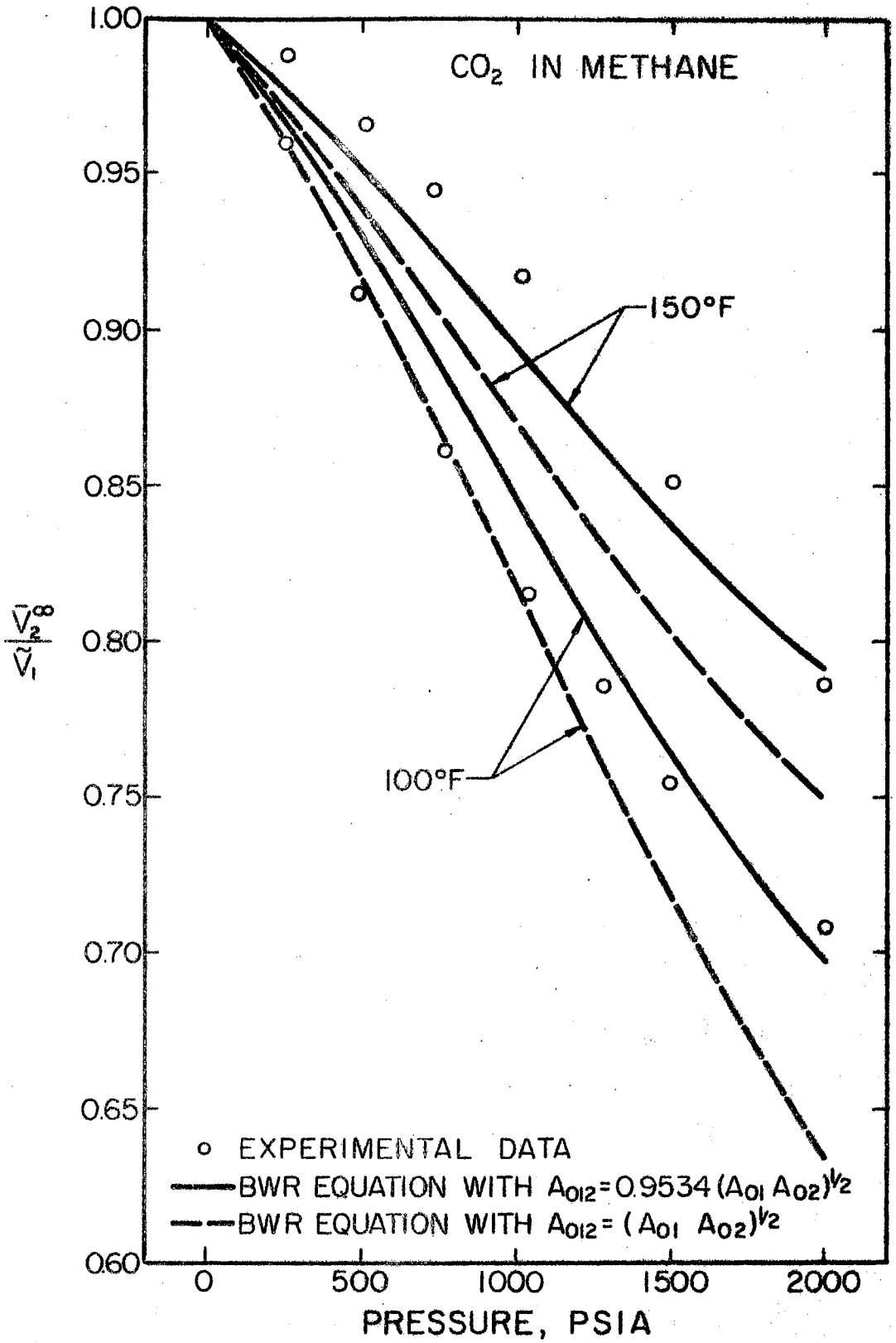

Figure 24. B-W-R Equation Fitting of the Volume Ratios at Infinite Dilution of Carbon Dioxide in Methane

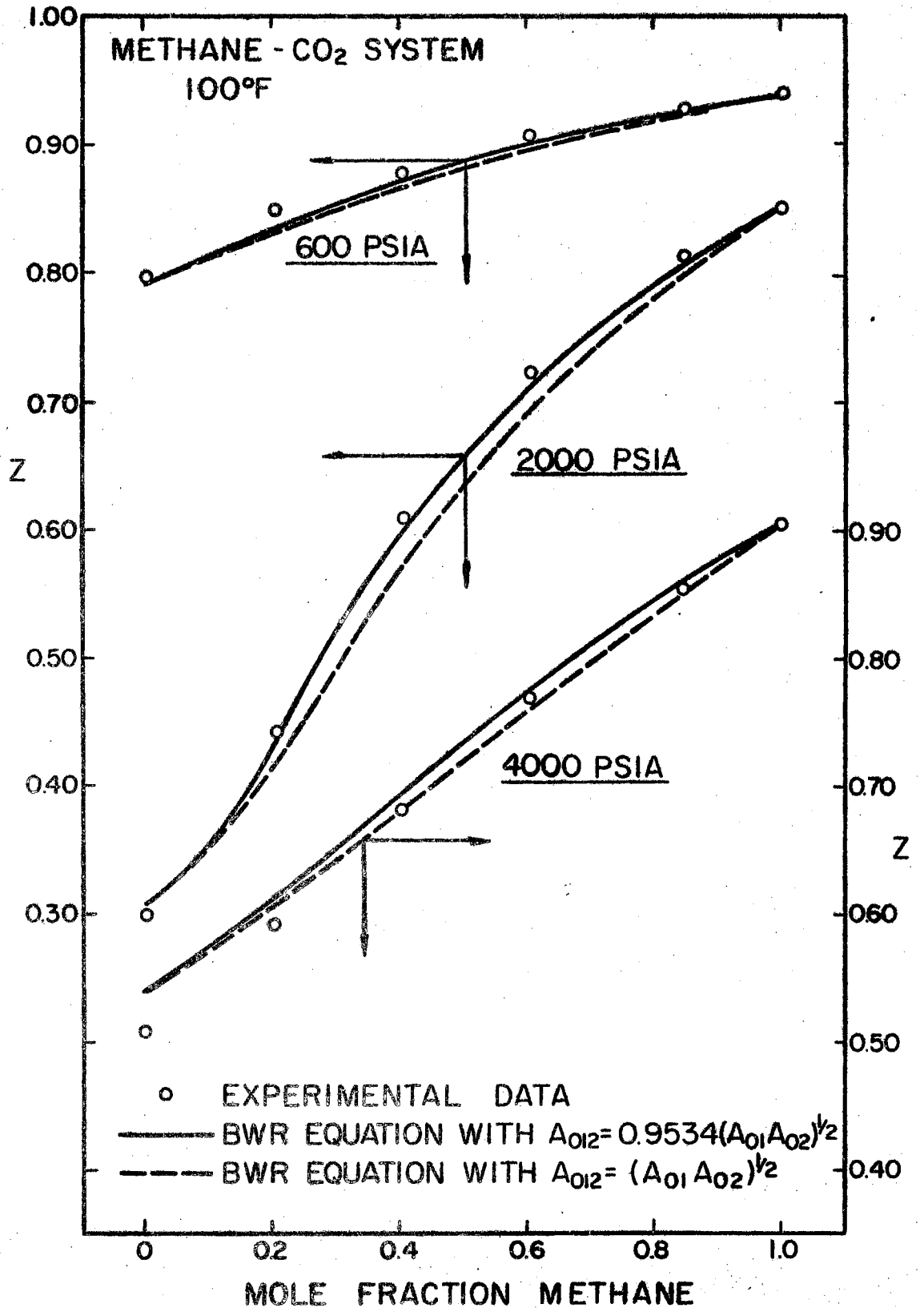

Figure 25. Volumetric Properties of Methane-Carbon Dioxide Mixtures at 100°F

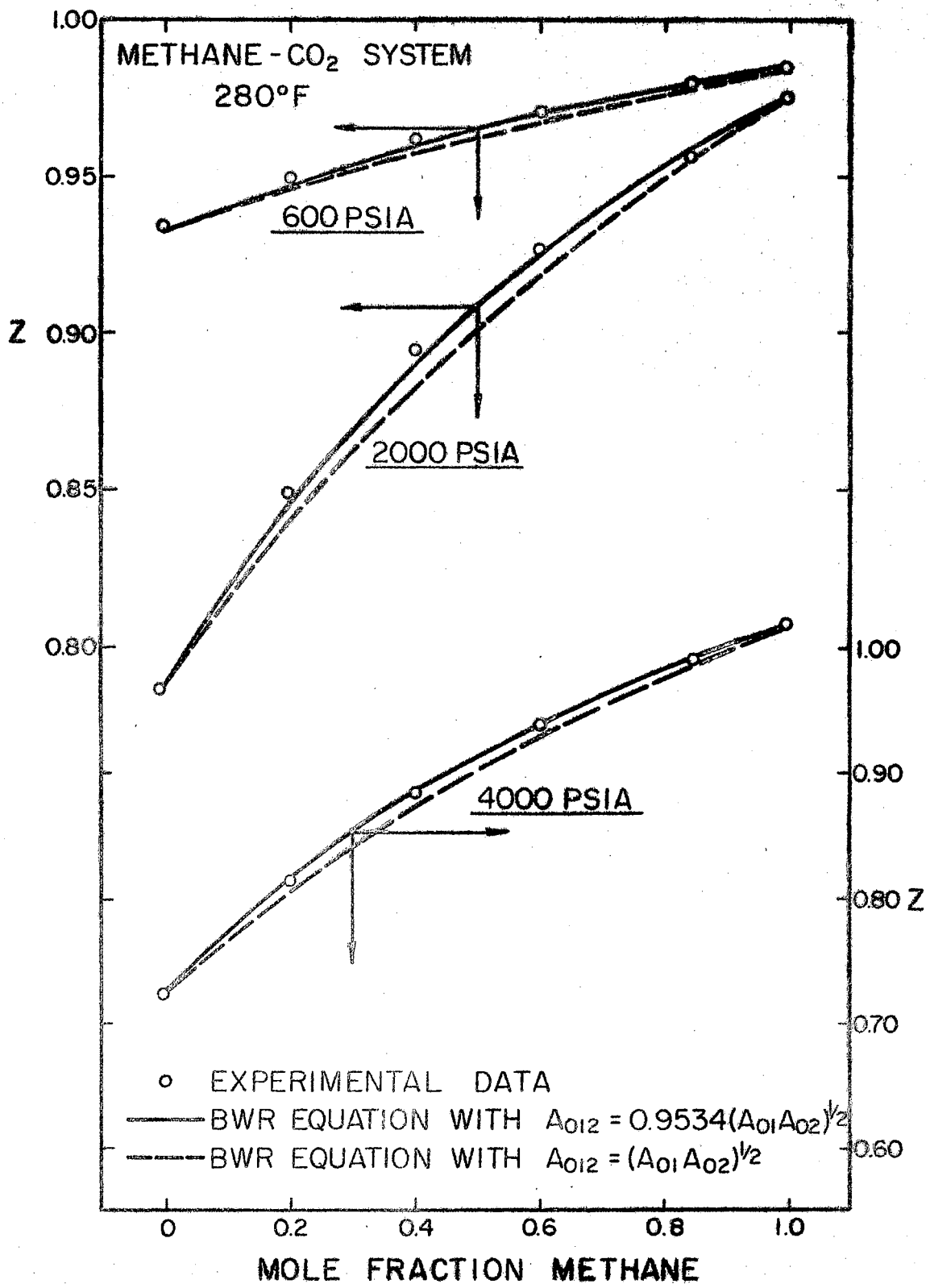

Figure 26. Volumetric Properties of Methane-Carbon Dioxide Mixtures at 280°F

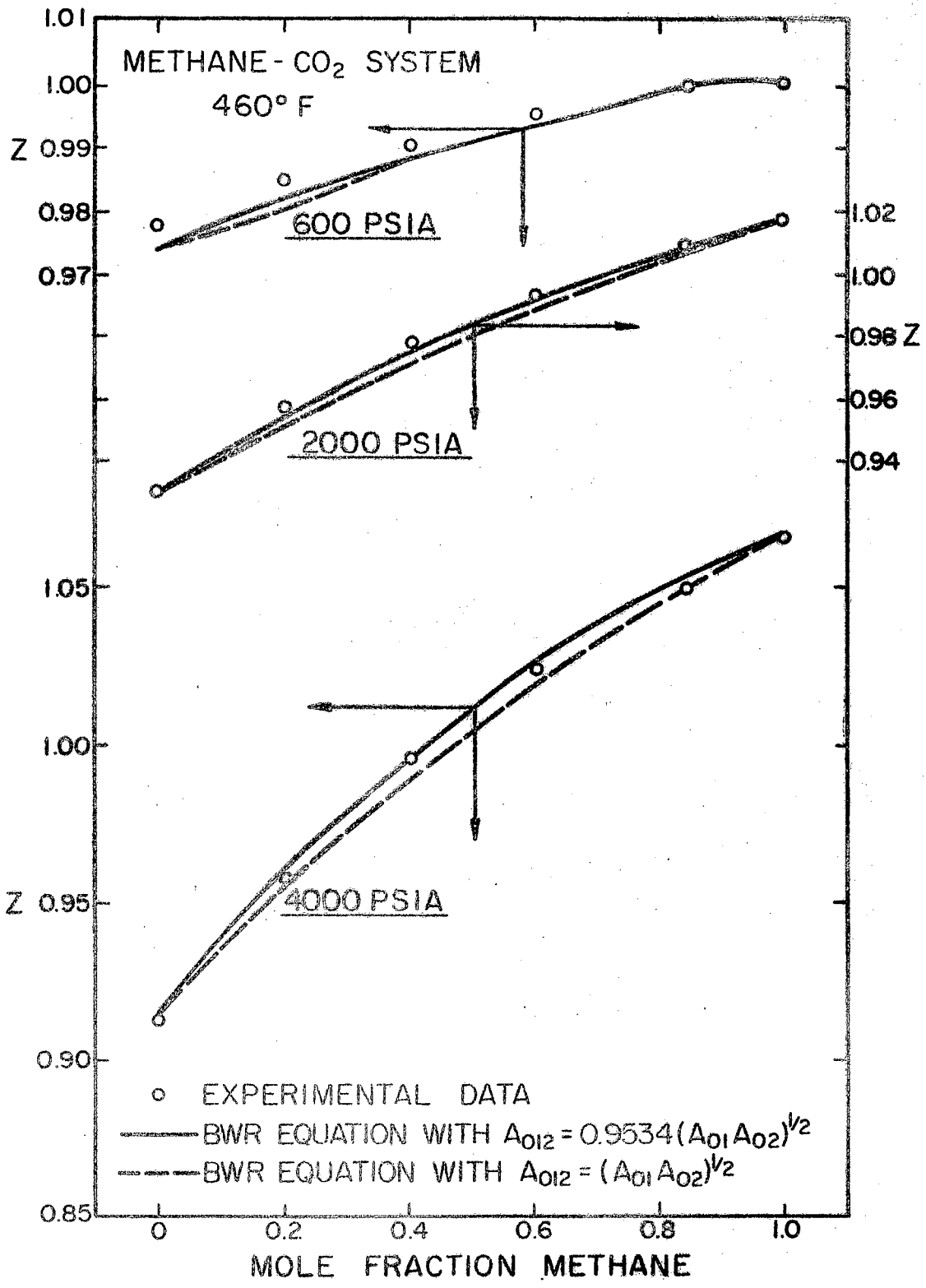

Figure 27. Volumetric Properties of Methane-Carbon Dioxide Mixtures at 460°F

tained solutes. Consequently, a given error in V_R or V_G will cause a larger relative error in K-value for the less soluble solutes. Furthermore, the relative error in K-value will generally be greater at higher temperature and lower pressure condition since the value of $(V_{R_i} - V_G)$ is smaller at this condition for a given solute.

The results of this study indicates that for the systems investigated in this work, the values of α_o for the postulated "zero-solubility" solutes were very close to zero, i.e., close "hard-sphere" solute gas.

The estimated uncertainties involved in the measurements of experimental parameters are listed below.

Experimental Measurement	Estimated Uncertainty
System temperature	$\pm$ 0.04°F
Room temperature	$\pm$ 0.2°F
System pressure	$\pm$ 1 psi
Atmospheric pressure	$\pm$ 0.02%
Time	$\pm$ 0.05 sec
Wt. of stationary liquid	$\pm$ 0.02%
Flow rate	$\pm$ 0.1%

The concentrations of methane in n-decane obtained from the literature (87, 6) carried an uncertainty of $\pm$ 0.2%. Since these data were interpolated, a conservative assumption of $\pm$ 0.4% uncertainty seemed reasonable. The uncertainty of molar volumes of saturated methane-n-decane solutions obtained from the literature (87, 6), was taken as $\pm$ 0.4%.

A detailed error analysis is presented in Appendix E, the results

are summarized in Table IX.

TABLE IX

ESTIMATED MAXIMUM ERROR IN EXPERIMENTALLY DETERMINED K-VALUES

	10°F		150°F	
Solute	100 psia	1750 psia	100 psia	1750 psia
N_2	2.9	0.8	3.9	1.3
Ar	2.6	0.8	3.2	1.1
CO_2	0.9	0.6	1.5	0.8
C_2H_2	0.8	0.6	1.1	0.7
C_3H_8	0.6	0.6	0.7	0.6

Table IX shows that the estimated maximum errors are higher for the lighter solutes and at lower pressures. This can be related to the fact that the retention time was shorter for a light solute at lower pressures, and, therefore, the relative error was larger. The retention time for a heavier solute such as propane was relatively high and, therefore, the pressure had negligible effect on values of $(V_R - V_G)$.

The maximum relative error for the experiment is:

N_2 - 3.9%

Ar - 3.2%

CO_2 - 1.5%

C_2H_2 - 1.1%

C_3H_8 - 0.7%

The uncertainty in the molal volume of methane-n-decane solutions had a negligible influence on the error in the K-values, (see Appendix E).

These error estimates were substantiated by the reproducibility of the data and by the cross plots shown in Figures 11 through 22, except for the K-values of nitrogen the errors of which were higher in some cases.

Comparison of the K-Value Data with Other Sources

The Propane-Methane-n-Decane System. The K-values of propane at infinite dilution in the methane-n-decane system determined in this study were compared with the data of Stalkup (93) and Koonce(50) who also obtained the K-values chromatographically. The comparison was made at $40^{o}F$ and $70^{o}F$ at pressures up to 1000 psia since this temperature and pressure range was common to the works of Stalkup, Koonce and this author.

Figure 28 illustrates a comparison of propane K-values determined from GLC data by Stalkup (93), Koonce (50) and this work. Table X shows a quantitative comparison of the propane K-values of Koonce (50), the more recent work of the two mentioned above, with those measured during this work. The agreement among the three different sources is apparent. Each of the three investigators used a different method for determining column void volume; the methods used by Stalkup (93) and Koonce (50) were discussed in Chapter II.

Table XI shows the comparison of propane K-values at infinite dilution in the C_3H_8-CH_4-n-C_{10} system with those predicted by the Chao-Seader correlation (12) and NGPSA Data Book (73). The comparison was made at $125^{o}F$ and $150^{o}F$ since at lower temperatures the methane concentration in the liquid phase exceeded 20%, which was beyond the range of conditions specified by the Chao-Seader correlation.

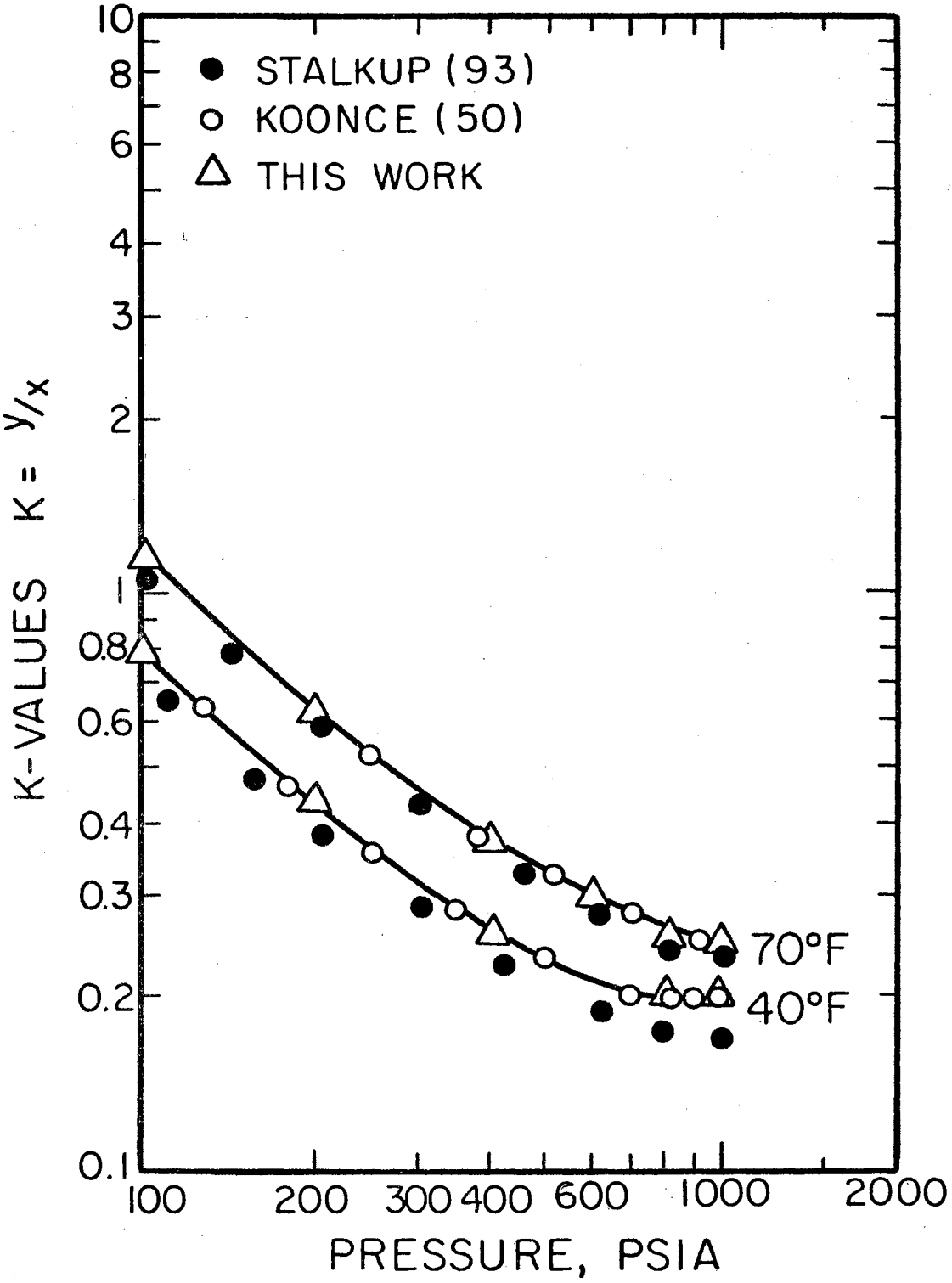

Figure 28. Comparison of K-Values for Propane at Infinite Dilution in the Methane-n-Decane System

TABLE X

COMPARISON OF K-VALUES FOR PROPANE AT INFINITE DILUTION IN THE C_3H_8-CH_4-n-C_{10} SYSTEM

	K-values		
Pressure, psia	This Work	Koonce (50)	% Deviation*
		40°F	
100	0.791	0.800	1.14
200	0.426	0.432	1.41
400	0.258	0.265	2.71
600	0.207	0.215	3.86
800	0.193	0.199	3.11
1000	0.192	0.200	4.17
		70°F	
100	1.179	1.180	0.10
200	0.626	0.633	1.12
400	0.373	0.377	1.07
600	0.292	0.300	2.74
800	0.255	0.264	3.53
1000	0.245	0.247	0.82

Average absolute % Deviation: @ 40°F - 2.73%

@ 70°F - 1.56%

*% Deviation = $100\ (K_{Koonce} - K_{This\ work})/K_{This\ work}$

The agreement between the correlated K-values and the data is noticeable, especially in the lower pressure range.

The Ethylene-Methane-n-Decane System. No comparable systems exist for the ethylene-methane-n-decane system.

Table XII shows a comparison of K-values for ethylene at infinite dilution in the C_2H_2-CH_4-n-C_{10} system at 125°F and 150°F with K-values

TABLE XI

COMPARISON OF K-VALUE FOR PROPANE AT INFINITE DILUTION IN THE C_3H_8-CH_4-n-C_{10} SYSTEM OBTAINED EXPERIMENTALLY WITH THOSE PREDICTED BY THE CHAO-SEADER CORRELATION (12) AND THE NGPSA CORRELATION (73)

	T=125°F			T=150°F		
P-psia	K_{exp}	K_{cs}	K_{NG}	K_{exp}	K_{cs}	K_{NG}
100	2.254	1.757*	2.30	2.852	2.089	2.85
200	1.134	0.998*	1.23	1.390	1.188	1.55
300	0.811	1.020	0.88	1.022	1.302	1.10
400	0.658	0.657	0.72	0.802	0.782	0.88
500	0.551	0.558	0.61	0.674	0.648	0.76
600	0.483	0.501	0.55	0.600	0.600	0.68
700	0.439	0.488	0.52	0.551	0.570	0.64
800	0.403	0.502*	0.50	0.486	0.566*	0.60
1000	0.367	0.458*	0.46	0.431	0.516*	0.56
1250	0.350	0.432*	0.44	0.395	0.487*	0.53
1500	0.341	0.437*	0.43	0.383	0.485*	0.52
1750	0.339	0.440*	0.47	0.377	0.489*	0.53

*Slightly beyond the limits of the correlation

TABLE XII

COMPARISON OF K-VALUES FOR ETHYLENE AT INFINITE DILUTION IN THE C_2H_2-CH_4-n-C_{10} SYSTEM OBTAINED EXPERIMENTALLY WITH THOSE PREDICTED BY THE CHAO-SEADER CORRELATION (12) AND THE NGPSA CORRELATION (73)

	T=125°F			T=150°F		
P-psia	K_{exp}	K_{cs}	K_{NG}	K_{exp}	K_{cs}	K_{NG}
100	9.804	8.671*	9.79	11.55	9.779	10.70
200	4.953	4.590*	5.00	5.635	5.177	5.70
300	3.258	3.984	3.50	3.694	4.744	4.00
400	2.506	2.611	2.75	2.792	2.934	3.15
500	1.975	2.115	2.25	2.228	2.332	2.65
600	1.720	1.802	1.98	1.906	2.024	2.30
700	1.515	1.635	1.75	1.644	1.800	2.05
800	1.348	1.543*	1.62	1.432	1.662*	1.85
1000	1.130	1.278*	1.40	1.207	1.366*	1.60
1250	0.973	1.072*	1.24	1.021	1.135*	1.40
1500	0.871	0.950	1.15	0.906	0.986*	1.29
1750	0.813	0.853*	1.08	0.845	0.868*	1.20

*Slightly beyond the limits of the correlation

predicted by the Chao-Seader correlation (12) and NGPSA correlation (73). The agreement between the K-values calculated by the correlation and those determined chromatographically is substantial, especially at pressures up to 1000 psia.

The Carbon-Dioxide-Methane-n-Decane System. K-value data of carbon dioxide at finite concentrations in n-decane were reported by Reamer and Sage (85). In the lower pressure range the infinite dilution K-value data and the finite concentration K-values are expected to be approximately equal.

A comparison between the chromatographically determined K-values with those reported by Reamer et. al. (85), in the lower pressure region, is shown in Table XIII. The deviations range from 0.2% to 9.5%. Taking into account the fact that the accuracy in finite concentration K-values determined by the static method is worst in the low solute concentrations region, the agreement of the data is reasonable.

A comparison of carbon dioxide K-values with those predicted by the Chao-Seader correlation (12) and NGPSA correlation (73) is also shown in Table XIV; the agreement is again substantial.

The Nitrogen-Methane-n-Decane System. Azarnoosh and McKetta (4) studied vapor-liquid equilibrium in the methane-n-decane-nitrogen system by a static method. They reported nitrogen K-values data at finite concentrations at 1000, 2000, 3000, 4000 and 5000 psia and temperatures of 100, 160, 220 and 280^{o}F. This author extrapolated the nitrogen K-values at 100^{o}F to infinite dilution and compared them to the data obtained in this work; the comparison is given below.

Figure 29 shows the temperature dependence of the nitrogen K-values

TABLE XIII

COMPARISON OF K-VALUES FOR CARBON DIOXIDE AT INFINITE DILUTION IN THE CO_2-CH_4-n-C_{10} SYSTEN OBTAINED EXPERIMENTALLY WITH FINITE CONCENTRATION K-VALUE OF CARBON DIOXIDE IN N-DECANE REPORTED BY REAMER ET.AL. (85) IN THE LOWER PRESSURE REGION

	T=40°F		T=70°F		T=100°F		T=125°F		T=150°F	
P-psi	K_{exp}	K^*	K_{exp}	K^*	K_{exp}	K^*	K_{exp}	K^*	K_{exp}	K^*
100	9.563	9.210	11.92	11.62	14.51	13.68				
200	4.819	4.590	6.064	6.052	7.217	6.950	8.539	7.760	9.841	8.570
300	3.322	2.980	4.123	3.670	4.933	4.693				
400			3.210	2.975	3.837	3.548	4.308	4.020	4.791	4.503

*CO_2 at finite concentration in n-C_{10} (85), K-values at 70°F, 125°F, and 150°F were interpolated.

TABLE XIV

COMPARISON OF K-VALUES FOR CARBON DIOXIDE AT INFINITE DILUTION IN THE CO_2-CH_4-n-C_{10} SYSTEM OBTAINED EXPERIMENTALLY WITH THOSE PREDICTED BY THE CHAO-SEADER CORRELATION (12) AND NGPSA CORRELATION (73).

	T=125°F			T=150°F		
P-psia	K_{exp}	K_{cs}	K_{NG}	K_{exp}	K_{cs}	K_{NG}
100	16.95	10.04*	18.30	19.21	11.58	21.00
200	8.539	5.196*	9.20	9.841	6.002	10.50
300	5.725	4.597	6.20	6.431	5.498	7.00
400	4.308	2.878	4.70	4.791	3.313	5.30
500	3.556	2.283	3.80	3.985	2.583	4.25
600	3.035	1.918	3.30	3.257	2.229	3.60
700	2.651	1.743	2.85	2.885	1.981	3.20
800	2.352	1.670*	2.60	2.525	1.844*	2.80
1000	1.975	1.382*	2.20	2.123	1.529*	2.40
1250	1.687	1.183*	1.90	1.801	1.316*	2.00
1500	1.481	1.115*	1.70	1.584	1.229*	1.80
1750	1.373	1.082*	1.50	1.475	1.202*	1.58

*Slightly beyond the limits of the correlation

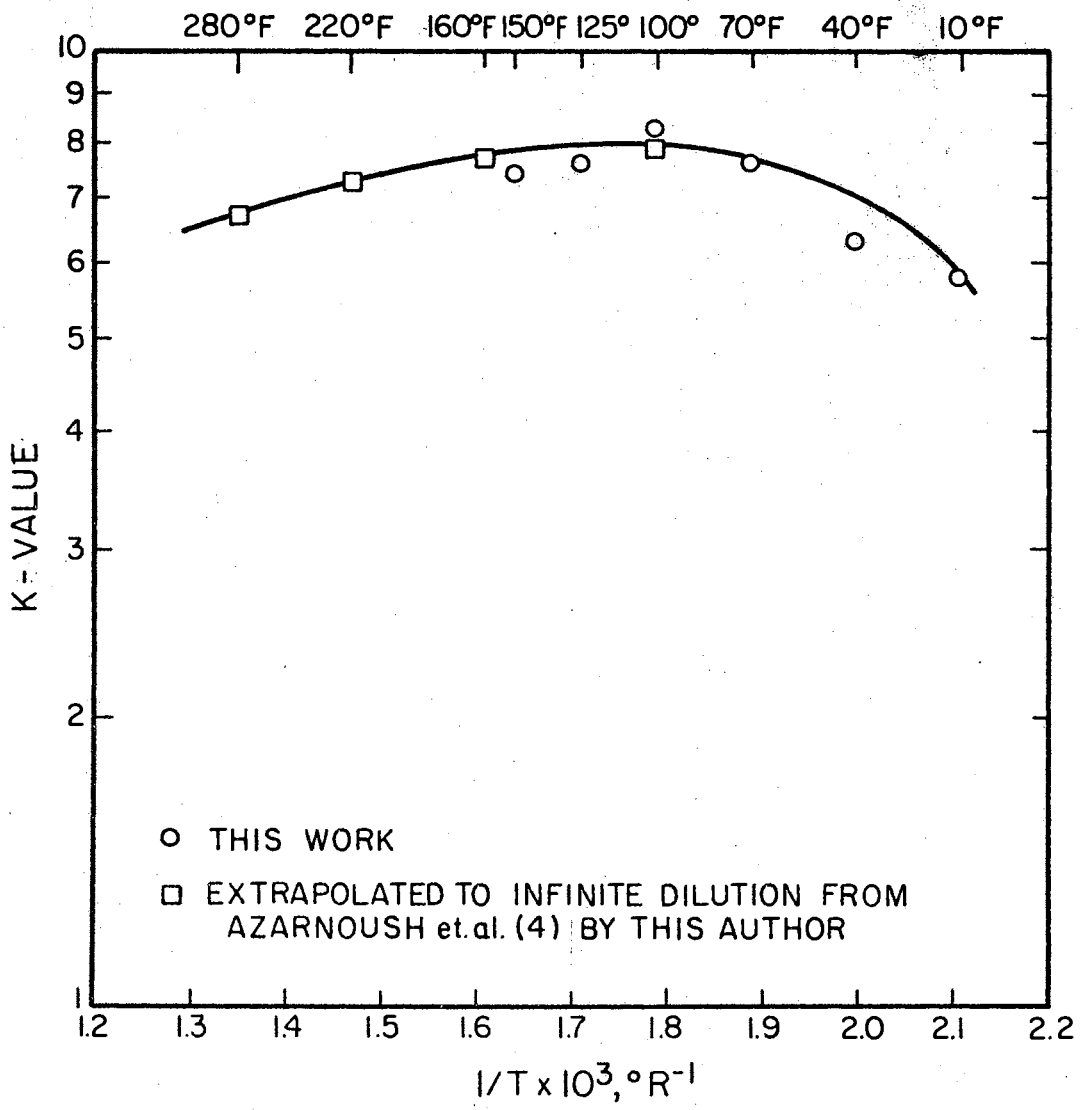

Figure 29. Temperature Dependence of Nitrogen K-Values at Infinite Dilution in the Methane-n-Decane System at 1000 psia

K-Value

Pressure, psia	This Work	From Azarnoosh et.at.*	% Deviation
800	11.42	11.10	2.79
1000	8.303	7.90	4.82
1250	6.625	6.45	2.63
1500	5.560	5.50	1.08
1750	4.647	4.80	-3.30

*Extrapolated to infinite dilution and interpolated pressure-wise from Azarnoosh and McKetta (4) by the present author.

at infinite dilution in the nitrogen-methane-n-decane system at pressure of 1000 psia using Azarnoosh and McKetta's data (4) and the data obtained in this work. The nitrogen K-values from Azarnoosh et. al. (4) were extrapolated to infinite dilution by the present author. Figure 29 shows that a combination of Azarnoosh et. al. K-value data in the higher temperature range and the data obtained chromatographically by this author in the lower temperature range results in a flatter profile of the curve compared to the curve based on the present author's data only (see Figure 18).

Table XV presents a comparison of K-values for nitrogen at infinite dilution in the N_2-CH_4-n-C_{10} system with those predicted by the Chao-Seader correlation (12). The agreement is seen to be good.

The Argon-Methane-n-Decane System. No comparable systems or correlations exist for the argon-methane-n-decane system and, therefore, no comparison of the experimental data was possible for this system. However, since the comparison of the other systems presented in this chapter are satisfactory, the probability that the experimental K-values for the argon-methane-n-decane system are of similar accuracy is rather high.

TABLE XV

COMPARISON OF K-VALUES FOR NITROGEN AT INFINITE DILUTION IN THE N_2-CH_4-n-C_{10} SYSTEM OBTAINED EXPERIMENTALLY WITH THOSE PREDICTED BY THE CHAO-SEADER CORRELATION (12).

	T=125°F		T=150°F	
P-psia	K_{exp}	K_{cs}	K_{exp}	K_{cs}
100	91.70	95.84*	80.23	92.92
200	45.31	47.57*	40.11	46.05
300	29.67	29.61	26.43	27.88
400	20.63	23.29	18.55	22.48
500	16.35	18.70	15.74	18.15
600	14.43	15.60	13.24	15.03
700	11.57	13.23	10.43	12.80
800	10.36	11.37*	8.802	11.05*
1000	7.609	9.124*	7.448	8.860*
1250	6.188	7.312*	5.413	7.088*
1500	4.701	6.049*	4.561	5.865*
1750	4.248	5.176*	3.885	4.990*

*Slightly beyond the limits of the correlation.

The Determination of Liquid Fugacities and Activity Coefficients from Gas Mixture Data and Chromatographically Determined K-values

A general method for determining liquid fugacities and activity coefficients from chromatographic measurements was outlined earlier in Chapter III. Eq. (3-87) shows that the fugacity of a solute in the liquid phase is determined from the measured K-value, the system pressure and the fugacity coefficient of the solute at infinite dilution in the vapor phase.

$$\left(\frac{f^{o}_{L_2}}{x_2}\right)^{\infty} = K_2^{\infty} \Psi_2^{\infty} P \qquad (3\text{-}87)$$

The vapor phase in the systems studied was taken as a solute at infinite dilution in the carrier gas, i.e., in pure methane, assuming that the amount of n-decane in the vapor phase is negligibly small. The later assumption was a valid one considering the very small vapor pressure of n-decane at temperature investigated in this study and was also substantiated by the phase behavior in the methane-n-decane binary system (87).

At the beginning of this chapter, the modification of the B-W-R equation of state for the carbon dioxide-methane system by fitting the A_{012} constant was discussed. The binary volumetric properties predicted by the modified B-W-R equation showed a considerable improvement over the basic B-W-R equation, even when compared with experimental data at temperature and pressure conditions well outside the range of the data used for fitting the A_{012} constant.

Based upon these findings a modified B-W-R equation of state was used for predicting fugacity coefficients of the solute carbon dioxide in methane gas for conditions not covered in the partial volume experiment.

The B-W-R equation of state was also modified for the following systems: nitrogen-methane, ethylene-methane and propane-methane by fitting A_{012} to published mixture volumetric data on the respective systems using a linear least square method.

The binary mixture data were at finite concentrations and were obtained from the literature (47, 56, 72, 87). No data were available for the argon-methane system, and, therefore, the basic B-W-R equation was used for the $Ar-CH_4$ system. The results of the modificiation of the B-W-R equation are summarized below, along with the errors involved in predicting the compressibility factor, Z, by the modified equation.

Mixture	α_{12}	Ave. Abs. % Error in Z	Conditions Covered T-°F	p-psia	Source of Mixture PVT Data
N_2-CH_4	0.8710	0.22	32-212	425-2500	(47)
$C_2H_4-CH_4$	0.9367	0.16	20-167	100-2500	(56,72)
$C_3H_8-CH_4$	0.9769	0.25	100-220	200-2250	(87)

where α_{12} is defined by

$$\alpha_{12} = \frac{A_{012}}{(A_{01}\, A_{02})^{\frac{1}{2}}} \tag{7-2}$$

The results for the CO_2-CH_4 system are given by Eq. (7-1).

The fugacity coefficient of a solute at infinite dilution in a pure gas solvent was derived by integrating the B-W-R equation according to Eq. (3-12); the results of this integration is shown by Eq. (7-3).

$$\ln \psi_2^{\infty} = \frac{1}{RT}\; 2(B_{012}RT - A_{012} - C_{012}/T^2)\rho_1 + \frac{3}{2}(b_1^{2/3} b_2^{1/3} RT$$

$$- a_1^{2/3} a_2^{1/3})\rho_1^2 + \frac{3}{5}(\alpha_1 a_1^{2/3} a_2^{1/3} + a_1 \alpha_1^{2/3} \alpha_2^{1/3})\rho_1^5$$

$$+ \frac{3}{T^2}\, \rho_1^2\, C_1^{2/3} C_2^{1/3}\, \left(\frac{1-e^{-\gamma_1 \rho_1^2}}{\gamma_1 \rho_1^2} - \frac{e^{-\gamma_1 \rho_1^2}}{2}\right)$$

$$-\frac{2}{T^2}\rho_1^2 C_1 \gamma_{12}\left[\frac{1-e^{-\gamma_1\rho_1^2}}{\rho_1^2}-\left(\gamma_1+\frac{\gamma_1^2\rho_1^2}{2}\right)e^{-\gamma_1\rho_1^2}\right]-\ln Z \qquad (7\text{-}3)$$

The mixture constants in Eq. (7-3) were determined according to Eqs. (3-15) and (3-16) using pure component constants except for A_{012} which was determined to fit mixture data. The pure component constants for the B-W-R equation were obtained from the literature; the references are listed below.

Component	Reference for B-W-R- constants
Methane	(26)
Carbon dioxide	(22)
Nitrogen	(19)
Argon	(106)
Ethylene	(8)
Propane	(7)

The fugacity coefficient of carbon dioxide at infinite dilution in methane at 100°F and 150°F was determined from the partial volume data. The deviations between the fugacity coefficients predicted by the modified B-W-R equation of state and those determined by a numerical integration of partial volumes at infinite dilution (Eq. (3-12)) were:

Isotherm	Maximum % Deviation	Average % Deviation
100°F	2.33(@ 800 psia)	1.20
150°F	-2.10(@ 1250 psia)	1.74

The values of $(f^o_{L_2}/x_2)^\infty$ based on experimental data for the five ternary systems: CO_2-CH_4-n-C_{10}, N_2-CH_4-n-C_{10}, Ar-CH_4-n-C_{10}, C_2H_2-CH_4-n-C_{10} and C_3H_8-CH_4-n-C_{10} are shown in Figures 30 through 34.

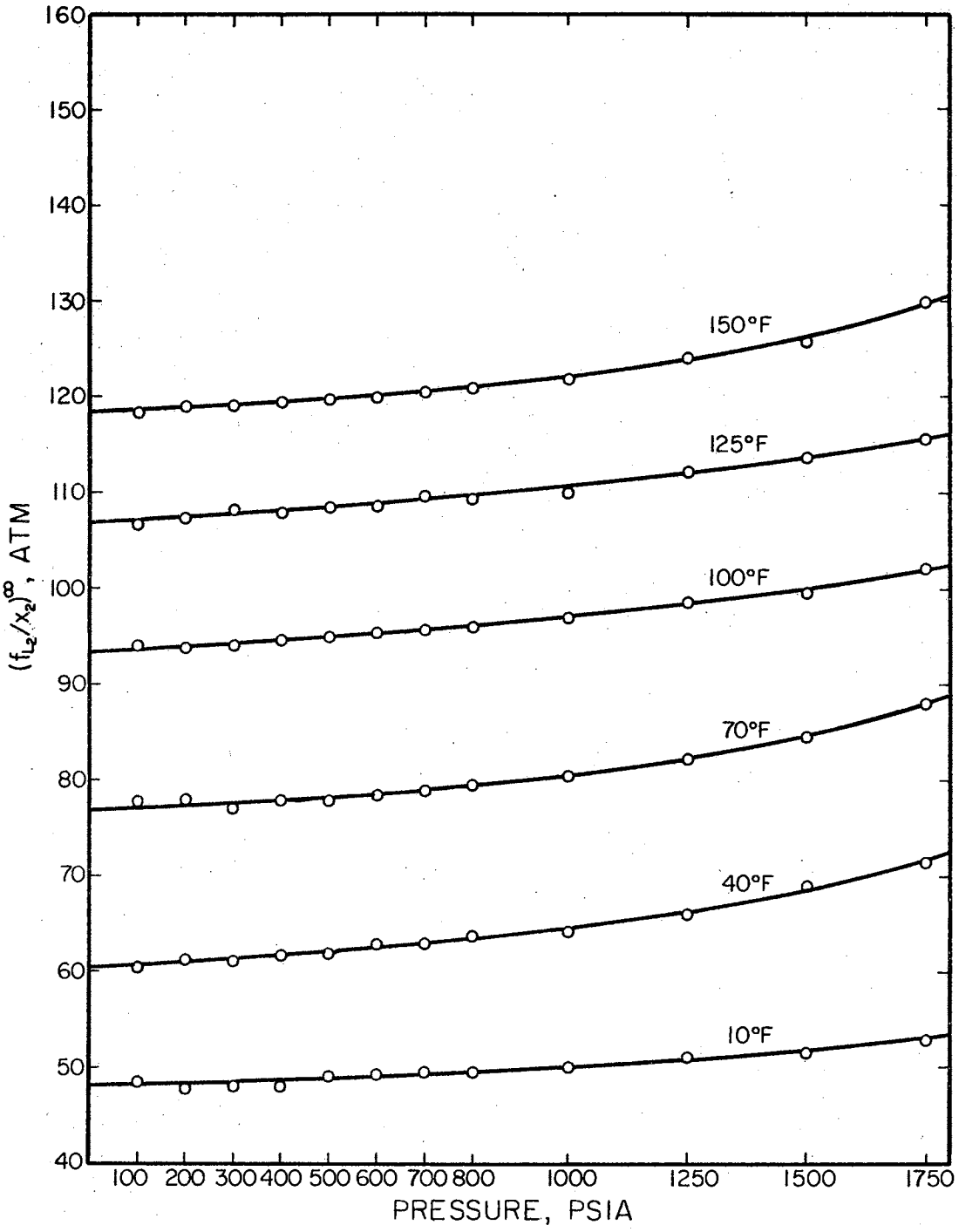

Figure 30. Liquid Phase Fugacity of Carbon Dioxide at Infinite Dilution in the Methane-n-Decane System

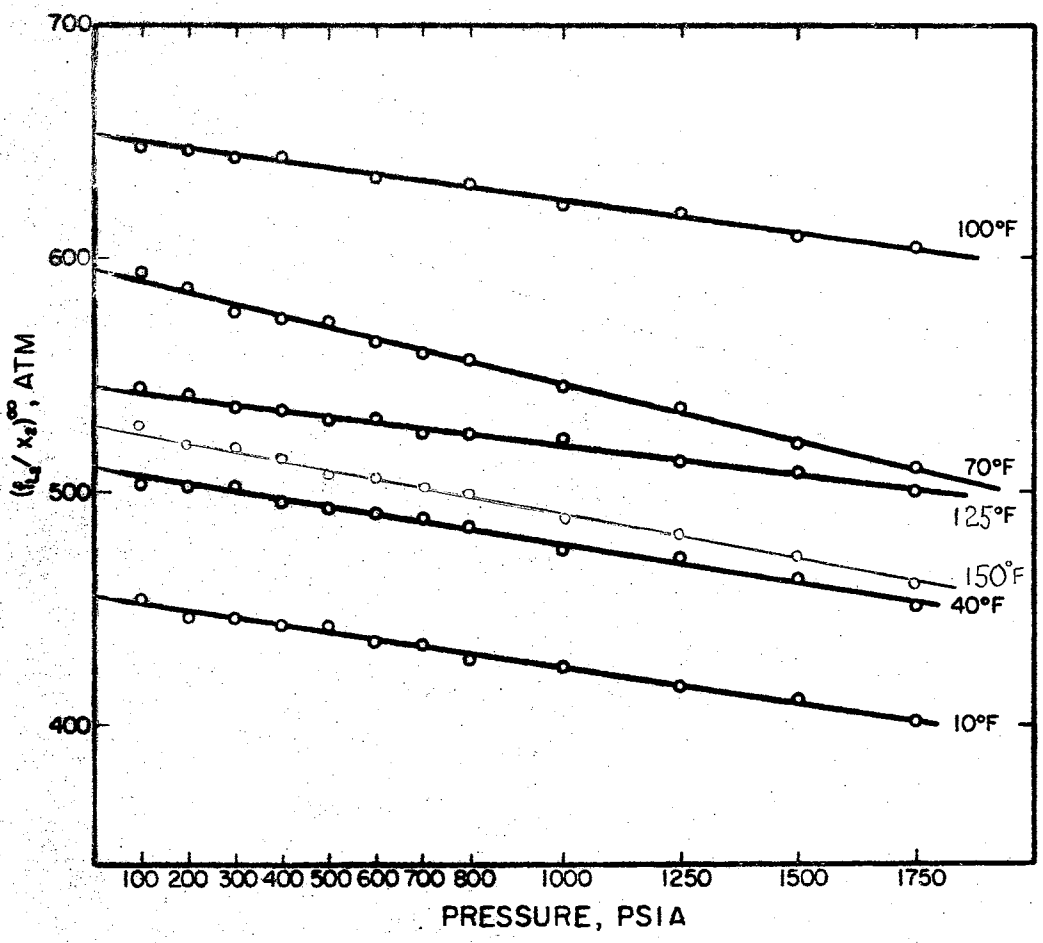

Figure 31. Liquid Phase Fugacity of Nitrogen at Infinite Dilution in the Methane-n-Decane System

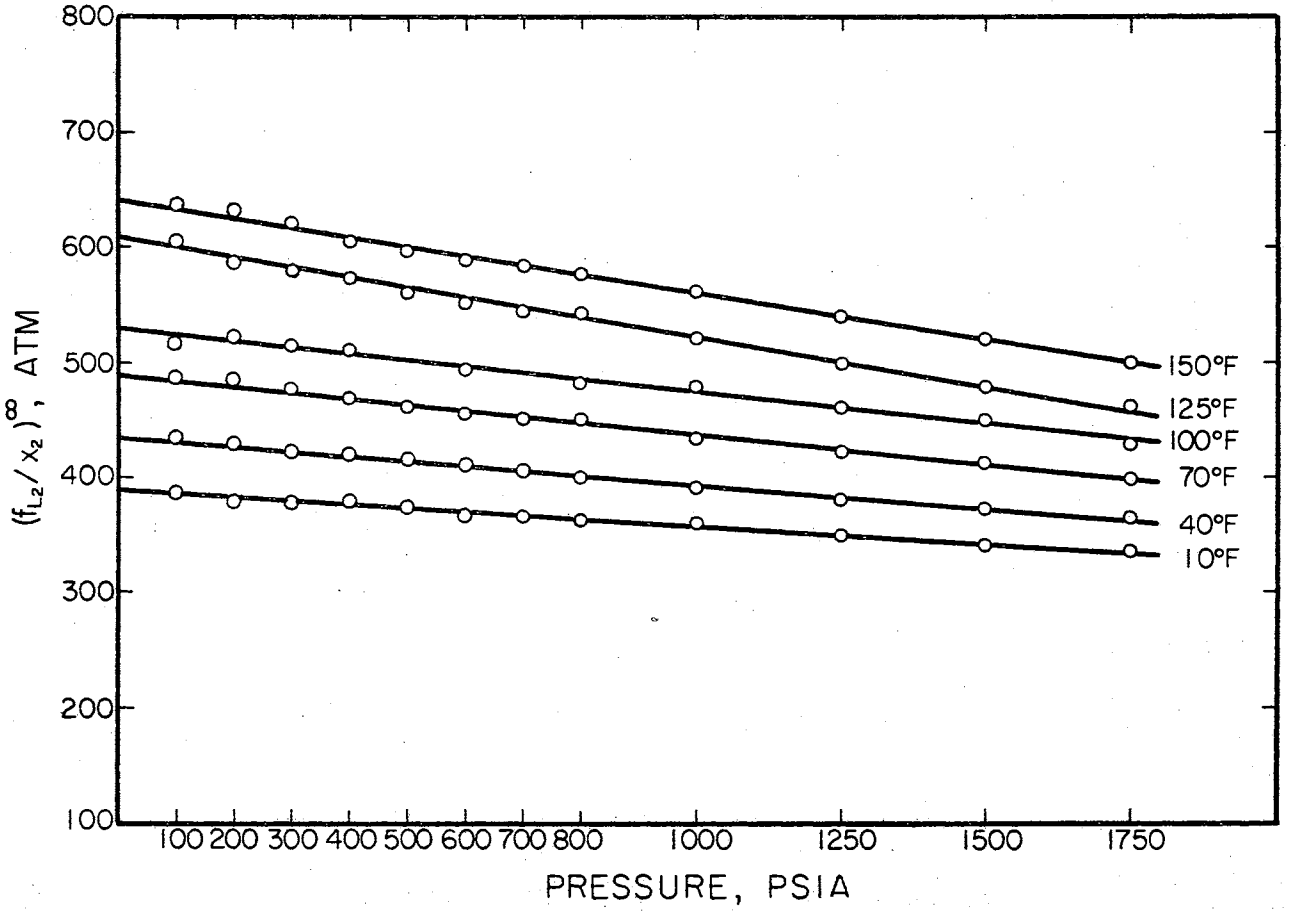

Figure 32. Liquid Phase Fugacity of Argon at Infinite Dilution in the Methane-n-Decane System

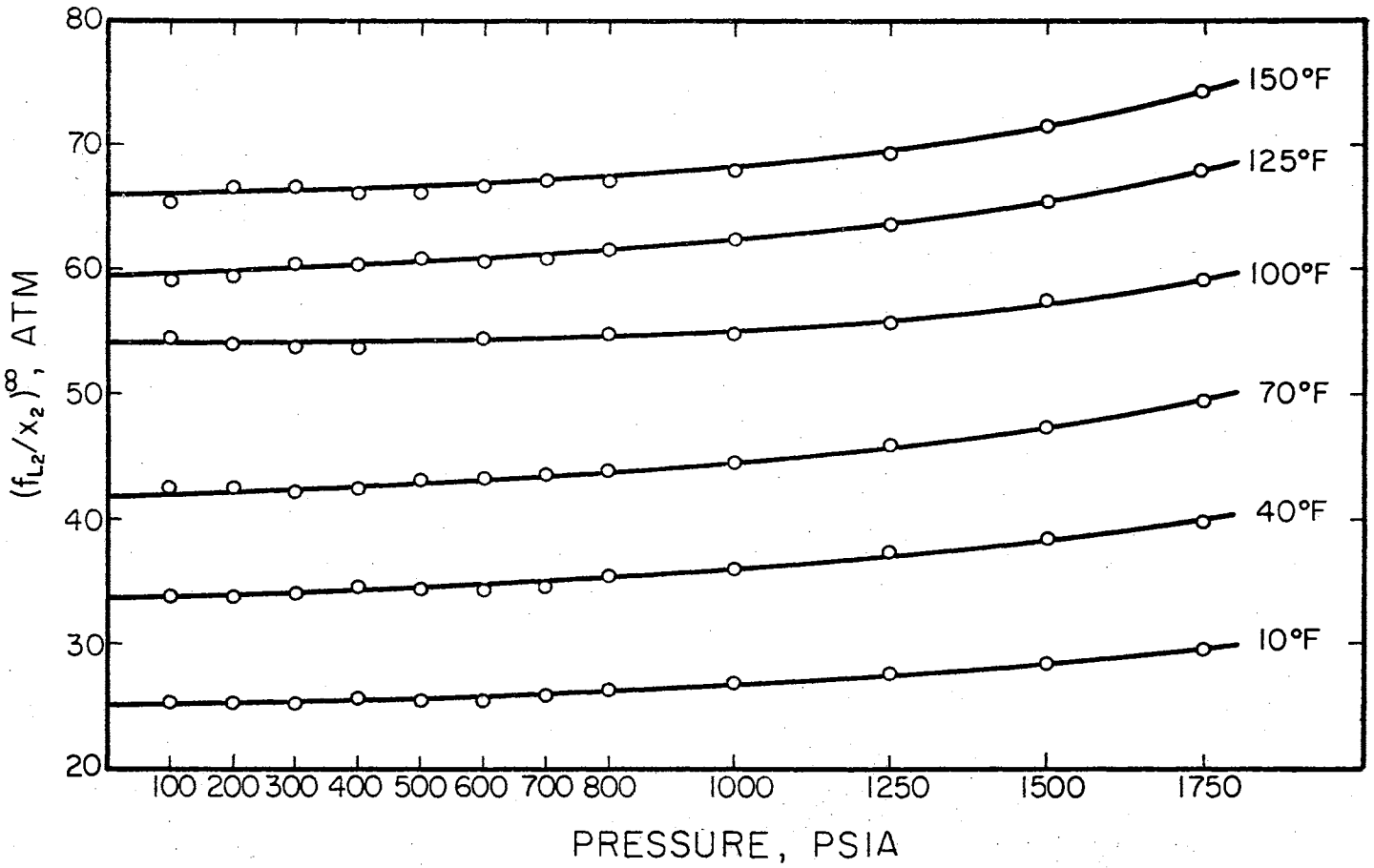

Figure 33. Liquid Phase Fugacity of Ethylene at Infinite Dilution in the Methane-n-Decane System

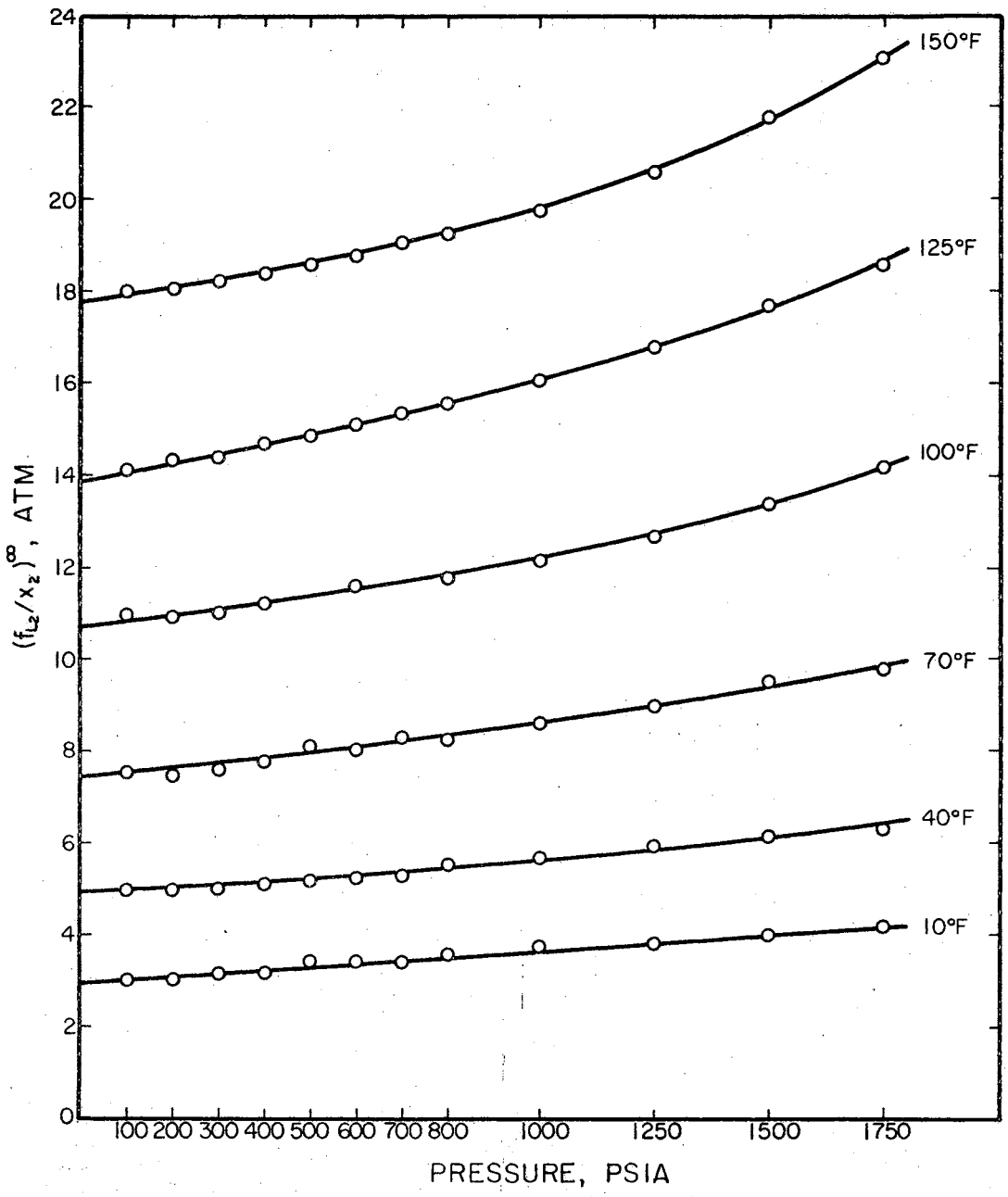

Figure 34. Liquid Phase Fugacity of Propane at Infinite Dilution in the Methane-n-Decane System

The standard state liquid fugacities were obtained from the plot shown in Figures 30 through 34 by extrapolating the data according to Eq. (3-89) as shown in Figure 3. Rigorously, the extrapolation should be to the vapor pressure of n-decane at the system temperature, but as was explained in Chapter III, the vapor pressure of n-decane at temperatures employed in this study is so small that the extrapolation could be carried out to zero pressure with a negligibly small error (see Eq. (3-91)). Consequently, the extrapolated values as shown in Figures 30 through 34 are regarded as standard state fugacities at zero reference pressure.

The standard state liquid fugacities for the five ternary systems are listed in Table XVI.

TABLE XVI

STANDARD STATE LIQUID FUGACITIES OF

THE FIVE EXPERIMENTAL SYSTEMS

	$f^{o}_{L_2}$ - psia					
System	10°F	40°F	70°F	100°F	125°F	150°F
CO_2-CH_4-C_{10}	682	889	1130	1370	1570	1740
N_2-CH_4-C_{10}	6690	7500	8740	9600	8010	7800
Ar-CH_4-C_{10}	5730	6410	7160	7640	9100	9420
C_2H_2-CH_4-C_{10}	368	492	617	715	875	967
C_3H_8-CH_4-C_{10}	42.6	72.1	109	157	203	260

The unsymmetric activity coefficients for the five ternary systems at each temperature and pressure condition were calculated via Eq. (3-88) using the experimental data. Figures 35 through 40 show the unsymmetric activity coefficients at infinite dilution for the five ternary systems

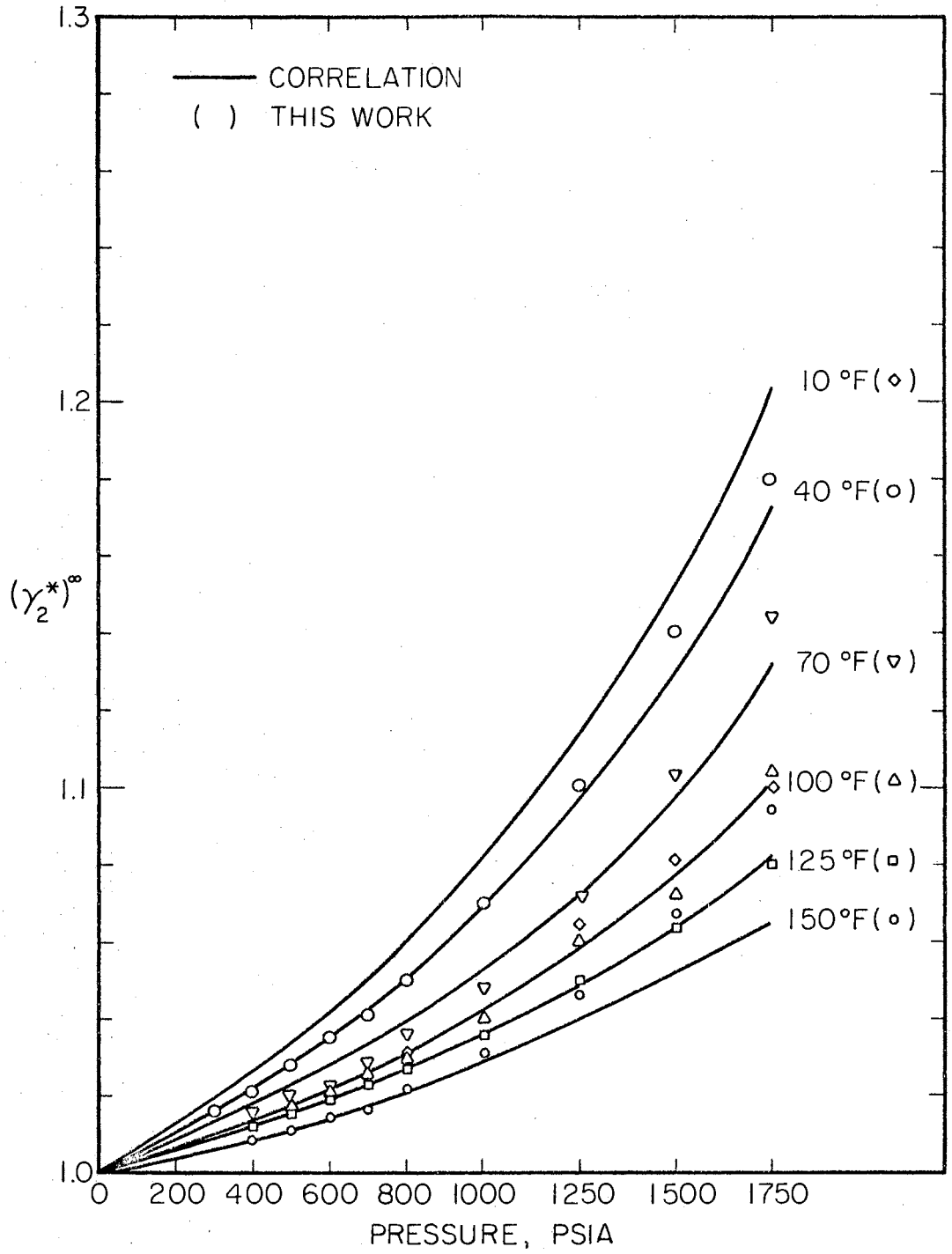

Figure 35. Activity Coefficient of Carbon Dioxide at Infinite Dilution in the Methane-n-Decane System

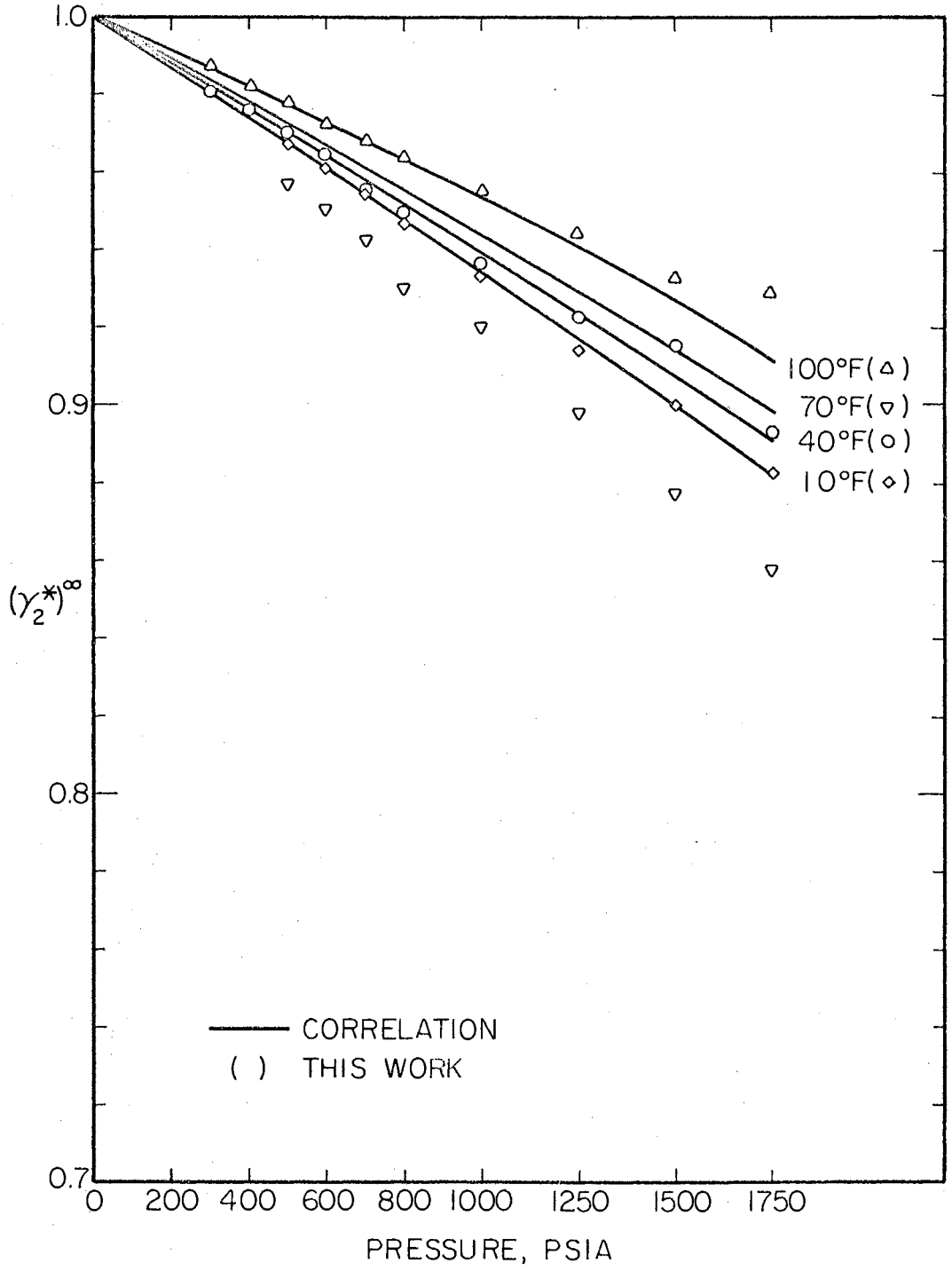

Figure 36. Activity Coefficient of Nitrogen at Infinite Dilution in the Methane-n-Decane System

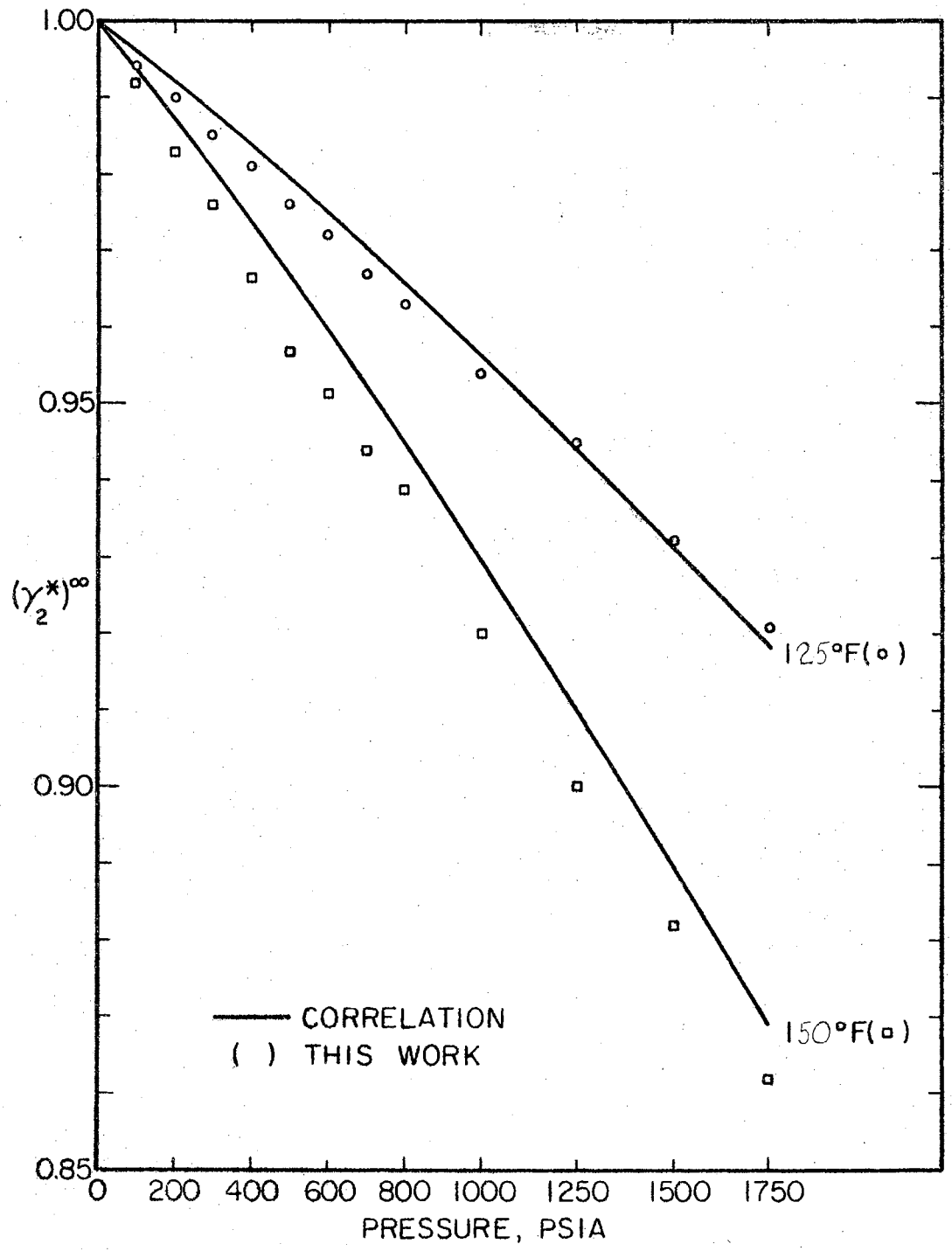

Figure 37. Activity Coefficient of Nitrogen at Infinite Dilution in the Methane-n-Decane System, High Temperature Range

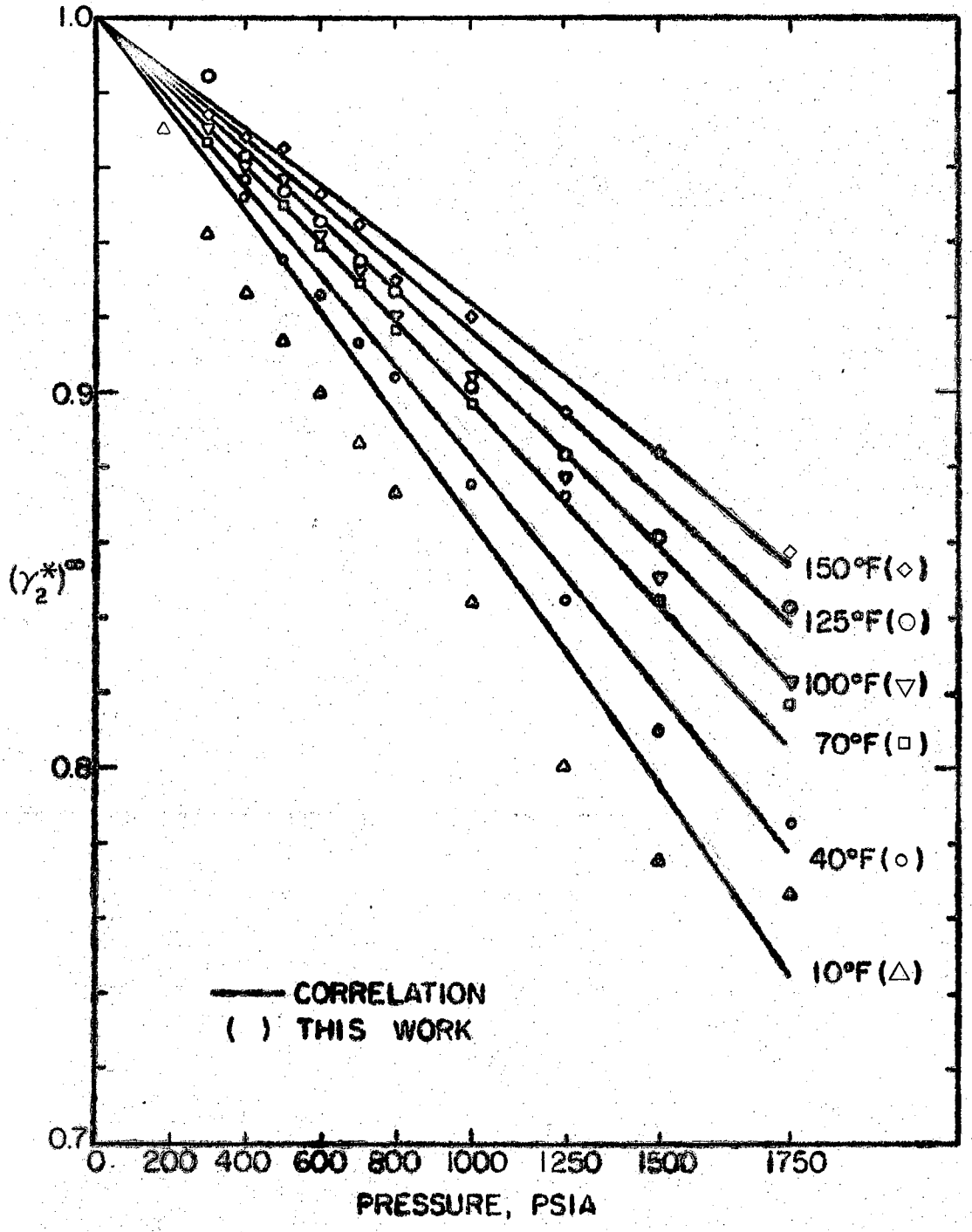

Figure 38. Activity Coefficient of Argon at Infinite Dilution in the Methane-n-Decane System

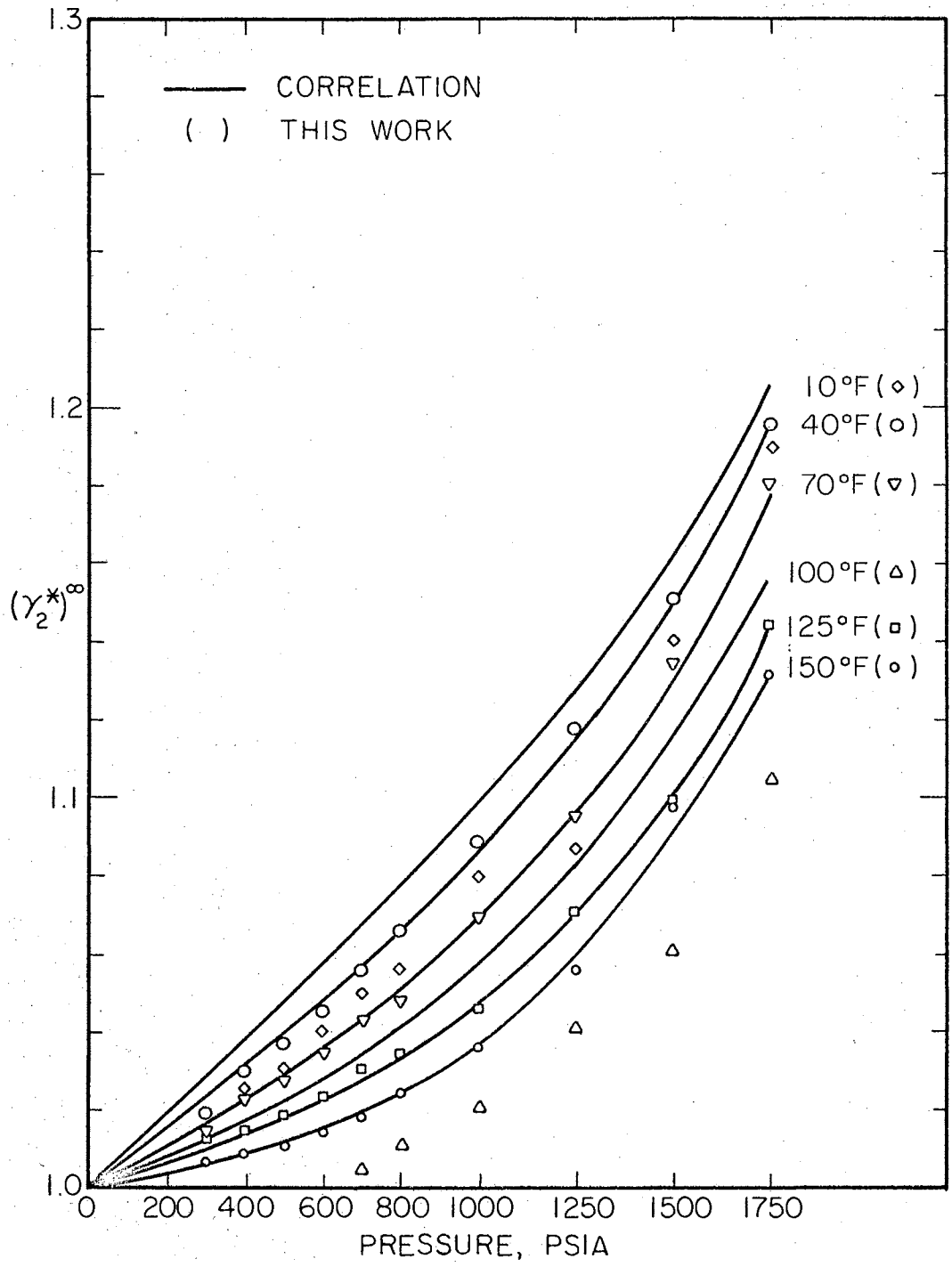

Figure 39. Activity Coefficient of Ethylene at Infinite Dilution in the Methane-n-Decane System

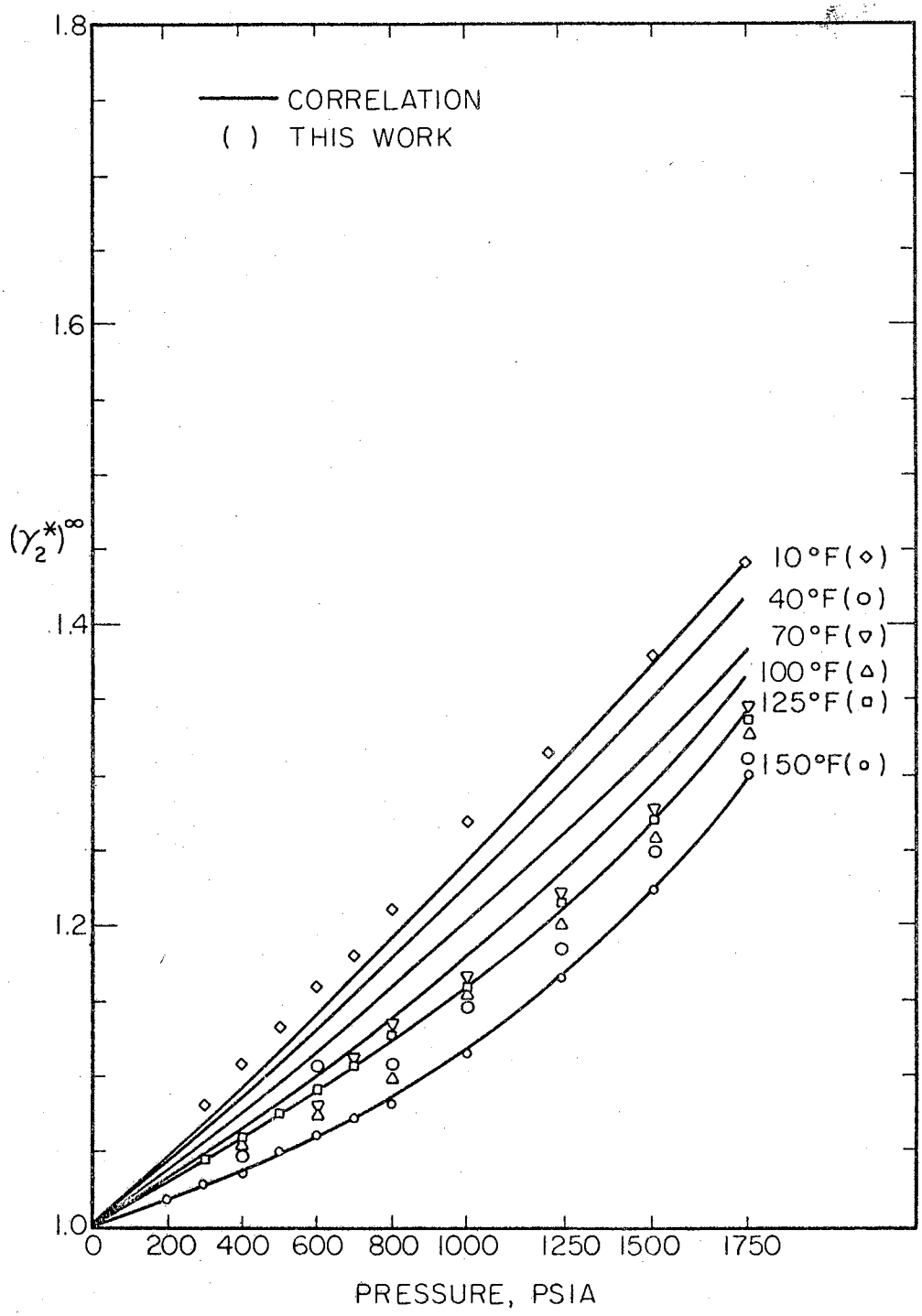

Figure 40. Activity Coefficient of Propane at Infinite Dilution in the Methane-n-Decane System

at $10^{o}F$, $40^{o}F$, $70^{o}F$, $100^{o}F$, $125^{o}F$, and $150^{o}F$ and pressures from 100 to 1750 psia.

Correlational Results for Liquid Phase Activity Coefficient

In Chapter III a general framework for correlation of activity coefficients in liquid solution at high pressures was presented. The various expressions for the activity coefficients were presented for the general case of a multi-component system and then reduced to the simple case of a binary solution.

The general correlation for the activity coefficient was applied to the experimental data first to fit the interaction constants of the activity coefficient equation for the five ternary systems and second to test the activity coefficients predicted by the correlation against those obtained from the experimental data.

One of the characteristics of the proposed correlation is that the interaction constants appearing in the equation can be determined from the respective binary phase equilibrium data. In this study the activity coefficients of the ternary system carbon dioxide-methane-n-decane were predicted by the correlation using interaction constants determined from binary equilibrium data on methane-n-decane (4, 87), carbon dioxide-n-decane (85), and carbon dioxide-methane (25).

The systems studied during the course of this work consisted of a solute "2" at infinite dilutions in a saturated methane solution (methane-component "1", n-decane, the solvent-component "3"). The Scatchard-Hildebrand activity coefficient in the unsymmetric convention for the systems studied in this work can be readily obtained from Eq. (3-60), recalling that for the above system $\Phi_1 = 1-\Phi_3$,

$$\ln(\gamma_2^{*\infty})_{SH} = 2\frac{V_2}{RT}\Phi_1(a_{23}-a_{12}) + \frac{V_2}{RT}\left[\Phi_1^2 a_{11} + a_{33}(\Phi_3^2 - 1) + 2\Phi_1\Phi_3 a_{13}\right] \tag{7-4}$$

Substituting the following into Eq. (7-4)

$$a_{11} = \delta_1^2$$
$$a_{22} = \delta_2^2$$
$$a_{33} = \delta_3^2$$

where δ_i is the solubility parameter of component i as defined by Hildebrand (91),

$$\ln(\gamma_2^{*\infty})_{SH} = 2\frac{V_2}{RT}\Phi_1(a_{23}-a_{12}) + \frac{V_2}{RT}\left[\Phi_1^2\delta_1^2 + \delta_3^2(\Phi_3^2-1) + 2\Phi_1\Phi_3 a_{13}\right] \tag{7-5}$$

Eq. (7-4) reduces to the following equation when a_{ij} is approximated by the geometric mean rule,

$$\ln \gamma_2^{*\infty} = \frac{V_2}{RT}\left[(\delta_2-\bar{\delta})^2 - (\delta_2-\delta_3)^2\right] \tag{7-6}$$

where

$$\bar{\delta} = \sum_i \Phi_1\delta_1 \tag{7-7}$$

Eq. (7-6) is obtained from Hildebrand's (36) equation for activity in a multicomponent system that was used by Chao and Seader (12) in their correlation,

$$\ln \gamma_i = \frac{V_i}{RT}(\delta_i - \bar{\delta})^2 \tag{7-8}$$

The expression for the pressure dependent activity coefficients for the experimental systems is derived from the general correlation given by Eq. (3-93) by taking the limit $x_2 \to 0$ noting that for these systems $P_{vp} \cong 0$ as shown previously, the resulting expression is,

$$\ln \gamma_2^{*\infty} = \frac{2V_2}{RT} \Phi_1(a_{23}-a_{12}) + \frac{V_2}{RT}\left[\Phi_1^2 \delta_1^2 + \delta_3^2(\Phi_3^2 - 1) + 2\,\Phi_1\Phi_3 a_{13}\right]$$

$$+ \ln \frac{V_3}{V_m} - \Phi_1\left(\frac{V_2}{V_1} - \frac{V_2}{V_3}\right) + \frac{1}{RT}\int_o^P \bar{V}_{L_2}^{\infty}\, dp \qquad (7\text{-}9)$$

where,

a_{12} = interaction constant between methane and solute

a_{13} = interaction constant between methane and n-decane

a_{23} = interaction constant between solute and n-decane

The parameters δ_i - solubility parameter, V_i - molar volume, V_m - molar volume of saturated methane-n-decane solution and x_1 - mole fraction of methane in the saturated methane-n-decane solution, were obtained from the literature; the literature references are listed below.

Parameter	Reference
δ_1, δ_3, V_1, V_3	(12)
δ_2, V_2 for C_2H_2 and C_3H_8	(12)
δ_2, V_2 for CO_2, N_2 and Ar	(36)
x_1	(87, 4)

The left hand side of Eq. (7-9) is evaluated from experimental data via Eq. (3-88).

$$\gamma_2^{*\infty} = \frac{K_2^{\infty}\,\psi_2^{\infty}\,P}{f_{L_2}^{o}} \qquad (3\text{-}88)$$

The right hand side of Eq. (7-9) contains the Scatchard-Hildebrand term, the Flory-Huggins term and the pressure term.

The liquid partial volumes of the solute at infinite dilution in the methane-n-decane system are required in the evaluation of the pressure term in Eq. (7-9). However, there are few data or correlations in the literature (17, 75, 99) for liquid partial volumes. The correlation

of Chueh and Prausnitz (17) for partial volumes in saturated liquids was used in this study. This correlation predicts partial volumes of a solute in a saturated liquid solution as a function of temperature, concentration and critical parameters of the solution using the modified Redlich-Kwong equation. The correlation was tested successfully by Chueh and Prausnitz (17) for the saturated liquid solutions of the n-butane-carbon dioxide and propane-methane systems and by this author for the methane-n-pentane and methane-n-decane systems and found to predict the experimental data of these systems (87) at temperatures of 100°F, 160°F and 220°F and pressures up to 2000 psia. The average absolute errors were 3.3% for the methane-n-pentane system and 2.8% for the methane-n-decane system.

The Redlich and Kwong equation of state is

$$P = \frac{RT}{v-b} - \frac{a}{T^{0.5}\, v(v+b)} \tag{7-10}$$

where,

$$a = \frac{\Omega_a R^2 T_c^{2.5}}{P_c} \tag{7-11}$$

$$b = \frac{\Omega_b R T_c}{P_c} \tag{7-12}$$

Ω_a and Ω_b are dimensionless constants. In this work Ω_a and Ω_b of pure n-decane were evaluated by fitting Eqs. (7-10) through (7-12) to the P-V-T data of saturated n-decane (87) at 100°F to 400°F using non-linear least squares method. The evaluated constants for n-decane were: Ω_a = 0.3779 and Ω_b = 0.0702.

The Chueh-Prausnitz correlation for liquid partial volume (17) is,

$$\bar{v}_k = \frac{\frac{RT}{v-b}\left(1 + \frac{b_k}{v-b} - \frac{2\left(\sum_i x_i a_{ki}\right) - a b_k/(v+b)}{v(v+b)T^{\frac{1}{2}}}\right)}{\frac{RT}{(v-b)^2} - \frac{a}{T^{\frac{1}{2}}}\left[\frac{2v+b}{v^2(v+b)^2}\right]} \tag{7-13}$$

where,

$$a = \sum_i \sum_j x_i x_j a_{ij} \quad [a_{ij} \neq (a_i a_j)^{\frac{1}{2}}] \tag{7-14}$$

$$b = \sum_i x_i b_i \tag{7-15}$$

$$a_{ii} = \frac{\Omega_{a_i} R^2 T_{c_i}^{2.5}}{P_{c_i}} \tag{7-16}$$

$$b_i = \frac{\Omega_{b_i} R T_{c_i}}{P_{c_i}} \tag{7-17}$$

$$a_{ij} = \frac{0.25(\Omega_{a_i} + \Omega_{a_j}) R\, T_{c_{ij}}^{1.5} (v_{c_i} + v_{c_j})}{0.291 - 0.04(\omega_i + \omega_j)} \tag{7-18}$$

and

$$T_{c_{ij}} = (T_{c_{ii}} T_{c_{jj}})(1 - k_{ij}) \tag{7-19}$$

where T_c, P_c and v_c are the critical temperature, pressure and volume respectively; ω is the acentric factor; Ω_a and Ω_b the dimensionless constant in the Redlich-Kwong equation. The Chueh-Prausnitz correlation was modified for the methane-n-decane and carbon dioxide-n-decane systems by evaluating the best k_{12} (see Eq. (7-19)) for those systems using the non-linear least squares method and liquid solution volumetric data of the respective systems reported in the literature (85, 87). The evaluated k_{12} are given below.

System	k_{12}	Conditions Covered		Source of Data
		T - °F	P - psia	
CH_4-n-C_{10}	0.105	100-160	60-2000	(87)
CO_2-n-C_{10}	0.152	40-160	50-2000	(85)

The partial volumes of the solutes at infinite dilution in the methane-n-decane system determined by the Chueh-Prausnitz correlation

(17) changed slightly with system pressure (or with methane concentration). This phenomenon was partly explained by the fact that the system pressures were considerably removed from the critical pressures of the methane-n-decane system. The critical pressures of the methane-n-decane system were:

System Temperature - ^{o}F	Critical Pressure - psia
10	4990
40	5020
70	5110
100	5310
125	5160
150	5100

while the maximum system pressure was 1750 psia. Partial volume data of liquid hydrocarbon solutions reported by Sage and Lacey (87) also show that in the range of bubble-point pressures below about 60% of the solution critical pressures the change of solute partial volume with pressure is very small.

In the present work the experimental activity coefficients of the various solutes were used to evaluate $(a_{23} - a_{12})$ in Eq. (7-9) based on least squares fit to the activity coefficients. The interaction constant between methane and n-decane a_{13} is independent of the nature of the solute used; a_{13} was, therefore, determined from binary solution phase equilibrium information on methane-n-decane.

Eq. (3-94) expresses the proposed correlation for a binary mixture. Substituting $a_{11} = \delta_1^2$ and $a_{22} = \delta_2^2$ into Eq. (3-94),

$$\ln\left(\frac{K_2 \Psi_2 P}{f_{i_2}}\right) = \frac{V_2}{RT}(\Phi_1^2 - 1)(\delta_1^2 + \delta_2^2 - 2a_{12}) + \ln \frac{V_1}{V_m}$$

$$-\Phi_2\left(1 - \frac{V_2}{V_1}\right) + \frac{1}{RT}\int_o^P \bar{V}_{L_2}\, dp \qquad (7\text{-}20)$$

The constant a_{12} for a binary system can be evaluated by fitting Eq. (7-20) to binary solution phase equilibrium data using the linear least squares method. The procedure is similar to that used for fitting Eq. (7-9) to experimental data of ternary systems obtained in this work, the only difference is that Eq. (7-20) is expressed for a solute at finite concentrations.

The fugacity coefficient of the solute in the vapor phase on the left hand side of Eq. (7-20), Ψ_2, was evaluated by the Redlich-Kwong equation of state modified by Chueh and Prausnitz. The vapor liquid equilibrium coefficient K_2, was obtained from the binary phase equilibrium data and the standard state fugacity $f^o_{L_2}$, was determined by graphical extrapolation of $(K_2\Psi_2 P)$ to infinite dilution according to Eq. (3-84).

The constant a_{12} for methane-n-decane interaction was evaluated according to the procedure outlined above. Vapor-liquid equilibrium data of the methane-n-decane system at temperatures of 32^oF to 160^oF and pressures up to 2000 psia were taken from the literature (6, 87). Liquid partial volumes of methane in n-decane were evaluated from methane-n-decane solution volumetric data (6, 87). The constant k_{12} previously determined by this author for the methane-n-decane interaction was used in the Redlich-Kwong equation to predict Ψ_2.

Having determined the methane-n-decane interaction constant (a_{13} in Eq. (7-9)), the interaction constants of solute-methane and solute-n-decane (a_{12} and a_{23} in Eq. (7-9)) were fitted to the experimentally determined activity coefficients based on data from the present work.

Basically the same procedure used to evaluate the methane-n-decane

interaction constant can be used for each binary constant, a_{ij}, in Eq. (7-9), providing the appropriate binary phase equilibrium data is available. This method was employed with the carbon dioxide-methane-n-decane system (in addition to determining a_{12} and a_{23} from the present experimental data).

The binary interaction constant of carbon dioxide-n-decane was determined using phase equilibrium data of carbon dioxide-n-decane system at temperatures of $40^{\circ}F$ to $160^{\circ}F$ and pressures up to 2000 psia taken from Reamer et. al. (85). Liquid partial volumes of carbon dioxide in n-decane were evaluated from volumetric data on the carbon dioxide-n-decane system (85). The constant k_{12}, previously determined by this author for the carbon dioxide-n-decane system was used in the Redlich-Kwong equation to predict the vapor phase fugacity coefficient.

The carbon dioxide-methane interaction constant was determined from Donnelly et. al. data (25) at $29^{\circ}F$ and $8^{\circ}F$ and pressures up to 1000 psia. Liquid partial volumes were determined via Chueh-Prausnitz correlation (17) and k_{12} for carbon dioxide-methane was taken from the literature (15). Thus, all three binary interaction constants in Eq. (7-9) for the CO_2-CH_4-n-C_{10} system were determined independently of the ternary system.

The procedure used for predicting the activity coefficient of the ternary systems in this work is summarized below.

1. The CH_4-n-C_{10} interaction constant a_{13} was determined using Eq. (7-20) and binary phase equilibrium data (87) (6) by least square fit. The constant a_{13} was used for the five experimental systems.
2. Eq. (7-9) was fitted to the activity coefficient data of the five ternary systems in order to evaluate the combined constant

$(a_{23}-a_{12})$ for each system.

3. The activity coefficients for the five ternary systems predicted by the correlations were compared to the activity coefficient obtained experimentally.

4. In addition to the above, all binary interaction constants in Eq. (7-9) were determined for the ternary CO_2-CH_4-n-C_{10} from phase equilibrium data on the constituent binary systems (25, 85). The binary constants, a_{ij}, were substituted into Eq. (7-9) and the predicted activity coefficients were compared to the experimental data.

The fitting of the constants in Eq. (7-9) was based on 70 experimental points for each ternary system.

The calculations were carried out on an IBM 7040 digital computer. The Fortran listings of the programs are given in Appendix H.

The constants used in the empirical correlations for the five ternary systems obtained from the fitting of the data are tabulated in Table XVII.

TABLE XVII

CONSTANTS OF THE ACTIVITY COEFFICIENT CORRELATIONS FOR THE FIVE TERNARY SYSTEMS.

System	$(a_{23}-a_{12})$ - cal/cc*	a_{13} - cal/cc**
CO_2-CH_4-n-C_{10}	-4.696	40.79
N_2-CH_4-n-C_{10}	-15.41	40.79
Ar-CH_4-n-C_{10}	-28.12	40.79
C_2H_2-CH_4-η-C_{10}	7.664	40.79
C_3H_8-CH_4-n-C_{10}	11.91	40.79

*From experimental data on ternary solution.

**From CH_4-n-C_{10} binary solution data (6, 87).

The interaction constants for the CO_2-n-C_{10} and CH_4-CO_2 binaries determined by fitting Eq. (7-20) to the respective phase equilibrium data (25,85) are given below.

CO_2-n-C_{10}	a_{23} = 45.389 cal/cc
CH_4-CO_2	a_{12} = 45.505 cal/cc

The numerical value of $(a_{23}-a_{12})$ obtained from the experimental data on the ternary system carbon dioxide-methane-n-decane is -4.696 cal/cc compared with -4.116 cal/cc determined from binary phase equilibrium data of the carbon dioxide-n-decane and methane-carbon dioxide systems. This agreement seems quite good and indicates that phase behavior of the ternary system carbon dioxide-methane-n-decane can be predicted using the proposed correlation with all interaction constants determined from data on the constituent binary systems. The value of such a prediction scheme is obvious.

Comparison of Experimental Activity Coefficients with Those Predicted by the Correlations

The experimentally-based a_{12}, a_{13} and a_{23} for each of the five ternary systems were used with the correlation (Eq. (7-9)) to predict the unsymmetric activity coefficients of the solute at infinite dilution in the methane-n-decane system.

The following equation is derived from Eq. (7-9):

$$\ln K_2^{\infty} = \frac{2V_2}{RT}\Phi_1(a_{23}-a_{12}) + \frac{V_2}{RT}\left[\Phi_1\delta_1^2 + \delta_3^2(\Phi_3^2-1) + 2\Phi_1\Phi_3 a_{13}\right]$$

$$+ \ln \frac{V_3}{V_m} - \Phi_1 \left(\frac{V_2}{V_1} - \frac{V_2}{V_3}\right) + \frac{1}{RT} \int_o^P \bar{V}_{L_2}^{\infty} dp - \ln \psi_2^{\infty} - \ln P + \ln f_{L_2}^{o} \quad (7\text{-}21)$$

The vapor-liquid equilibrium constant of a solute at infinite dilution, K_2^{∞}, can be predicted by Eq. (7-21) providing a correlation for the standard state liquid fugacity $f_{L_2}^{o}$ (defined as Henry's law constant of solute "2") is available. Since $f_{L_2}^{o}$ was determined in this work experimentally, a more meaningful test of the correlation is a comparison of the activity coefficients predicted by Eq. (7-9) with the experimentally determined ones, thus eliminating the use of a correlation for predicting Henry's law constant. A direct comparison of the predicted activity coefficients to the experimental ones would, therefore, make it possible to assess the correlation model based on the Scatchard-Hildebrand and Flory-Huggins theories more meaningful. Furthermore, if the experimental value of $f_{L_2}^{o}$ is used in Eq. (7-21), this equation becomes virtually identical to Eq. (7-9) and therefore, the error involved in predicting the activity coefficient via Eq. (7-9) becomes identical to that involved in predicting the K-value by Eq. (7-21).

Figures 35 to 40 show comparisons of the predicted activity coefficients along with the experimentally determined ones for the five ternary systems. The comparisons illustrate the capability of the correlation to predict satisfactorily the activity coefficients for the five experimental systems.

The maximum errors, average absolute errors and average errors involved in predicting the experimental unsymmetric activity coefficients by the proposed correlation for the systems studied in this work are listed in Table XVIII.

Table XVIII reveals that the average error in predicting the experimental data ranges from 2.02% for the CO_2-CH_4-n-C_{10} system to 4.47% for

TABLE XVIII

ERRORS IN PREDICTING THE EXPERIMENTAL UNSYMMETRIC ACTIVITY COEFFICIENTS OF FIVE TERNARY SYSTEMS

System	Max. % Error	Ave. Abs. % Error	Ave. % Error
CO_2-CH_4-n-C_{10}	9.5 (10°, 1750 psia)	2.0	-0.5
N_2-CH_4-n-C_{10}	4.7 (70°, 1750 psia)	3.3	-0.5
A_r-CH_4-n-C_{10}	12.9 (100°, 1500 psia)	4.5	-2.6
C_2H_2-CH_4-n-C_{10}	5.3 (100°, 1500 psia)	4.1	-0.2
C_3H_8-CH_4-n-C_{10}	8.5 (40°, 1250 psia)	2.2	-0.1

where, $\%\ \text{Error} = \frac{\text{Act.corr.} - \text{Act. exp.}}{\text{Act. exp.}} \times 100$

for the Ar-CH_4-n-C_{10} system, and that on the average, the activity coefficients predicted by the correlation are slightly lower than the experimental ones for all the systems studied.

A comparison between the correlation for the CO_2-CH_4-n-C_{10} system using (a_{23}-a_{12}) fitted to ternary data of that system (correlation A) and the correlation using a_{23} and a_{21} obtained by fitting Eq. (7-10) to CO_2-n-C_{10} and CH_4-CO_2 binary data respectively (25, 85). (Correlation B) is shown below:

System: CO_2-CH_4-n-C_{10}

Correlation A - (a_{23}-a_{12}) fitted to ternary data.			Correlation B - All binary interaction constants obtained from binary data.		
Ave.Abs. % Error	Max. % Error	Ave. % Error	Ave.Abs. % Error	Max. % Error	Ave. % Error
2.0	9.5	-0.5	2.2	12.9	1.2

This comparison shows that the ternary equilibrium data of the CO_2-CH_4-n-C_{10} system obtained in this experiment can be predicted accurately by the proposed correlation using only phase equilibrium data on the three binaries CH_4-n-C_{10}, CO_2-n-C_{10}, and CH_4-CO_2. This finding indicates that phase equilibria of a multi-component system could possibly be predicted using binary phase equilibrium data only. However, further investigation is required to establish the generality of this method.

The correction factor to the geometric mean assumption, l_{ij}, is defined by Eq. (3-64). The correction factor l_{ij} is derived from Eq. (3-64) as,

$$l_{ij} = 1 - \frac{a_{ij}}{\delta_i \delta_j} \tag{7-11}$$

The correction factor l_{12} for the CO_2-CH_4 interaction was derived from a_{12} according to Eq. (7-11). The a_{12} was previously determined from fitting the correlational expression (Eq. (7-9)) to the CO_2-CH_4-n-C_{10} ternary data and found to be a_{12} = 49.09 cal/cc. A comparison of l_{12} for the pair CO_2-CH_4 determined in this study to other sources is shown below.

l_{12}(or k_{12}) for CO_2-CH_4 interaction

l_{12}- This work	k_{12} - Chueh-Prausnitz (15)	l_{12}-Cheung-Zander(13)
0.029	0.05 ± 0.02	0.028 to 0.031
Temp. 10°F to 160°F	Estimated from binaries	Temp. -175°F to -260°F

The agreement among the three sources is excellent.

In order to check the individual effects of the Scatchard-Hildebrand and Flory-Huggins terms on the predicted activity coefficients, the following equations were employed to evaluate the binary interation

parameters and to predict the experimental data using the same methods outlined previously in this section:

Binary System, Scatchard-Hildebrand term only.

$$\ln\left(\frac{K_2 \psi_2 P}{f^o_{L_2}}\right) = \frac{V_2}{RT}(\psi_1^2-1)(\delta_1^2 + \delta_2^2 - 2a_{12}) + \frac{1}{RT}\int_o^P \bar{V}_{L_2} dp \qquad (7\text{-}22)$$

Ternary System, Scatchard-Hildebrand term only.

$$\ln\gamma_2^{*\infty} = 2\frac{V_2}{RT}\Phi_1(a_{23}-a_{12}) + \frac{V_2}{RT}\left[\Phi_1^2\delta_1^2 + \delta_3^2(\Phi_3^2-1) + 2\Phi_1\Phi_3 a_{13}\right] + \frac{1}{RT}\int_o^P \bar{V}_{L_2}^{\infty} dp \qquad (7\text{-}23)$$

Eqs. (7-22) and (7-23) were obtained from Eqs. (7-20) and (7-9) respectively by deleting the Flory-Huggins term.

The procedure used for predicting activity coefficients for the five experimental systems by Eq. (7-22) and (7-23) is identical to that discussed previously.

A comparison of the activity coefficients predicted by the correlation including the Scatchard-Hildebrand and the Flory-Huggins terms (Eqs. (7-20) and (7-9)) to those predicted by the correlation including the Scatchard-Hildebrand term only (Eqs. (7-23) and (7-24)) is given in Table XIX.

Table XIX shows that the errors resulting from prediction of the activity coefficients by the basic correlation were of the same order of magnitude as those predicted by the modified version of the correlation, i.e., by Eq. (7-23).

The interaction constants for the CO_2-n-C_{10} and CH_4-CO_2 binaries determined by fitting Eq. (7-22) to the respective phase equilibrium data (25, 85) are given below.

CO_2-n-C_{10}	a_{23} = 71.531 cal/cc
CH_4-CO_2	a_{12} = 26.283 cal/cc

TABLE XIX

A COMPARISON BETWEEN THE CORRELATION INCLUDING THE SCATCHARD-HILDEBRAND AND FLORY-HUGGINS TERMS TO THAT INCLUDING THE SCATCHARD-HILDEBRAND TERM ONLY

	Ave. Abs. % Error in Activity Coefficient	
System	S-H and F-H terms	S-H term only
CO_2-CH_4-n-C_{10}	2.0	2.0
N_2-CH_4-n-C_{10}	3.3	3.3
Ar-CH_4-n-C_{10}	4.5	4.2
C_2H_2-CH_4-n-C_{10}	4.1	4.5
C_3H_8-CH_4-n-C_{10}	2.2	2.3

A comparison of the numerical value of $(a_{23}-a_{12})$ obtained from experimental data on the ternary system carbon dioxide-methane-n-decane and from the constituent binary systems using the basic correlation and the one without the Flory-Huggins term is shown below.

$(a_{23}-a_{12})$ cal/cc

Correlation Contains S-H and F-H Terms		Correlation Contains S-H Term Only	
From Binaries	From Ternary	From Binary	From Ternary
-4.116	-4.696	45.248	16.970

The above comparison shows that the value of $(a_{23}-a_{12})$ obtained from the experimental ternary data is close to that obtained from the constituent binary system for the correlation that includes the Flory-Huggins term. These two values differ considerably when predicted by the correlation that does not include the Flory-Huggins term. These results indicate that the includion of the Flory-Huggins term gives more consistency in

the interaction parameters and therefore, the combination of the Scatchart-Hildebrand and the Flory-Huggins terms appears to form a more realistic basis for the correlation of the activity coefficients.

The experimentally determined activity coefficients shown in Figures 35 through 40 require further discussion. In certain systems, there is a particular isotherm which appears inconsistent with the other isotherms. The following cases of unexpected activity coefficient behavior deserve mention: the 10°F isotherm for CO_2 (Figure 35) is about 10% lower at the highest pressure than would be expected; the 70°F isotherm for nitrogen (Figure 36) is about 5% low; the 10°F isotherm for ethylene (Figure 39) is about 2% low; the 10°F isotherm for propane (Figure 40) is about 10% high. A detailed analysis of such activity coefficient behavior is given in Appendix I. The results of this analysis is given below.

Random scatter in activity coefficients of a few percent might be expected due to experimental uncertainties. However, the results in Figure 35 through 40 show very small scatter of a random nature, but rather the unexpected behavior of certain isotherms is of a systematic nature. Based on the analysis given in Appendix I, this author concludes that the unexpected behavior, if incorrect, must be attributed to systematic errors of unknown origin to the extent of few percent in the K-values along the subject isotherms.

In summary, the small temperature effect on the non-ideality (activity coefficients) in the solutions studied, on the order of 10% change in the 140°F interval studied, combined with the sensitivity of the activity coefficients to any small systematic errors in the K-values, could cause the unexpected behavior in four of the thirty activity coefficients isotherms presented.

CHAPTER VIII

CONCLUSIONS AND RECOMMENDATIONS

The present study involved measurement of infinite dilution partial volumes of dense gas mixtures and of vapor-liquid equilibrium ratios using the "injection method" and chromatographic techniques, respectively.

The non-ideality of liquid solutions at high pressures was determined by combining the experimental results of the two sets of experiments. A framework of correlation was developed for predicting liquid phase activity coefficients.

The conclusions reached and the recommendations made based upon this work are given in this chapter.

The Partial Volume Experiment

Conclusions

The conclusions reached from the partial volume are:

1. The infinite dilution technique is a useful method for studying thermodynamic properties of binary gas mixtures.
2. For binary systems that exist as a gas mixture in the entire composition range, two sets of infinite dilution data can be obtained, one in each pure gas component as the solvent. The two sets of data provide a convenient interpolation basis for the complete description of the volumetric properties of the

binary mixture system. The accuracy of this description depends upon the interpolation scheme employed. The generality of this method deserve further investigation.

3. When an empirical equation of state is used, infinite dilution data for only one pure component contributes all the necessary mixture information for the determination of binary interaction constants. Present indications are that binary interaction constants are usually sufficient when combined with pure component properties for the complete description of gas phase mixture volumetric behavior, i.e., higher order interactions may be neglected.

Recommendations

The following recommendations are made for future work:

1. There is at present an appreciable error associated with the total pressure measurement. A Bourdon type Heise gauge is used for this purpose. The relative accuracy of pressure reading at 2000 psia is about 0.1% and about 1% at 200 psia The use of a dead weight gauge is recommended in order to eliminate this error at the low pressure range.
2. The present method for mixing the solute calls for "jetting" the solute gas into the main bomb. The "jetting" technique caused considerable pressure fluctuations. An excessive amount of time, sometimes two hours or more, was required for equilibrium to be restored. A slow motion magnetic stirrer placed inside the mainbomb will improve mixing and will shorten the time required for a solute injection.

The Gas-Liquid Chromatography Experiment

Conclusions

The conclusions drawn from this experiment are as follows:

1. Phase equilibrium of carbon dioxide, nitrogen, argon, ethylene and propane in the methane-n-decane system was successfully studied chromatographically.
2. The extrapolation scheme used for determining the chromatograph column void volume increased the accuracy of the experimental results.
3. The vapor-liquid equilibrium constants at infinite dilution on the systems: carbon dioxide-methane-n-decane
   nitrogen-methane-n-decane
   argon-methane-n-decane
   ethylene-methane-n-decane
   propane-methane-n-decane
   obtained in this experiment are self-consistent and in reasonable agreement with comparable work of other investigators.
4. The comparisons of K-values obtained during the course of this experiment with those from other sources, furnish further confirmation of chromatography as a sound and reliable technique for studying phase equilibrium.
5. The use of vapor phase partial volume data in conjunction with the chromatographically determined K-values provided a successful method for determining liquid phase fugacities.
6. The correlation method presented, based on a combination of the Scatchard-Hildebrand and Flory-Huggins theories, can be

used to predict liquid non-idealities of binary and ternary solutions. Agreement between experimental data and predictions of the new correlation is good.

7. Ternary solution phase behavior can be predicted by the correlation using binary interaction constants obtained from solution data on the constituent binary systems.
8. Phase behavior of higher order multicomponent systems might be predicted by the correlation using the respective binary data only, but there is a need for further investigation before a complete generality of the correlation can be asserted.

Recommendations

The following recommendations are made for future work:

1. The presently used sample valve often leaked internally at high pressures. The high pressure carrier gas leaked into the sample cavity and prevented the sample solute from being trapped inside the cavity. The reason for the malfunction of the sample valve was that small Teflon flakes, scraped off the packing by the moving valve stem settled on the valve seat and prevented good sealing. The scraping of the valve packing by the stem can be minimized by tapering the valve stem.
2. One of the characteristics of thermistors is their high signal-to-noise ratio. Advantage should be taken of this characteristic by using a dc amplifier. This will produce a higher signal that will make easier the study of solutes which thermal conductivities close to that of the carrier gas.

3. A detector cell, capable of operating under high pressures might ease the electrical noise problem resulting from the turbulance induced in the cell due to the expansion of the column effluent gas.
4. Further study is recommended to establish the generality of the correlation to multicomponent systems of higher order than studied in this work.

A SELECTED BIBLIOGRAPHY

(1) Ambrose, D. and B. A. Ambrose, "Gas Chromatography," D. Van Nostrand, Princeton, N. J.w (1962).

(2) Anderson, J. R. and K. H. Napier, Austral. J. Chem. 10, 250 (1957).

(3) Ashworth, A. J. and D. H. Everett, Trans. Faraday Soc. 56, 1609 (1960).

(4) Azarnoosh, A. and J. J. McKetta, J. Chem. Eng. Data, 8, 513 (1963).

(5) Barker, P. E. and A. K. Hilmi, J. Gas Chromat. 5, 119 (1967).

(6) Beaudin, J. M. and J. P. Kohn, J. Chem. Eng. Data 12, 189 (1967).

(7) Benedict, M., G. B. Webb and L. C. Rubin, J. Chem. Phys. 8, 334 (1940).

(8) Benedict, M., G. B. Webb and L. C. Rubin, J. Chem. Eng. Progr. 47, 419 (1951).

(9) Bennett, C. E., S. Dal Nogare, L. W. Safranski and C. D. Lewis, Anal. Chem. 30, 898 (1958).

(10) Blanks, R. F. and J. M. Prausnitz, Ind. Eng. Chem. 3, 1 (1964).

(11) Chang, H. L., P. S. Chappelear and R. Kobayashi, AICHE J. 14, 318 (1968).

(12) Chao, K. C. and J. D. Seader, AICHE J. 7, 598 (1961).

(13) Cheung, H. and E. H. Zander, Chem. Eng. Progr. Symp. Series 64, 34 (1968)

(14) Chueh, P. L., N. K. Muirbrook and J. M. Prausnitz, AICHE J. 11, 1097 (1965).

(15) Chueh, P. L. and J. M. Prausnitz, Ind. Eng. Chem. Fund. 6, 492 (1967).

(16) Chueh, P. L. and J. M. Prausnitz, AICHE J. 13, 1107 (1967).

(17) Chueh, P. L. and J. M. Prausnitz, AICHE J. 13, 1099 (1967).

(18) Chueh, P. L. and J. M. Prausnitz, Ind. Eng. Chem. 60, 34 (1968).

(19) Crain, R. W. and R. E. Sonntag, J. Chem. Eng. Data 12, 73 (1967)

(20) Cruikshank, A. J. B., D. H. Everett and M. J. Westway, Trans. Faraday Soc. 61, 235 (1965).

(21) Cruickshank, A. J. B., M. L. Windsor and C. L. Young, Proc. Royal. Soc. (London) 295, 259 (1966).

(22) Cullen, E. J. and K. A. Kobe, AICHE J. 1, 452 (1955).

(23) Dal Nogare, S. and R. S. Juvet, "Gas Liquid Chromatography," Interscience Publisher, New York, N. Y. (1962).

(24) Desty, D. H. and W. T. J. Swanton, J. Phys. Chem. 65, 766 (1961).

(25) Donnelly, H. G. and D. L. Katz, Ind. Eng. Chem. 46, 511 (1954).

(26) Douslin, D. R., R. H. Harrison, R. T. Moore and J. P. McCullough, J. Chem. Eng. Data 9, 358 (1964).

(27) Eckert, C. A. and J. M. Prausnitz, AICHE J. 11, 886 (1965).

(28) Everett, D. H. and C. T. H. Stoddart, Trans. Faraday Soc. 57, 746 (1961).

(29) Flory, P. J., J. Chem. Phys. 9, 660 (1941).

(30) Flory, P. J., J. Chem. Phys, 10, 51 (1942).

(31) Giddings, J. C., "Dynamics of Chromatography, Part I - Principle and Theory," Marcel Dekker Inc., New York, N. Y. (1965).

(32) Glueckauf, E., Trans. Faraday Soc. 51, 34 (1955).

(33) Hardy, C. J., J. Chromat. 2, 490 (1959).

(34) Hensel, B. H., W. C. Edmister and K. C. Chao, AICHE J. 13, 784 (1967).

(35) Heric, E. L., and C. D. Posey, J. Chem. Eng. Data 9, 61 (1964).

(36) Hildebrand, J. H. and R. L. Scott, "Solubility of Nonelectrolytes," 3rd Ed., Reinhold, N. Y. (1950).

(37) Hildebrand, J. H. and R. L. Scott, "Regular Solutions," Prentice Hall, Englewood Cliffs, N. J. (1962).

(38) Huggins, M. L., J. Chem. Phys. 9, 440 (1941).

(39) Huggins, M. L. Ann. N. Y. Acad. Sci. 43, 1 (1942).

(40) Hurt, L. J., "Low Temperature Vapor-Liquid Equilibria of the Paraffin Hydrocarbon: The Methane-Propane-n-Heptane System," PhD Thesis, Rice University, July 1962.

(41) James, A. T. and A. J. P. Martin, Biochem. J. 50, 679 (1952).

(42) James, M. R., J. C. Giddings and H. J. Eyring, J. Phys. Chem. 69, 2351 (1965).

(43) Joffe, J. and D. Zudkevitch, Ind. Eng. Chem. Fund. 5, 455 (1966).

(44) Kate, F. H., "Infinite Dilution Study of Methane-Hydrogen Sulfide Binary System," M.S. Thesis, Oklahoma State University, May 1968.

(45) Kate, F. H., R. L. Robinson and K. C. Chao, Chem. Eng. Progr. Symp. Series 64, 91 (1968).

(46) Keulemans, A. I. M., "Gas Chromatography," Reinhold Publishing Corp., N. Y. (1957).

(47) Keyes, F. G. and H. G. Burks, J. Am. Chem. Soc. 50, 1100 (1928).

(48) Kobayashi, K., P. S. Chappelear and H. A. Deans, Ind. Eng. Chem. 59, 63 (1967).

(49) Kohn, J. P., Chem. Eng. Progr. Symp. Series 63, 57 (1967).

(50) Koonce, K. T., "Generalization of Gas Liquid Partition Chromatography to Study Multicomponent Vapor-Liquid Equilibria at High Pressures," PhD Thesis, Rice University, November 1963.

(51) Koonce, K. T. and R. Kobayashi, J. Chem. Eng. Data 9, 494 (1964).

(52) Koonce, K. T. and R. Kobayashi, J. Chem. Eng. Data 9, 490 (1964).

(53) Kurkchi, G. A. and A. V. Iogansen, Akademiia Nauk SSSR Doklady 145, 1085 (1962).

(54) Kwantes, A. and G. W. A. Rijnders, "Gas Chromatography," D. H. Desty ed., Academic Press, N. Y. (1958).

(55) Langer, S. H. and J. H. Purnell, J. Phys. Chem. 67, 263 (1963).

(56) Lee, R. C., "Compressibility Factors and Virial Coefficients for Methane, Ethylene and Their Mixtures Using an Isothermal Expansion Ratio Apparatus," PhD Thesis, Oklahoma State University, 1969.

(57) Lin, H. M. and K. C. Chao, "A Group Contribution Theory of Gas Solubility," to be published.

(58) Lin, H. M., Personal Communication.

(59) Littlewood, A. B., C. S. G. Phillips, and D. T. Price, J. Chem. Soc. 1480 (1955).

(60) Littlewood, A. B., "Gas Chromatography," Academic Press, N. Y. (1962).

(61) Lopez, M. G. and R. Kobayashi, Pet. Ref. 39, 125 (1960).

(62) Martin, A. J. P., Symp. Gas Chromatography, Soc. for Analytical Chemistry, Stevenston, Scotland, May 1955.

(63) Martin, A. J. P. and R. L. M. Synge, Biochem. J. 35, 1358 (1941).

(64) Martin, R. L., Anal. Chem. 33, 34 (1961).

(65) Martin, R. L., Anal. Chem. 35, 116 (1963).

(66) Martire, D. E., Anal. Chem. 33, 1143 (1961).

(67) Martire, D. E., "Gas Chromatography," L. Fowler, ed., Academic Press, N. Y. (1963).

(68) Martire, D. E. and L. Z. Pollara, J. Chem. Engr. Data 10, 40 (1965).

(69) Martire, D. E., R. L. Pecsok and J. H. Purnell, Nature 203, 1279 (1964).

(70) Masukawa, S., J. I. Alyea and R. Kobayashi, paper submitted for publication in the J. Gas Chromat.

(71) Masukawa, S. and R. Kobayashi, J. Gas Chromat. 6, 257 (1968).

(72) McMath, H. G., "Volumetric Properties and Virial Coefficients of the Methane-Ethylene System Using the Technique of Isochoric Changes of Pressure with Temperature, PhD Thesis, Oklahoma State University (1967).

(73) Natural Gas Processors Suppliers Association, "Engineering Data Book," Tulsa, Oklahoma (1967).

(74) Natural Gasoline Association of America, "Equilibrium Ratio Data Book," Tulsa, Oklahoma (1957).

(75) Orentlicher, M. and J. M. Prausnitz, Chem. Eng. Sci. 19, 775 (1964).

(76) Pecsok, R. L., "Principles and Practice of Gas Chromatography," John Wiley and Sons Inc., N. Y. (1959).

(77) Pierotti, G. J., C. H. Deal, E. L. Derr and P. E. Porter, J. Am. Chem. Soc. 78, 2989 (1956).

(78) Pierotti, R. A., J. Phys. Chem. 67, 1840 (1963).

(79) Pierotti, R. A., J. Phys. Chem. 69, 281 (1965).

(80) Porter, P. E., C. H. Deal and F. H. J. Stross, Am. Chem. Soc. 78, 2999 (1956).

(81) Prausnitz, J. M., Chem. Eng. Sci. 18, 613 (1963).

(82) Rangel, E. T., "Analysis of Low Temperature Chromatographic Separation of Methane-Propane Mixtures with n-Decane on Celite," M.S. Thesis, Rice University (1956).

(83) Reamer, H. H., R. H. Olds, B. H. Sage and W. N. Lacey, Ind. Eng. Chem. 34, 1526 (1942).

(84) Reamer, H. H., R. H. Olds and W. N. Lacey, Ind. Eng. Chem. 36, 88 (1944).

(85) Reamer, H. H. and B. H. Sage, J. Chem. Eng. Data 8, 508 (1963).

(86) Robinson, R. L., and R. H. Jacoby, Hydrocar. Proc. Pet. Ref. 44, 141 (1965).

(87) Sage, B. H. and W. N. Lacey, "Thermodynamic Properties of Lighter Paraffin Hydrocarbon and Nitrogen," American Petroleum Institute, N. Y. (1950).

(88) Sage, B. H. and W. N. Lacey, "Some Properties of the Lighter Hydrocarbons, Hydrogen Sulfide and Carbon Dioxide," American Petroleum Institute, N. Y. (1955).

(89) Saylor, J. H. and R. Battino, J. Phys. Chem. 62, 1334 (1958).

(90) Scatchard, G., Chem. Rev. 8, 321 (1931).

(91) Scatchard, G., Trans. Faraday Soc. 33, 160 (1937).

(92) Scott, R. L., J. Phys. Chem. 62, 136 (1958).

(93) Stalkup, F. I., "The Study of High Pressure Vapor Liquid Equilibrium by Gas Liquid Partition Chromatography," PhD Thesis, Rice University (1961).

(94) Stalkup, F. I. and H. A. Deans, AICHE J. 9, 106 (1963).

(95) Stalkup, F. I. and R. Kobayashi, AICHE J. 9, 121 (1963).

(96) Stalkup, F. I. and R. Kobayashi, J. Chem. Eng. Data 8, 564 (1963).

(97) Stotler, H. H. and M. Benedict, Chem. Eng. Progr. Symp. Series 49, No. 6, 25 (1953).

(98) Van Deemter, J. J., F. J. Zuiderweg and A. Klinkenberg, Chem. Eng. Sci. 5, 271 (1956).

(99) Van Horn, L. D., "A Study of Low Temperature Vapor-Liquid Equilibria in Light Hydrocarbon Solvents," PhD Thesis, Rice University (1966).

(100) Van Horn, L. D. and R. Kobayashi, J. Chem. Eng. Data 12, 294 (1967).

(101) Vennix, A. J., "Low Temperature Volumetric Properties and the Development of an Equation of State for Methane," PhD Thesis, Rice University (1966).

(102) Wilson, G. M., Advanced Cryog. Eng. 9, 168 (1964).

(103) Wilzbach, K. E. and P. Riez, Science 126, 1062 (1957).

(104) Yorizane, M., S. Yoshimura and H. Masuoka, Kagaku Kogaku 30, 1093 (1966).

(105) Yudovich, A., R. L. Robinson and K. C. Chao, Chem. Eng. Progr. Symp. Series 64, 85 (1968).

(106) Zudkevitch, D. and T. Kaufmann, AICHE J. 12, 577 (1966).

(107) Pecsar, R. E. and J. J. Martin, J. Anal. Chem. 38, 1661 (1966).

APPENDIX A

DERIVATION OF EQUATIONS (3-9) THROUGH (3-11)

From Eq. (3-8)

$$RT\ell n\gamma_2 = \int_0^P (\bar{V}_2 - \tilde{\bar{V}}_2)dP \tag{A-1}$$

the molar volume of the binary mixture, $\tilde{\tilde{V}}$, is expressed by Eqs. (3-4) and (3-5) as

$$\tilde{\tilde{V}} = x_1\tilde{\bar{V}}_1 + x_2\tilde{\bar{V}}_2 + x_1x_2[a + b(x_2 - x_1) + \ldots] \tag{A-2}$$

also

$$\bar{V}_2 = \tilde{\tilde{V}} - x_1\left(\frac{\partial\tilde{\tilde{V}}}{\partial x_1}\right)_{P,T} \tag{A-3}$$

The partial volume, $\bar{V}_2$, is obtained by differentiating Eq. (A-2) according to Eq. (A-3). When $\bar{V}_2$ is substituted into Eq. (A-1) and the constants "a" and "b" are expressed in terms of partial volume at infinite dilution as given by Eqs. (3-6) and (3-7), the following relation is obtained,

$$RT\ell n\gamma_2 = \int_0^P \left[\frac{1}{2}(\bar{\bar{V}}_1^{\infty} - \tilde{\bar{V}}_1)x_1^2 + \frac{1}{2}(\bar{\bar{V}}_2^{\infty} - \tilde{\bar{V}}_2)\,x_1^2 + \frac{3}{2}(\bar{\bar{V}}_1^{\infty} - \tilde{\bar{V}}_1)x_1^2\right.$$

$$\left. - \frac{3}{2}(\bar{\bar{V}}_2^{\infty} - \tilde{\bar{V}}_2)x_1^2 - 2(\bar{\bar{V}}_1^{\infty} - \tilde{\bar{V}}_1)x_1^3 + 2(\bar{\bar{V}}_2^{\infty} - \tilde{\bar{V}}_2)x_1^3\right]dP \tag{A-4}$$

Equation (A-4) is reduced to the following expression using Eq. (3-8)

$$\ell n\gamma_2 = \ell n\frac{\gamma_1^{\infty 2}}{\gamma_2^{\infty}}x_1^2 + \ell n\frac{\gamma_2^{\infty 2}}{\gamma_1^{\infty 2}}x_1^3 \tag{A-5}$$

or,

$$\ell n\gamma_2 = x_1^2(\alpha + \beta x_1) \tag{A-6}$$

where,

$$\alpha = \ell n \frac{\gamma_1^{\infty_2}}{\gamma_2^{\infty}}$$

and,

$$\beta = \ell n \frac{\gamma_2^{\infty_2}}{\gamma_1^{\infty_2}} \tag{A-7}$$

APPENDIX B

DERIVATION OF EQUATION (3-57)

The general equation for the activity coefficient of component k in a multicomponent system based on Scatchard's regular solution theory will be developed in this appendix.

The cohesive energy density "a" is defined by

$$a = \frac{\tilde{U}^* - \tilde{U}}{\tilde{V}} \tag{B-1}$$

where $\tilde{U}$ is the molar internal energy of the liquid; $\tilde{U}^*$ is the molar internal energy of the same material at the ideal gas state; $\tilde{V}$ is the molar volume of the solution.

The cohesive energy density for a solution, a_m, is defined by

$$a_m = \sum_{ij}^{nn} \Phi_i \Phi_j a_{ij} \tag{B-2}$$

where n is the number of components in the solution; Φ_i is the volume fraction of component i and is given by

$$\Phi_i = \frac{x_i \tilde{V}_i}{\sum_j^n \tilde{V}_j x_j} = \frac{x_i V_i}{\tilde{V}_m} \tag{B-3}$$

The molar energy of mixing is expressed by

$$\Delta\tilde{U}^M = \tilde{U}^M - \Sigma x_i \tilde{U}_i = (\tilde{U}^{M*} - \Sigma x_i \tilde{U}_i) - (\tilde{U}^{M*} - \tilde{U}^M) \tag{B-4}$$

noting that $\tilde{U}^{M*} = \Sigma x_i \tilde{U}^*$, Eq. (B-4) becomes

$$\Delta\tilde{U}^M = \Sigma x_i(\tilde{U}^* - \tilde{U}_i) - (\tilde{U}^{M*} - \tilde{U}^M) \tag{B-5}$$

substituting Eqs. (B-1) and (B-2) into Eq. (B-5)

$$\Delta\tilde{U}^M = \Sigma x_i a_i \tilde{V}_i - a_m \tilde{V}_m = \Sigma_i x_i a_i \tilde{V}_i - \tilde{V}_m \Sigma\Sigma_{ij} \Phi_i \Phi_j a_{ij} \tag{B-6}$$

Rearranging Eq. (B-6)

$$\Delta\tilde{U}^M = \tilde{V}_m \Sigma\Sigma_{ij} \Phi_i \Phi_j (a_{ii} - a_{ij}) \tag{B-7}$$

From regular solution theory

$$\Delta\tilde{G}^E = \Delta\tilde{U}^E = \Delta\tilde{U}^M = \tilde{V}_m \Sigma\Sigma_{ij} \Phi_i \Phi_j (a_{ii} - a_{ij}) \tag{B-8}$$

For a mixture containing n_ℓ moles of ℓ,

$$\Delta G^E = \Sigma_\ell n_\ell \tilde{V}_m \left[\Sigma\Sigma_{ij} \Phi_i \Phi_j (a_{ii} - a_{ij})\right] = \Sigma\Sigma_{ij} n_i \tilde{V}_i n_i \tilde{V}_j \frac{(a_{ii} - a_{ij})}{\Sigma_\ell \tilde{V}_\ell} \tag{B-9}$$

The activity coefficient of a component k at constant temperature and pressure will therefore be

$$\ell n \gamma_k = \frac{\Delta \overline{G}^E_k}{RT} = \frac{1}{RT} \Sigma\Sigma_{ij} (a_{ii} - a_{ij}) \left[\delta_{ik} \tilde{V}_i \frac{n_j \tilde{V}_j}{\Sigma n_\ell \tilde{V}_\ell} + n_i \tilde{V}_i \frac{\delta_{jk} \tilde{V}_j}{\Sigma n_\ell \tilde{V}_\ell} + n_i \tilde{V}_i n_j \tilde{V}_j \frac{(-\delta_{\ell k} \tilde{V}_\ell)}{(\Sigma n_\ell \tilde{V}_\ell)^2}\right] \tag{B-10}$$

where δ_{ij}, the Kronecker delta, is defined to be unity if $i = j$ and zero if $i \neq j$.

From Eq. (B-10),

$$RT\ell n\gamma_k = \sum_j \tilde{\tilde{V}}_k \Phi_j (a_k - a_{kj}) + \sum_i \tilde{\tilde{V}}_k \Phi_i (a_{ii} - a_{ik})$$

$$- \sum_{ij} \sum \tilde{\tilde{V}}_k \Phi_i \Phi_j (a_{ii} - a_{ij}) \qquad \text{(B-11)}$$

Rearranging Eq. (B-11),

$$\ell n\gamma_k = \frac{\tilde{\tilde{V}}_k}{RT}\left[a_k - 2\sum_j^n \Phi_j a_{kj} + \sum_{ij}^{nn} \Phi_i \Phi_j a_{ij}\right] \qquad \text{(B-12)}$$

The activity coefficient of component k in a multicomponent system based on the regular solution theory at constant temperature and pressure is obtained from Eq. (B-12).

APPENDIX C

CALIBRATION OF THERMOCOUPLE

A copper-constantan thermocouple was used to measure the system temperature. The thermocouple was calibrated in a constant temperature bath containing ethylene glycol-water solution. The temperature of the bath was controlled with a Model 1053A Hallikainen temperature controller within ±0.04°F. The temperature of the bath was measured with a precision a mercury in glass thermometer with 0.02°F subdivisions. This thermometer was calibrated and certified by the National Bureau of Standards. In addition, the thermocouple was calibrated at ice-water mixture temperature.

The thermocouple EMF output was measured with a Leeds and Northrup potentiometer (catalog No. 8687) to a precision of 0.001 mv.

The results of the thermocouple calibration are tabulated below.

TABLE C-I

THERMOCOUPLE CALIBRATION

Temperature, °F	Thermocouple EMF, mv
22.12	-0.208
32.00 (ice-water)	0.000
40.80	0.187
61.48	0.644
79.64	1.050
101.20	1.546
126.36	2.141

APPENDIX D

EVALUATION OF OPTIMUM THERMISTOR RESPONSE

The optimal thermistor power for maximum response was established by plotting the thermistor power dissipation, i.e., the product of the current through the thermistor and the voltage drop across it.

The experimental procedure of this experiment was discussed in Chapter V.

The optimum thermistor power dissipation obtained from Figure 41 was about 9 mw, this corresponded to bridge voltage of 18.5 volt.

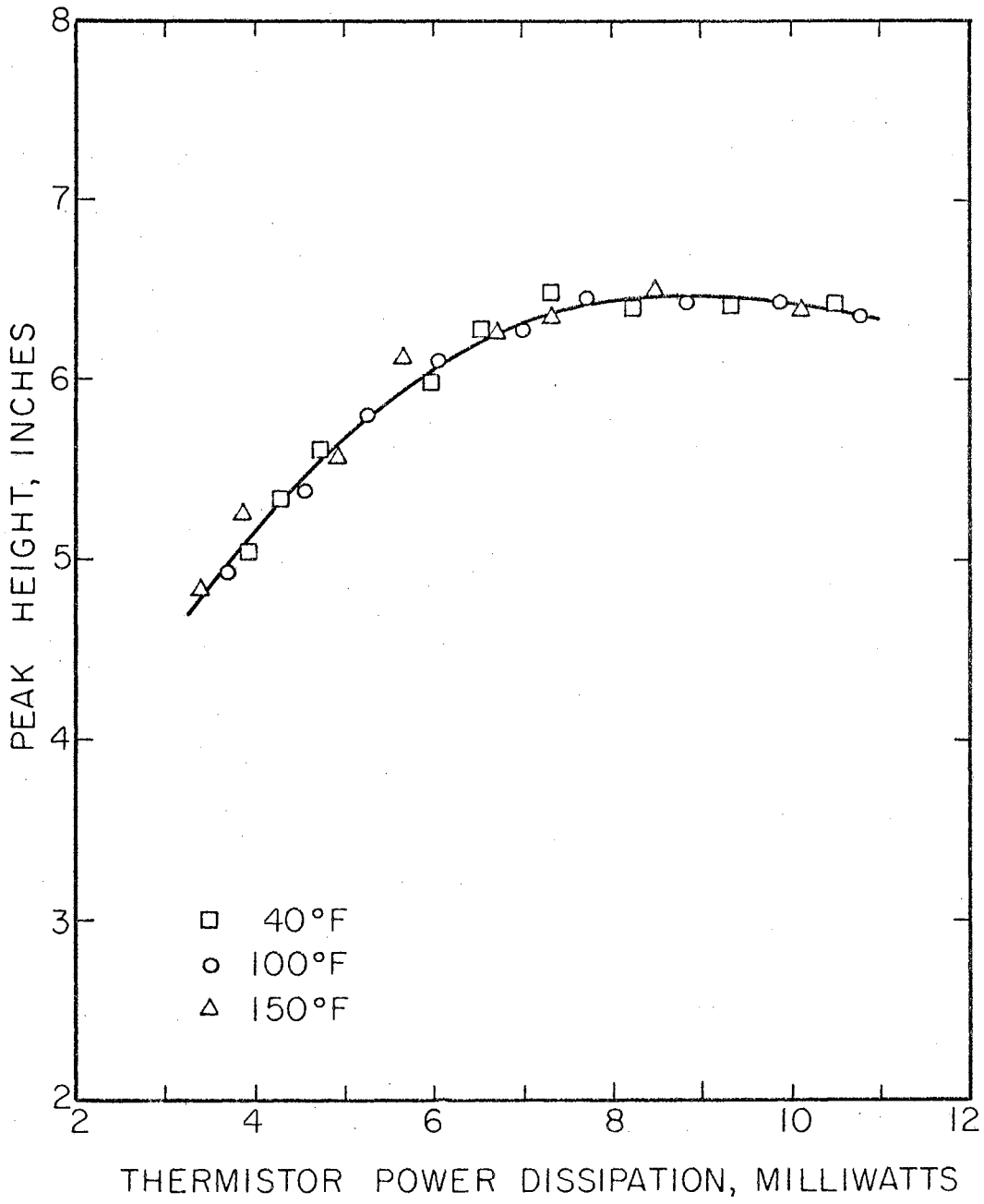

Figure 41. Power Dissipation-Response Curve for the 30K Ohm Thermistors

APPENDIX E

ERROR ANALYSIS

The Gas Liquid Chromatography Experiment

The K-values are calculated from experimental data according to Eq. (3-36)

$$K_i = \frac{W_L^o}{(1 - x_1)\rho G(V_{R_i} - V_G)} \tag{3-36}$$

where V_{R_i} is given by Eq. (3-37)

$$V_{R_i} = t_{R_i} f_a \frac{P_a}{P} \frac{T}{T_a} Z_G \tag{3-37}$$

V_G is determined experimentally by extrapolating the retention volumes of helium, neon and argon.

A variable t_G is defined by the following relation:

$$t_G = \frac{V_G}{f_a} \tag{E-1}$$

t_G is the retention time of an imaginary unsoluble gas which retention volume equal to the void volume of the column. Since the carrier gas flow rate at a given temperature and pressure condition was kept constant, the term $(V_{R_i} - V_G)$ in Eq. (3-36) can be combined with Eq. (3-37) to yield the following expression:

$$(V_{R_i} - V_G) = (t_{R_i} - t_G) f_a \frac{P_a}{P} \frac{T}{T_a} Z_G \tag{E-2}$$

Substituting Eq. (E-2) into Eq. (3-36),

$$K_i = \frac{RW_L^o T_a}{(1 - x_1) f_a P_a (t_{R_i} - t_G)} \qquad \text{(E-3)}$$

t_G in Eq. (E-3), although not measured directly, can be determined by Eq. (E-1).

Differentiating Eq. (E-3)

$$dK_i = \frac{RW_L^o T_a}{f_a P_a (t_{R_i} - t_G)(1 - x_1)^2} dx_1 + \frac{RT_a}{(1 - x_1) f_a P_a (t_{R_i} - t_G)} dW_L^o$$

$$+ \frac{RW_L^o}{(1 - x_1) f_a P_a (t_{R_i} - t_G)} dT_a - \frac{RW_L^o T_a}{(1 - x_1) f_a^2 P_a (t_{R_i} - t_G)} df_a$$

$$- \frac{RW_L^o T_a}{(1 - x_1) f_a P_a^2 (t_{R_i} - t_G)} dP_a - \frac{RW_L^o T_a}{(1 - x_1) f_a P_a (t_{R_i} - t_G)^2} d(t_{R_i} - t_G) \qquad \text{(E-4)}$$

The differentials dx_1, dw_L^o etc. are approximated by small finite increments Δx_1, Δw_L^o etc. and Eq. (E-4) is divided through by the right hand side of Eq. (E-3). In order to obtain the maximum error, the signs of Δf_a, ΔP_a and $\Delta(t_{R_i} - t_G)$ will be taken as negative and all other increments will be taken as positive.

The maximum relative error in K-value is therefore,

$$\frac{\Delta K}{K} = \frac{\Delta W_L^o}{W_L^o} + \frac{\Delta x_1}{(1 - x_1)} + \frac{\Delta T_a}{T_a} + \frac{\Delta f_a}{f_a} + \frac{\Delta P_a}{P_a} + \frac{\Delta(t_{R_i} - t_G)}{(t_{R_i} - t_G)} \qquad \text{(E-5)}$$

The estimated uncertainties in Eq. (E-5) are given in Chapter VII. The maximum errors in the K-values were evaluated via Eq. (E-5) at the lowest and highest pressures used in this work, i.e., at 100 and 1750 psia for the 10°F and 150°F isotherms respectively and are given in Table IX.

Equation (E-5) shows that the uncertainty of the molar volume of the saturated methane-n-decane solution has negligible effect on the error in the K-value.

The results of this error analysis are discussed in Chapter VII.

The Partial Volume Experiment

The volume ratios are calculated from experimental data according to Eqs. (3-1) and (5-2)

$$\text{Volume Ratio (VR)} = \frac{\bar{V}_2^{\infty}}{\bar{V}_1^{o}} = \frac{\dfrac{e_2}{(\pi/Z)_2}}{\dfrac{e_1}{(\pi/Z)_1}} \qquad \text{(E-6)}$$

Differentiating and rearranging Eq. (E-6) using the same procedure outlined previously in this Appendix, the maximum expected error in the slope ratio is expressed by

$$\frac{\Delta(VR)}{(VR)} = \frac{\Delta e_1}{e_1} + \frac{\Delta e_2}{e_2} + \frac{\Delta Z_1}{Z_1} + \frac{\Delta Z_2}{Z_2} \qquad \text{(E-7)}$$

The relative error in the injecting pressures π, is negligible (see Chapter VII).

The uncertainty in the compressibility factors of pure methane and carbon dioxide was taken as ±0.2% respectively. The uncertainty in measuring the pressure transducer output was 0.1%.

The estimated maximum error of the volume ratio according to Eq. (E-7) is therefore 0.6%.

APPENDIX F

SAMPLE CALCULATIONS

The calculations used in determining the K-value from chromatography elution data are demonstrated here using the following experimental run:

System temperature: $40^{o}F$

System pressure: 1000 psia

1. Amount of Pure Decane in Column.

   Length of Column: 14 inches

   Net weight of column: 68.6413 gms

   Weight of column with packing: 72.6518 gms

   Net weight of packing: 4.0105 gms

   Net weight of weighing bottle: 15.5711 gms

   Weight of weighing bottle containing wet column packing: 20.2509 gms

   Weight of weighing bottle containing dry column packing: 18.9402 gms

$$\text{Decane load} = \frac{20.2509-18.9402}{20.2509-15.5711} = 0.2801 \ \frac{\text{gm decane}}{\text{gm wet packing}}$$

$$W_L^{o} = \frac{(0.2801)(4.0105)}{(142.276)} = 0.00789 \text{ gm-mole decane}$$

The system and ambient temperatures and pressures for this run were:

$T = 40^{o}F$

$T_a = 81.4^{o}F$

$P = 1000$ psia

$P_a = 741.2$ mm Hg

The properties of methane gas phase and methane-n-decane solution at the system conditions were:

$Z_G = 0.8446$

$\rho_G = 0.00353$ gm-mole/cc

$x_1 = 0.3107$ mole fraction of methane in liquid solution

The K-values were calculated from experimental data via Eqs. (3-36) and (3-37).

$$K_i = \frac{W_L^{o}}{(1-x_1)\rho_G(V_{R_i}-V_G)} \tag{3-36}$$

$$V_{R_i} = t_{R_i} f_a \left(\frac{P_a}{P}\right)\left(\frac{T}{T_a}\right)Z_G \tag{3-37}$$

2. Calculation of Retention Time

For carbon dioxide

$t_{R_i} = 9' 0.10'' = 9.0016$ min

$f_a = 118.891$ cc/min

From Eq. (3-37)

$$V_{R_i} = (9.0016)(118.891)\frac{(741.2)(0.01934)}{(1000)} \times \frac{(40+460)}{(81.4+460)}(0.8446) = 11.964\text{cc}$$

3. Calculation of Void Volume

The retention times and flow rates for helium, neon and argon are:

	t_{R_i}	f_a
He	7′ 13.51″	117.996 cc/min
Ne	7′ 16.41″	118.038 cc/min
Ar	7′ 38.72″	118.421 cc/min

Using these experimental data, the retention volumes were calculated via Eq. (3-37). The retention volumes and normalized polarizabilities are given below.

	V_{R_i}	α/α_{He}
He	9.634 cc	1.000
Ne	9.700 cc	1.926
Ar	10.121 cc	7.990

Moles of stationary liquid solution at given T & P = $\frac{W_L^o}{1-x_1}$

Moles of stationary solution @ 100 psia: $\frac{0.00789}{1-0.042} = 0.00823$ mole

Moles of stationary solution @ 1000 psia: $\frac{0.00789}{1-0.3107} = 0.01144$ mole

Density of C_1-C_{10} solution @ 100 psia = 0.04693 cc/gm mole

Density of C_1-C_{10} solution @ 1000 psia = 0.03814 cc/gm mole

The calculated change in stationary solution volume is, therefore,

$$(V_L)_P = 4\text{x}10^{-4} \text{ cc}$$

This value smaller than the precision in measuring the retention volume and, therefore, the change in solution volume due to pressure is negligible for this system.

A straight line was fitted to the retention volumes and polarizabil-

ity ratios of the solutes He, Ne and Ar using a linear least square technique programmed for a digital computer. The void volume V_G, was taken as the intersection of the line with lines of different system pressures. The evaluated void volume was:

$$V_G = 9.565 \text{ cc}$$

4. Calculation of the K-Value

The K-value of the system CO_2-CH_4-C_{10} was determined through Eq. (3-36).

$$K_{CO_2} = \frac{0.00789}{(1-0.3107)(0.00353)(11.964-9.565)} = 1.351$$

The retention time for propane was 19.8478 min and its retention volume was 26.449 cc and, therefore,

$$K_{C_3} = \frac{0.00789}{(1-0.3107)(0.00353)(26.449-9.565)} = 0.192$$

APPENDIX G

TABULATION OF DATA

TABLE G-I

DATA FROM THE GAS-LIQUID CHROMATOGRAPHY EXPERIMENT

$T = 10^{o}F$

$W_L^{o} = 0.0074$ gm-mole

$P = 100$ psia

$T_a = 77.6^{o}F$

$P_a = 740.0$ mm Hg

$V_G = 9.719$ cc

Solute	t_{R_i} Min	t_{R_i} Sec	fa-cc/min
He	2	21.94	33.924
Ne	2	22.64	33.900
N_2	2	26.31	33.670
Ar	2	27.65	33.573
CO_2	3	9.90	33.504
C_2H_2	3	59.82	33.554
C_3H_8	14	4.54	33.526

$T = 10^{o}F$

$W_L^{o} = 0.0074$ gm-mole

$P = 200$ psia

$T_a = 77.6^{o}F$

$P_a = 745.5$ mm Hg

$V_G = 9.667$ cc

Solute	t_{R_i} Min	t_{R_i} Sec	fa-cc/min
He	4	30.69	35.598
Ne	4	32.09	35.600
N_2	4	39.52	35.580
Ar	4	40.69	35.658
CO_2	5	56.75	35.814
C_2H_2	7	14.93	35.721
C_3H_8	25	7.85	35.792

TABLE G-I (Continued)

$T = 10^{o}F$				$T = 10^{o}F$			
$W_L^{o} = 0.0074$ gm-mole				$W_L^{o} = 0.0074$ gm-mole			
$P = 300$ psia				$P = 400$ psia			
$T_a = 78.0^{o}F$				$T_a = 78.1^{o}F$			
$P_a = 739.0$ mm Hg				$P_a = 738.5$ mm Hg			
$V_G = 9.610$ cc				$V_G = 9.501$ cc			
	t_{R_i}				t_{R_i}		
Solute	Min	Sec	fa-cc/min	Solute	Min	Sec	fa-cc/min
He	5	42.95	43.578	He	5	30.21	60.596
Ne	5	44.76	43.609	Ne	5	31.97	60.500
N_2	5	54.72	43.166	N_2	5	42.79	60.443
Ar	5	54.77	43.394	Ar	5	43.97	60.362
CO_2	7	35.66	43.073	CO_2	7	13.22	60.443
C_2H_2	9	0.60	43.254	C_2H_2	8	32.29	60.525
C_3H_8	29	39.42	42.816	C_3H_8	26	39.35	60.060

TABLE G-I (Continued)

$T = 10^{o}F$

$W_L^{o} = 0.0074$ gm-mole

$P = 500$ psia

$T_a = 78.2^{o}F$

$P_a = 741.2$ mm Hg

$V_G = 9.270$ cc

Solute	t_{R_i} Min	t_{R_i} Sec	fa-cc/min
He	8	8.87	50.750
Ne	8	11.66	50.750
N_2	8	29.12	50.758
Ar	8	29.99	50.752
CO_2	10	39.42	50.750
C_2H_2	12	32.63	50.800
C_3H_8	35	27.32	50.805

$T = 10^{o}F$

$W_L^{o} = 0.0074$ gm-mole

$P = 600$ psia

$T_a = 79.0^{o}F$

$P_a = 744.0$ mm Hg

$V_G = 9.235$ cc

Solute	t_{R_i} Min	t_{R_i} Sec	fa-cc/min
He	6	28.84	77.855
Ne	6	31.20	77.890
N_2	6	44.18	77.922
Ar	6	41.50	78.913
CO_2	8	27.86	77.956
C_2H_2	9	50.94	78.295
C_3H_8	26	39.96	78.261

TABLE G-I (Continued)

$T = 10^{o}F$

$W_L^{o} = 0.0074$ gm-mole

$P = 700$ psia

$T_a = 78.7^{o}F$

$P_a = 744.8$ mm Hg

$V_G = 9.152$ cc

Solute	t_{R_i} Min	t_{R_i} Sec	fa-cc/min
He	7	36.56	78.452
Ne	7	39.35	78.450
N_2	7	55.23	78.450
Ar	7	57.58	78.450
CO_2	9	53.83	78.455
C_2H_2	11	27.96	78.461
C_3H_8	28	35.20	78.462

$T = 10^{o}F$

$W_L^{o} = 0.0074$ gm-mole

$P = 800$ psia

$T_a = 78.5^{o}F$

$P_a = 741.0$ mm Hg

$V_G = 9.138$ cc

Solute	t_{R_i} Min	t_{R_i} Sec	fa-cc/min
He	8	44.80	80.431
Ne	8	48.08	80.343
N_2	9	7.94	80.214
Ar	9	8.61	80.357
CO_2	11	16.75	80.071
C_2H_2	12	58.94	80.214
C_3H_8	30	7.49	80.357

TABLE G-I (Continued)

$T = 10^{o}F$

$W_L^{o} = 0.0074$ gm-mole

$P = 1000$ psia

$T_a = 78.5^{o}F$

$P_a = 740.0$ mm Hg

$V_G = 9.099$ cc

Solute	t_{R_i} Min	t_{R_i} Sec	fa-cc/min
He	10	54.22	84.318
Ne	10	58.34	84.316
N_2	11	24.18	84.312
Ar	11	25.31	84.310
CO_2	13	54.24	84.315
C_2H_2	15	52.65	84.310
C_3H_8	32	16.86	84.318

$T = 10^{o}F$

$W_L^{o} = 0.0074$ gm-mole

$P = 1250$ psia

$T_a = 78.6^{o}F$

$P_a = 740.2$ mm Hg

$V_G = 9.078$ cc

Solute	t_{R_i} Min	t_{R_i} Sec	fa-cc/min
He	13	30.82	90.125
Ne	13	36.32	90.122
N_2	14	11.02	90.120
Ar	14	12.30	90.128
CO_2	17	4.99	90.130
C_2H_2	19	6.72	90.132
C_3H_8	34	10.75	90.128

TABLE G-I (Continued)

$T = 10^{\circ}F$	$T = 10^{\circ}F$
$W_L^{\circ} = 0.0074$ gm-mole	$W_L^{\circ} = 0.0074$ gm-mole
$P = 1500$ psia	$P = 1750$ psia
$T_a = 78.2^{\circ}F$	$T_a = 78.0^{\circ}F$
$P_a = 741.4$ mm Hg	$P_a = 741.0$ mm Hg
$V_G = 9.068$ cc	$V_G = 8.973$ cc

	t_{R_i}				t_{R_i}		
Solute	Min	Sec	fa-cc/min	Solute	Min	Sec	fa-cc/min
He	16	1.29	95.213	He	13	17.00	98.814
Ne	16	8.28	95.210	Ne	13	27.52	98.875
N_2	16	49.05	95.300	N_2	14	19.39	98.902
Ar	16	54.52	95.250	Ar	14	36.39	98.900
CO_2	19	59.86	95.284	CO_2	17	40.37	98.900
C_2H_2	22	6.53	95.291	C_2H_2	19	38.79	99.553
C_3H_8	35	50.95	95.274	C_3H_8	32	15.86	99.040

TABLE G-I (Continued)

$T = 40^{\circ}F$

$W_L^{\circ} = 0.0079$ gm-mole

$P = 100$ psia

$T_a = 76.8^{\circ}F$

$P_a = 740.2$ mm Hg

$V_G = 9.832$ cc

Solute	t_{R_i} Min	t_{R_i} Sec	fa-cc/min
He	2	15.63	33.404
Ne	2	16.28	33.406
N_2	2	19.81	33.318
Ar	2	20.51	33.340
CO_2	2	53.96	33.309
C_2H_2	3	32.71	33.237
C_3H_8	10	8.75	33.180

$T = 40^{\circ}F$

$W_L^{\circ} = 0.0079$ gm-mole

$P = 200$ psia

$T_a = 79.0^{\circ}F$

$P_a = 738.5$ mm Hg

$V_G = 9.757$ cc

Solute	t_{R_i} Min	t_{R_i} Sec	fa-cc/min
He	4	24.54	34.843
Ne	4	25.89	34.844
N_2	4	32.94	34.682
Ar	4	34.50	34.716
CO_2	5	39.85	34.803
C_2H_2	6	46.04	34.810
C_3H_8	18	49.98	34.816

TABLE G-I (Continued

T = 40°F	T = 40°F
W_L^o = 0.0079 gm-mole	W_L^o = gm-mole
P = 300 psia	P = 400 psia
T_a = 78°F	T_a = 79°F
P_a = 738.0°F	P_a = 733.5 mm Hg
V_G = 9.727 cc	V_G = 9.686 cc

	t_{R_i}				t_{R_i}		
Solute	Min	Sec	fa-cc/min	Solute	Min	Sec	fa-cc/min
He	5	9.66	45.587	He	5	16.86	59.890
Ne	5	11.36	45.590	Ne	5	18.59	59.890
N_2	5	20.12	45.000	N_2	5	28.44	59.840
Ar	5	21.18	45.181	Ar	5	29.05	60.000
CO_2	6	39.141	44.910	CO_2	6	44.641	59.801
C_2H_2	7	51.23	44.979	C_2H_2	7	45.30	61.017
C_3H_8	21	35.13	44.754	C_3H_8	20	9.57	61.017

TABLE G-I (Continued)

$T = 40^{\circ}F$

$W_L^{\circ} = 0.0079$ gm-mole

$P = 500$ psia

$T_a = 79.4^{\circ}F$

$P_a = 737.2$ mm Hg

$V_G = 9.639$ cc

Solute	t_{R_i} Min	t_{R_i} Sec	fa-cc/min
He	6	10.14	64.493
Ne	6	12.30	64.496
N_2	6	23.45	64.562
Ar	6	26.03	64.632
CO_2	7	50.51	64.888
C_2H_2	9	7.89	64.702
C_3H_8	22	40.79	64.982

$T = 40^{\circ}F$

$W_L^{\circ} = 0.0079$ gm-mole

$P = 600$ psia

$T_a = 79.4^{\circ}F$

$P_a = 737.4$ mm Hg

$V_G = 9.632$ cc

Solute	t_{R_i} Min	t_{R_i} Sec	fa-cc/min
He	6	2.51	80.718
Ne	6	4.59	80.720
N_2	6	16.10	80.393
Ar	6	16.56	80.754
CO_2	7	37.53	80.681
C_2H_2	8	51.92	80.321
C_3H_8	20	56.75	81.448

TABLE G-I (Continued)

$T = 40^{o}F$

$W_L^{o} = 0.0079$ gm-mole

$P = 700$ psia

$T_a = 80.2^{o}F$

$P_a = 743.2$ mm Hg

$V_G = 9.619$ cc

Solute	t_{R_i} Min	t_{R_i} Sec	fa-cc/min
He	7	2.36	81.319
Ne	7	4.95	81.317
N_2	7	19.76	81.310
Ar	7	21.83	81.315
CO_2	8	50.82	81.383
C_2H_2	10	13.81	81.370
C_3H_8	23	16.38	81.402

$T = 40^{o}F$

$W_L^{o} = 0.0079$ gm-mole

$P = 800$ psia

$T_a = 80.8^{o}F$

$P_a = 740.4$ mm Hg

$V_G = 9.590$ cc

Solute	t_{R_i} Min	t_{R_i} Sec	fa-cc/min
He	8	20.16	79.983
Ne	8	23.34	79.993
N_2	8	41.33	80.036
Ar	8	46.71	79.646
CO_2	10	25.37	80.000
C_2H_2	12	1.67	79.929
C_3H_8	25	56.05	79.505

TABLE G-I (Continued)

$T = 40^{o}F$

$W_L^{o} = 0.0079$ gm-mole

$P = 1000$ psia

$T_a = 81.4^{o}F$

$P_a = 741.2^{o}F$

$V_G = 9.565$ cc

Solute	t_{R_i} Min	t_{R_i} Sec	fa-cc/min
He	7	13.51	117.996
Ne	7	16.41	118.038
N_2	7	33.43	119.284
Ar	7	38.72	118.421
CO_2	9	0.10	118.891
C_2H_2	10	13.62	119.205
C_3H_8	19	50.87	119.205

$T = 40^{o}F$

$W_L^{o} = 0.0079$ gm-mole

$P = 1250$ psia

$T_a = 81.0^{o}F$

$P_a = 741.0^{o}F$

$V_G = 9.556$ cc

Solute	t_{R_i} Min	t_{R_i} Sec	fa-cc/min
He	9	16.35	120.806
Ne	9	20.30	120.802
N_2	9	41.70	120.996
Ar	9	45.63	121.105
CO_2	11	21.90	121.100
C_2H_2	12	51.10	121.174
C_3H_8	22	39.00	121.182

TABLE G-I (Continued)

$T = 40^{\circ}F$

$W_L^{\circ} = 0.0079$ gm-mole

$P = 1500$ psia

$T_a = 81.2^{\circ}F$

$P_a = 740.8$ mm Hg

$V_G = 9.537$ cc

Solute	t_{R_i} Min	t_{R_i} Sec	fa-cc/min
He	11	25.00	122.883
Ne	11	30.06	122.684
N_2	11	59.13	122.000
Ar	12	2.49	122.112
CO_2	13	45.53	122.115
C_2H_2	15	35.82	122.250
C_3H_8	25	15.35	122.314

$T = 40^{\circ}F$

$W_L^{\circ} = 0.0079$ gm-mole

$P = 1750$ psia

$T_a = 81.6^{\circ}F$

$P_a = 741.6$ mm Hg

$V_G = 9.505$ cc

Solute	t_{R_i} Min	t_{R_i} Sec	fa-cc/min
He	13	11.89	125.746
Ne	13	17.85	125.720
N_2	13	55.60	125.707
Ar	13	57.25	125.652
CO_2	15	34.03	126.085
C_2H_2	17	29.30	126.124
C_3H_8	26	13.18	126.100

TABLE G-I (Continued)

$T = 70^{o}F$	$T = 70^{o}F$
$W_L^{o} = 0.0073$ gm-mole	$W_L^{o} = 0.0073$ gm-mole
$P = 100$ psia	$P = 200$ psia
$T_a = 82.0^{o}F$	$T_a = 82.1^{o}F$
$P_a = 747.0$ mm Hg	$P_a = 747.0$ mm Hg
$V_G = 10.193$ cc	$V_G = 10.189$ cc

	t_{R_i}				t_{R_i}		
Solute	Min	Sec	fa-cc/min	Solute	Min	Sec	fa-cc/min
He	1	59.30	37.272	He	3	1.44	49.180
Ne				Ne			
N_2	2	2.31	37.272	N_2	3	6.17	49.180
Ar	2	2.91	37.272	Ar	3	7.21	49.180
CO_2	2	24.33	37.272	CO_2	3	40.06	49.180
C_2H_2	2	46.87	37.272	C_2H_2	4	12.44	49.180
C_3H_8	6	17.02	37.272	C_3H_8	9	23.02	49.180

TABLE G-I (Continued)

$T = 70^{o}F$

$W_L^{o} = 0.0073$ gm-mole

$P = 400$ psia

$T_a = 82.0^{o}F$

$P_a = 747.0$ mm Hg

$V_G = 10.355$ cc

Solute	t_{R_i} Min	t_{R_i} Sec	fa-cc/min
He	4	27.46	66.914
Ne			
N_2	4	44.80	66.914
Ar	4	47.04	66.914
CO_2	5	34.80	66.914
C_2H_2	6	20.22	66.914
C_3H_8	13	1.75	66.914

$T = 70^{o}F$

$W_L^{o} = 0.0073$ gm-mole

$P = 600$ psia

$T_a = 82.0^{o}F$

$P_a = 747.0$ mm Hg

$V_G = 10.343$ cc

Solute	t_{R_i} Min	t_{R_i} Sec	fa-cc/min
He	6	0.01	79.471
Ne			
N_2	6	11.13	79.471
Ar	6	13.46	79.471
CO_2	7	11.58	79.471
C_2H_2	8	8.62	79.471
C_3H_8	15	41.07	79.471

TABLE G-I (Continued)

$T = 70^{o}F$	$T = 70^{o}F$
$W_L^{o} = 0.0073$ gm-mole	$W_L^{o} = 0.0073$ gm-mole
$P = 800$ psia	$P = 1000$ psia
$T_a = 82.0^{o}F$	$T_a = 82.0^{o}F$
$P_a = 747.5$ mm Hg	$P_a = 746.8$ mm Hg
$V_G = 10.235$ cc	$V_G = 10.163$ cc

	t_{R_i}				t_{R_i}		
Solute	Min	Sec	fa-cc/min	Solute	Min	Sec	fa-cc/min
He	6	29.36	99.448	He	7	44.35	105.950
Ne				Ne			
N_2	6	41.80	99.448	N_2	8	0.13	105.950
Ar	6	44.16	99.448	Ar	8	3.62	105.950
CO_2	7	43.58	99.448	CO_2	9	10.80	105.950
C_2H_2	8	45.90	99.448	C_2H_2	10	21.25	105.950
C_3H_8	15	47.63	99.448	C_3H_8	17	25.32	105.950

TABLE G-I (Continued)

$T = 70^{o}F$

$W_L^{o} = 0.0079$ gm-mole

$P = 300$ psia

$T_a = 81.2^{o}F$

$P_a = 741.2$ mm Hg

$V_G = 10.249$ cc

Solute	t_{R_i} Min	t_{R_i} Sec	fa-cc/min
He	5	10.24	44.250
Ne	5	11.71	44.250
N_2	5	19.59	44.255
Ar	5	21.31	44.257
CO_2	6	21.60	44.257
C_2H_2	7	19.39	44.255
C_3H_8	16	14.99	44.220

$T = 70^{o}F$

$W_L^{o} = 0.0079$ gm-mole

$P = 500$ psia

$T_a = 80.4^{o}F$

$P_a = 742.0$ mm Hg

$V_G = 10.158$ cc

Solute	t_{R_i} Min	t_{R_i} Sec	fa-cc/min
He	7	11.52	53.810
Ne	7	13.79	53.805
N_2	7	25.89	53.800
Ar	7	28.63	53.805
CO_2	8	49.53	53.803
C_2H_2	10	6.12	53.804
C_3H_8	20	28.36	53.812

TABLE G-I (Continued)

$T = 70^{o}F$

$W_L^{o} = 0.0079$ gm-mole

$P = 700$ psia

$T_a = 79.6^{o}F$

$P_a = 741.5$ mm Hg

$V_G = 10.138$ cc

Solute	t_{R_i} Min	t_{R_i} Sec	fa-cc/min
He	9	57.42	55.516
Ne	10	0.70	55.515
N_2	10	17.21	55.515
Ar	10	22.15	55.515
CO_2	12	6.32	55.515
C_2H_2	13	49.04	55.519
C_3H_8	26	15.23	55.524

$T = 70^{o}F$

$W_L^{o} = 0.0079$ gm-mole

$P = 1250$ psia

$T_a = 79.4^{o}F$

$P_a = 740.8$ mm Hg

$V_G = 10.063$ cc

Solute	t_{R_i} Min	t_{R_i} Sec	fa-cc/min
He	12	43.77	82.445
Ne	12	48.54	82.446
N_2	13	16.76	82.458
Ar	13	20.22	82.409
CO_2	15	14.77	82.413
C_2H_2	17	12.48	82.441
C_3H_8	27	35.53	82.437

TABLE G-I (Continued)

$T = 70^{o}F$	$T = 70^{o}F$
$W_L^{o} = 0.0079$ gm-mole	$W_L^{o} = 0.0079$ gm-mole
$P = 1500$ psia	$P = 1750$ psia
$T_a = 79.2^{o}F$	$T_a = 79.0^{o}F$
$P_a = 740.4$ mm Hg	$P_a = 740.0$ mm Hg
$V_G = 10.077$ cc	$V_G = 10.090$ cc

	t_{R_i}				t_{R_i}		
Solute	Min	Sec	fa-cc/min	Solute	Min	Sec	fa-cc/min
He	14	20.25	89.979	He	15	37.77	98.514
Ne	14	26.14	89.981	Ne	15	44.71	98.512
N_2	15	0.45	89.983	N_2	16	23.28	98.471
Ar	15	5.07	89.946	Ar	16	29.82	98.499
CO_2	17	1.18	89.984	CO_2	18	18.94	98.765
C_2H_2	19	5.33	90.018	C_2H_2	20	25.68	98.813
C_3H_8	28	35.33	89.912	C_3H_8	29	15.61	98.902

TABLE G-I (Continued)

$T = 100^{o}F$	$T = 100^{o}F$
$W_L^{o} = 0.0077$ gm-mole	$W_L^{o} = 0.0077$ gm-mole
$P = 100$ psia	$P = 200$ psia
$T_a = 83.0^{o}F$	$T_a = 83.0^{o}F$
$P_a = 741.0$ mm Hg	$P_a = 741.2$ mm Hg
$V_G = 10.921$ cc	$V_G = 10.702$ cc

	t_{R_i}				t_{R_i}		
Solute	Min	Sec	fa-cc/min	Solute	Min	Sec	fa-cc/min
He	2	9.50	34.783	He	3	26.76	43.114
Ne				Ne			
N_2	2	12.64	34.783	N_2	3	32.04	43.114
Ar	2	13.24	34.783	Ar	3	33.11	43.114
CO_2	2	33.15	34.783	CO_2	4	6.12	43.114
C_2H_2	2	51.72	34.783	C_2H_2	4	35.48	43.114
C_3H_8	5	33.52	34.783	C_3H_8	9	2.99	43.114

TABLE G-I (Continued)

$T = 100^{o}F$	$T = 100^{o}F$
$W_L^{o} = 0.0077$ gm-mole	$W_L^{o} = 0.0073$ gm-mole
$P = 400$ psia	$P = 600$ psia
$T_a = 83.1^{o}F$	$T_a = 83.2^{o}F$
$P_a = 740.0$ mm Hg	$P_a = 741.0$ mm Hg
$V_G = 10.634$ cc	$V_G = 10.522$ cc

	t_{R_i}				t_{R_i}		
Solute	Min	Sec	fa-cc/min	Solute	Min	Sec	fa-cc/min
He	5	3.63	59.583	He	6	30.58	70.148
Ne				Ne			
N_2	5	11.83	59.583	N_2	6	42.35	70.148
Ar	5	13.76	59.583	Ar	6	45.16	70.148
CO_2	6	1.11	59.583	CO_2	7	44.387	70.148
C_2H_2	6	45.69	59.583	C_2H_2	8	42.52	70.148
C_3H_8	12	14.20	59.583	C_3H_8	15	7.29	70.148

TABLE G-I (Continued)

$T = 100^{o}F$

$W_L^{o} = 0.0077$ gm-mole

$P = 800$ psia

$T_a = 83.0^{o}F$

$P_a = 741.4$ mm Hg

$V_G = 10.507$ cc

Solute	t_{R_i} Min	t_{R_i} Sec	fa-cc/min
He	5	25.72	114.213
Ne			
N_2	5	35.53	114.213
Ar	5	38.58	114.213
CO_2	6	25.85	114.213
C_2H_2	7	13.58	114.213
C_3H_8	12	3.92	114.213

$T = 100^{o}F$

$W_L^{o} = 0.0077$ gm-mole

$P = 1000$ psia

$T_a = 83.0^{o}F$

$P_a = 741.0$ mm Hg

$V_G = 10.444$ cc

Solute	t_{R_i} Min	t_{R_i} Sec	fa-cc/min
He	6	36.84	118.514
Ne			
N_2	6	50.84	118.514
Ar	6	53.34	118.514
CO_2	7	48.52	118.514
C_2H_2	8	45.47	118.514
C_3H_8	13	58.66	118.514

TABLE G-I (Continued)

$T = 100^{o}F$

$W_L^{o} = 0.0077$ gm-mole

$P = 1250$ psia

$T_a = 83.2^{o}F$

$P_a = 742.0$ mm Hg

$V_G = 10.422$ cc

Solute	t_{R_i} Min	t_{R_i} Sec	fa-cc/min
He	8	16.55	120.715
Ne			
N_2	8	34.91	120.715
Ar	8	39.22	120.715
CO_2	9	47.31	120.715
C_2H_2	10	53.07	120.715
C_3H_8	16	25.73	120.715

$T = 100^{o}F$

$W_L^{o} = 0.0079$ gm-mole

$P = 300$ psia

$T_a = 80.6\ ^{o}F$

$P_a = 738.2$ mm Hg

$V_G = 10.977$ cc

Solute	t_{R_i} Min	t_{R_i} Sec	fa-cc/min
He	5	4.63	45.572
Ne	5	5.88	45.570
N_2	5	12.30	45.604
Ar	5	13.99	45.615
CO_2	6	1.09	45.766
C_2H_2	6	43.81	45.810
C_3H_8	12	40.12	45.793

TABLE G-I (Continued)

$T = 100^{\circ}F$

$W_L^{\circ} = 0.0079$ gm-mole

$P = 1500$ psia

$T_a = 79.8^{\circ}F$

$P_a = 739.9$ mm Hg

$V_G = 10.445$ cc

Solute	t_{R_i} Min	t_{R_i} Sec	fa-cc/min
He	13	24.19	90.837
Ne	13	29.39	90.824
N_2	13	55.86	90.810
Ar	14	3.35	90.815
CO_2	15	48.74	90.815
C_2H_2	17	43.81	90.854
C_3H_8	25	16.25	90.860

$T = 100^{\circ}F$

$W_L^{\circ} = 0.0079$ gm-mole

$P = 1750$ psia

$T_a = 79.6^{\circ}F$

$P_a = 741.2$ mm Hg

$V_G = 10.390$ cc

Solute	t_{R_i} Min	t_{R_i} Sec	fa-cc/min
He	14	18.37	100.027
Ne	14	24.59	100.027
N_2	14	54.97	100.000
Ar	15	4.30	100.118
CO_2	16	46.58	100.129
C_2H_2	18	34.12	100.187
C_3H_8	25	42.21	100.202

TABLE G-I (Continued)

$T = 125^{o}F$	$T = 125^{o}F$
$W_L^{o} = 0.0073$ gm-mole	$W_L^{o} = 0.0073$ gm-mole
$P = 100$ psia	$P = 200$ psia
$T_a = 83.0^{o}F$	$T_a = 81.0^{o}F$
$P_a = 733.8$ mm Hg	$P_a = 734.4$ mm Hg
$V_G = 11.131$ cc	$V_G = 11.108$ cc

	t_{R_i}			t_{R_i}		
Solute	Min	Sec	fa-cc/min	Solute	Min	Sec	fa-cc/min
He	2	8.26	34.500	He	3	34.22	41.450
N_2	2	11.44	34.500	N_2	3	39.72	41.450
Ar	2	11.76	34.500	Ar	3	39.95	41.450
CO_2	2	27.52	34.500	CO_2	4	6.92	41.450
C_2H_2	2	41.90	34.500	C_2H_2	4	31.18	41.450
C_3H_8	4	36.12	34.500	C_3H_8	7	45.82	41.450

TABLE G-I (Continued)

$T = 125^{o}F$

$W_L^{o} = 0.0073$ gm-mole

$P = 300$ psia

$T_a = 79.5^{o}F$

$P_a = 735.0$ mm Hg

$V_G = 11.019$ cc

Solute	t_{R_i} Min	t_{R_i} Sec	fa-cc/min
He	4	24.57	50.462
N_2	4	31.60	50.462
Ar	4	31.95	50.462
CO_2	5	5.43	50.462
C_2H_2	5	37.16	50.462
C_3H_8	9	19.42	50.462

$T = 125^{o}F$

$W_L^{o} = 0.0073$ gm-mole

$P = 400$ psia

$T_a = 79.5^{o}F$

$P_a = 736.0$ mm Hg

$V_G = 10.967$ cc

Solute	t_{R_i} Min	t_{R_i} Sec	fa-cc/min
He	5	28.07	54.071
N_2	5	37.96	54.071
Ar	5	38.20	54.071
CO_2	6	20.57	54.071
C_2H_2	6	59.27	54.071
C_3H_8	11	19.47	54.071

TABLE G-I (Continued)

$T = 125^{o}F$

$W_L^{o} = 0.0073$ gm-mole

$P = 500$ psia

$T_a = 79.5^{o}F$

$P_a = 736.6$ mm Hg

$V_G = 10.956$ cc

Solute	t_{R_i} Min	t_{R_i} Sec	fa-cc/min
He	4	25.55	84.000
N_2	4	33.82	84.000
Ar	4	34.10	84.000
CO_2	5	7.78	84.000
C_2H_2	5	42.53	84.000
C_3H_8	9	4.41	84.000

$T = 125^{o}F$

$W_L^{o} = 0.0073$ gm-mole

$P = 600$ psia

$T_a = 80.0^{o}F$

$P_a = 739.2$ mm Hg

$V_G = 10.937$ cc

Solute	t_{R_i} Min	t_{R_i} Sec	fa-cc/min
He	5	41.26	78.773
N_2	5	51.44	78.773
Ar	5	52.01	78.773
CO_2	6	35.41	78.773
C_2H_2	7	17.99	78.773
C_3H_8	11	29.89	78.773

TABLE G-I (Continued)

$T = 125^{o}F$

$W_L^{o} = 0.0073$ gm-mole

$P = 700$ psia

$T_a = 81.0^{o}F$

$P_a = 738.6$ mm Hg

$V_G = 10.921$ cc

Solute	t_{R_i} Min	Sec	fa-cc/min
He	6	34.67	80.432
N_2	6	47.54	80.432
Ar	6	47.95	80.432
CO_2	7	37.13	80.432
C_2H_2	8	25.39	80.432
C_3H_8	13	0.95	80.432

$T = 125^{o}F$

$W_L^{o} = 0.0073$ gm-mole

$P = 800$ psia

$T_a = 80.5^{o}F$

$P_a = 738.0$ mm Hg

$V_G = 10.917$ cc

Solute	t_{R_i} Min	Sec	fa-cc/min
He	7	27.83	81.262
N_2	7	42.37	81.262
Ar	7	42.80	81.262
CO_2	8	39.20	81.262
C_2H_2	9	33.95	81.262
C_3H_8	14	34.67	81.262

TABLE G-I (Continued)

$T = 125^{o}F$

$W_L^{o} = 0.0073$ gm-mole

$P = 1000$ psia

$T_a = 79.4^{o}F$

$P_a = 738.0$ mm Hg

$V_G = 10.183$ cc

Solute	t_{R_i} Min	Sec	fa-cc/min
He	8	36.62	83.457
N_2	8	57.11	83.457
Ar	8	57.75	83.457
CO_2	10	3.89	83.457
C_2H_2	11	11.31	83.457
C_3H_8	16	38.85	83.457

$T = 125^{o}F$

$W_L^{o} = 0.0073$ gm-mole

$P = 1250$ psia

$T_a = 80.4^{o}F$

$P_a = 737.0$ mm Hg

$V_G = 10.854$ cc

Solute	t_{R_i} Min	Sec	fa-cc/min
He	11	32.25	84.252
N_2	11	59.02	84.252
Ar	12	0.04	84.242
CO_2	13	21.06	84.242
C_2H_2	14	43.88	84.242
C_3H_8	20	32.53	84.242

TABLE G-I (Continued)

$T = 125^{\circ}F$

$W_L^{\circ} = 0.0073$ gm-mole

$P = 1500$ psia

$T_a = 79.0^{\circ}F$

$P_a = 739.0$ mm Hg

$V_G = 10.836$ cc

$T = 125^{\circ}F$

$W_L^{\circ} = 0.0073$ gm-mole

$P = 1750$ psia

$T_a = 79.5^{\circ}F$

$P_a = 738.4$ mm Hg

$V_G = 10.810$ cc

Solute	t_{R_i} Min	t_{R_i} Sec	fa-cc/min	Solute	t_{R_i} Min	t_{R_i} Sec	fa-cc/min
He	14	0.90	83.754	He	16	13.37	85.790
N_2	14	38.87	83.754	N_2	16	56.00	85.790
Ar	14	39.44	84.754	Ar	16	58.56	85.790
CO_2	16	12.89	84.754	CO_2	18	41.90	85.790
C_2H_2	17	49.09	84.754	C_2H_2	20	28.56	85.790
C_3H_8	23	51.63	84.754	C_3H_8	26	34.39	85.790

TABLE G-I (Continued)

$T = 150^{o}F$	$T = 150^{o}F$
$W_L^{o} = 0.0080$ gm-mole	$W_L^{o} = 0.0080$ mole
$P = 100$ psia	$P = 200$ psia
$T_a = 80.7^{o}F$	$T_a = 80.4^{o}F$
$P_a = 739.6$ mm Hg	$P_a = 740.1$ mm Hg
$V_G = 11.142$ cc	$V_G = 11.052$ cc

	t_{R_i}				t_{R_i}		
Solute	Min	Sec	fa-cc/min	Solute	Min	Sec	fa-cc/min
He	2	9.62	32.769	He	3	24.78	40.179
Ne	2	10.10	32.770	Ne	3	25.55	40.203
N_2	2	13.79	32.386	N_2	3	28.30	40.909
Ar	2	13.95	32.229	Ar	3	31.82	40.835
CO_2	2	30.36	32.143	CO_2	3	58.00	40.395
C_2H_2	2	43.49	32.206	C_2H_2	4	20.00	40.733
C_3H_8	4	26.07	32.300	C_3H_8	7	13.03	40.674

TABLE G-I (Continued)

$T = 150^{o}F$

$W_L^{o} = 0.0080$ gm-mole

$P = 300$ psia

$T_a = 81.6^{o}F$

$P_a = 741.4$ mm Hg

$V_G = 10.944$ cc

Solute	t_{R_i} Min	t_{R_i} Sec	fa-cc/min
He	4	5.10	50.919
Ne	4	6.09	50.923
N_2	4	10.70	51.355
Ar	4	13.80	51.107
CO_2	4	45.23	51.121
C_2H_2	5	16.27	50.905
C_3H_8	8	20.32	50.833

$T = 150^{o}F$

$W_L^{o} = 0.0080$ gm-mole

$P = 400$ psia

$T_a = 81.8^{o}F$

$P_a = 739.8$ mm Hg

$V_G = 10.941$ cc

Solute	t_{R_i} Min	t_{R_i} Sec	fa-cc/min
He			53.428
Ne	5	16.74	53.400
N_2	5	23.27	52.832
Ar	5	28.02	52.509
CO_2	6	9.77	52.601
C_2H_2	6	48.91	52.570
C_3H_8	10	43.29	52.326

TABLE G-I (Continued)

$T = 150^{o}F$

$W_L^{o} = 0.0080$ gm-mole

$P = 500$ psia

$T_a = 80.8^{o}F$

$P_a = 740.4$ mm Hg

$V_G = 10.935$ cc

Solute	t_{R_i} Min	t_{R_i} Sec	fa-cc/min
He	6	2.18	58.395
Ne	6	3.75	58.401
N_2	6	13.00	58.408
Ar	6	14.90	58.426
CO_2	7	0.52	58.480
C_2H_2	7	48.19	58.482
C_3H_8	11	57.50	58.505

$T = 150^{o}F$

$W_L^{o} = 0.0080$ gm-mole

$P = 600$ psia

$T_a = 84.0^{o}F$

$P_a = 738.5$ mm Hg

$V_G = 11.030$ cc

Solute	t_{R_i} Min	t_{R_i} Sec	fa-cc/min
He	5	27.63	79.330
Ne	5	29.10	79.330
N_2	5	36.30	79.470
Ar	5	40.65	79.017
CO_2	6	21.34	79.717
C_2H_2	7	1.63	79.646
C_3H_8	10	30.51	79.717

TABLE G-I (Continued)

$T = 150^{\circ}F$				$T = 150^{\circ}F$			
$W_L^{\circ} = 0.0080$ gm-mole				$W_L^{\circ} = 0.0080$ mole			
$P = 700$ psia				$P = 800$ psia			
$T_a = 83.5^{\circ}F$				$T_a = 82.8^{\circ}F$			
$P_a = 737.8$ mm Hg				$P_a = 738.0$ mm Hg			
$V_G = 10.814$ cc				$V_G = 10.798$ cc			
	t_{R_i}				t_{R_i}		
Solute	Min	Sec	fa-cc/min	Solute	Min	Sec	fa-cc/min
He	7	9.25	71.542	He	7	15.12	80.863
Ne	7	11.25	71.544	Ne	7	17.18	80.862
N_2	7	23.05	71.485	N_2	7	34.6	80.573
Ar	7	28.88	71.090	Ar	7	35.17	81.448
CO_2	8	16.36	72.000	CO_2	8	26.93	80.826
C_2H_2	9	11.89	71.885	C_2H_2	9	24.78	80.740
C_3H_8	13	29.61	71.372	C_3H_8	13	38.68	81.301

TABLE G-I (Continued)

$T = 150^{o}F$	$T = 150^{o}F$
$W_L^{o} = 0.0080$ gm-mole	$W_L^{o} = 0.0080$ mole
$P = 1000$ psia	$P = 1250$ psia
$T_a = 81.6^{o}F$	$T_a = 82.2^{o}F$
$P_a = 738.4$ mm Hg	$P_a = 740.2$ mm Hg
$V_G = 11.079$ cc	$V_G = 11.025$ cc

	t_{R_i}				t_{R_i}		
Solute	Min	Sec	fa-cc/min	Solute	Min	Sec	fa-cc/min
He	8	9.82	88.753	He	9	39.49	94.150
Ne	8	12.41	88.750	Ne	9	42.83	94.170
N_2	8	27.92	88.604	N_2	10	4.15	94.290
Ar	8	31.63	88.507	Ar	10	9.92	94.383
CO_2	9	31.15	88.944	CO_2	11	14.89	94.755
C_2H_2	10	36.35	88.950	C_2H_2	12	31.48	94.894
C_3H_8	15	8.91	88.887	C_3H_8	17	14.89	94.974

TABLE G-I (Continued)

$T = 150^{o}F$

$W_L^{o} = 0.0080$ gm-mole

$P = 1500$ psia

$T_a = 82.4^{o}F$

$P_a = 739.5$ mm Hg

$V_G = 10.771$ cc

Solute	t_{R_i} Min	t_{R_i} Sec	fa-cc/min
He	11	0.65	100.593
Ne	11	4.74	100.565
N_2	11	30.6	100.455
Ar	11	36.80	100.584
CO_2	12	52.71	100.502
C_2H_2	14	18.99	100.617
C_3H_8	18	56.29	100.773

$T = 150^{o}F$

$W_L^{o} = 0.0080$ gm-mole

$P = 1750$ psia

$T_a = 83.0^{o}F$

$P_a = 738.8$ mm Hg

$V_G = 10.763$ cc

Solute	t_{R_i} Min	t_{R_i} Sec	fa-cc/min
He	11	15.97	115.004
Ne	11	18.77	115.114
N_2	11	36.42	115.105
Ar	11	40.18	115.212
CO_2	12	24.72	115.100
C_2H_2	13	17.41	115.209
C_3H_8	15	53.08	115.185

APPENDIX H

LISTING OF COMPUTER PROGRAMS

COMPUTER PROGRAM FOR CALCULATING K-VALUES FROM CHROMATOGRAPHIC DATA

```
C       CALCULATION OF K VALUES FROM CHROMATOGRAPHIC MEASUREMENTS
C       THIS PROGRAM ALSO PLOTS THE K-VALUES VS. PRESS. FOR EACH SOLUTE
        DIMENSION P(20),V(20),XX(20),Y(20),   Z(20),DG(20),X(20),
     1CK(10,20),RT(10,20) ,RV(10,20),GRT(20),VG(20) ,TRM(20),PATM(20)
     2 ,FLOW(10,20),C(10,20)
  200  FORMAT(1X,11HROOM TEMP =,F6.3,6H DEG F/)
  201  FORMAT(1X,14HATM PRESSURE =,F7.1,5H PSIA////)
  202  FORMAT(1X,13HSYSTEM TEMP =,F4.0,6H DEG F//)
  203  FORMAT(1X,10F8.1 )
  204  FORMAT(1X,10(1X,F8.5,2X))
  205  FORMAT(1X,9F8.6)
  206  FORMAT(1X,/////)
  208  FORMAT(1X,70H1=HELIUM  2=NITROGEN  3=ARGON  4=CARBON DIOXIDE  5=ET
     1HYLENE  6=PROPANE////)
  209  FORMAT(10X,10HPRESS PSIA,10X,2H K,16X,7HRET VOL,16X,8HRET TIME//)
  210   FORMAT(10X,F8.0,10X,F10.4,10X,F10.7,10X,F10.5////)
  198   FORMAT(10F8.6)
  199   FORMAT(2F10.8)
  299   FORMAT(2X,F10.8,6X,F10.8)
  300   FORMAT(1H1)
C
C       N=TOTAL NO. OF PRESS. POINTS
C       L=TOTAL NO. OF SOLUTES
C       WL=WT. OF DECANE IN GMS.
C       TRM=RM. TEMP.
C       PATM=ATM. PRESS.
C       T=SYST. TEMP.
C       P=SYST. PRESS.
C       Z=COMPRESS. FACTOR OF CARRIER GAS
C       X= MOLE FRACTION OF C1 IN C10 AT EQUILIB.
C       RT= RETENTION TIME
C       RV=RETENTION VOLUME
C       VG=VOID VOLUME
C       CK= K-VALUE
C
  4     CONTINUE
        READ(5,199)XN
        N=XN
        READ(5,199)WL
        READ(5,198)(TRM(J),J=1,N)
        READ(5,198)(PATM(J),J=1,N)
        READ(5,199)T
        READ(5,198) (P(J),J=1,N)
        READ(5,198) (Z(J),J=1,N)
        READ(5,198) ( X(J),J=1,N)
```

```
      L=7
      WLM=WL/142.276
      T=T+460.
C     SUBROUTINE DEADVL CALCULATES VOID VOLUME IN COLUMN USING LINEAR
C     FITTING TECHNIQUE
      DO 999J=1,N
      PATM(J)=PATM(J)*14.696/760.
      TRM(J)=TRM(J)+460.
      V(J)=Z(J)*T*10.73/P(J)
      DG(J)=1./V(J)*453.59/28320.
      READ(5,198)(FLOW(I,J),I=1,L)
      READ(5,198) (RT(I,J),I=1,L)
      DO 3 I=1,L
      C(I,J)=Z(J)*FLOW(I,J)*PATM(J)*T/P(J)/TRM(J)
3     RV(I,J)=C(I,J)*RT(I,J)
      HEV=C(1,J)*RV(1,J)
      VNE=C(2,J)*RV(2,J)
      ARV=C(3,J)*RT(3,J)
      CALL DEADVL(HEV,VNE,ARV,DVL)
      VG(J)=DVL
      DO90 I=1,L
      CK(I,J)=WLM/((1.-X(J))*DG(J)    *(RV(I,J)-VG(J)))
90    CONTINUE
999   CONTINUE
      WRITE(6,204)(DG(J),J=1,N)
      WRITE(6,203)(P(J),J=1,N)
      WRITE(6,204)(V(J),J=1,N)
      WRITE(6,204)(Z(J),J=1,N)
      WRITE(6,204)(X(J),J=1,N)
      WRITE(6,299 )WL,WLM
      WRITE(6,204)(VG(J),J=1,N)
      WRITE(6,206)
      T=T-460.
      DO 66J=1,N
      TRM(J)=TRM(J)-460.
      WRITE(6,200)TRM(J)
      WRITE(6,201)PATM(J)
66    CONTINUE
      WRITE(6,202)T
      WRITE(6,208)
      DO 888I=1,L
      WRITE(6,209)
      DO 777J=1,N
      WRITE(6,210) P(J),CK(I,J),RV(I,J),RT(I,J)
      Y(J)=CK(I,J)
      DG(J)=P(J)
777   CONTINUE
      CALL PLOT (DG,0,Y,0,Z,0,N,1,1,3,2,0,1)
888   CONTINUE
      WRITE(6,300)
      GO TO 4
      END
```

COPUTER PROGRAM FOR CALCULATING FUGACITY COEFFICIENT OF A SOLUTE AT INFINITE DILUTION IN GAS SOLVENT USING THE B-W-R EQUATION OF STATE

```
C     1 IS THE SOLVENT, 2 IS THE SOLUTE
C     CHROMATOGRAPHICALLY DETERMINED K-VALUE IS USED FOR CALCULATING
C     LIQUID FUGACITY OF THE SOLUTE
C
      COMMON Z,P,T,XR,AO1,BO1,CO1,A1,B1,C1,AL1,G1,DZ,DK
      DIMENSION P(100),T(20),SYS(12),CK(100),HENCON(100)
   10 FORMAT(8F10.5)
 50   FORMAT(1X,8E14.7/)
  55  FORMAT(1X,///,2X,14HSYSTEM TEMP IS,F10.2,6H DEG F//)
     115X,6HHENCON//)
  60  FORMAT(5X,7HDENSITY,19X,8HCOMPRESS,21X,8HFUGACITY,19X,9HPRESS-PSI,
  70  FORMAT(1X,E14.7,14X,E14.7,14X,E14.7,14X,E14.7 , 9X,E14.7/)
  75  FORMAT(1H1)
  90  FORMAT(12A6)
  95  FORMAT(1X,///,12A6)
 97   FORMAT(8F10.5)
 98   FORMAT(1X,///////,12F10.4)
C
C     N= NO. OF PRESS POINTS
C     L= NO. OF ISOTHERMS
C     XA12=MODIFIED AO12 FROM B-W-R EQ.
C     HENCON=LIQUID FUGACITY
C     CK=K-VALUE OBTAINED FROM CHROMAT. EXP.
C
   4  READ(5,90)(SYS(I),I=1,12)
      READ(5,10)XR
      READ(5,10) XN,XL
      READ(5,10) XA12
      N=XN
      L=XL
C
C     THE FOLLOWING ARE B-W-R CONSTANTS
      READ(5,10) AO1,BO1,CO1,B1,A1,AL1,C1,G1
      READ(5,10)AO2,BO2,CO2,B2,A2,AL2,C2,G2
      WRITE(6,50)XA12
      WRITE(6,50)AO1,BO1,CO1,B1,A1,AL1,C1,G1
      WRITE(6,50) AO2,BO2,CO2,B2,A2,AL2,C2,G2
      READ(5,10)(T(J),J=1,L)
      READ(5,10)(P(I),I=1,N)
      A112=A1**0.667*A2**0.333
      B112=B1**0.667*B2**0.333
      C112=C1**0.667*C2**0.333
      AL112=AL1**0.667*AL2**0.333
      BO12=(BO1*BO2)**0.5
      AO12=XA12*(AO1*AO2)**0.5
      CO12=(CO1*CO2)**0.5
      G12=(G1*G2)**0.5
      WRITE(6,95)(SYS(I),I=1,12)
```

```
      DO111 J=1,L
      WRITE(6,55) T(J)
      T(J)=(T(J)+459.6)/1.8
      WRITE(6,60)
      READ(5,10)(CK(I),I=1,N)
      DO222 I=1,N
      P(I)=P(I)/14.696
      CALL DENS (I,J)
      E=1./EXP(G1*DZ**2)
      Z=P(I)/(XR*T(J)*DZ)
      FUGL=1./XR/T(J)*(2.*(BO12*XR*T(J)-AO12-CO12/T(J)**2)*DZ+3./2.*
     1(B112*XR*T(J)-A112)*DZ**2+3./5.*(AL1*A112+A1*AL112)*DZ**5+
     23./T(J)**2*DZ**2*C112*((1.-E)/G1/DZ**2-E/2.)-2./T(J)**2*DZ**2
     3*C1*G12*((1.-E)/DZ**2-(G1+G1**2*DZ**2/2.)*E))-ALOG(Z)
      FUG=EXP(FUGL)
      P(I)=P(I)*14.696
      HENCON(I)=CK(I)*FUG*P(I)
      WRITE(6,70) DZ,Z,FUG,P(I),HENCON(I)
  222 CONTINUE
   35 WRITE(6,98)(CK(I),I=1,N)
      WRITE(7,97) (HENCON(I),I=1,N)
  111 CONTINUE
      WRITE(6,75)
      GO TO 4
      END
C     SUBROUTINE DENS CALCULATES VAPOR PHASE DENSITY DZ
      SUBROUTINE DENS (I,J)
      COMMON Z,P,T,XR,AO1,BO1,CO1,A1,B1,C1,AL1,G1,DZ,DK
      DIMENSION P(100),T(20),SYS(12)
      XU=P(I)/(.2*XR*T(J))
      XL=P(I)/(2.*XR*T(J))
   40 DZ=.5*(XU+XL)
      PC=DZ*XR*T(J)+(BO1*XR*T(J)-AO1-CO1/T(J)**2)*DZ**2+(B1*XR*T(J)-A1)*
     2DZ**3+A1*AL1*DZ**6+(C1*DZ**3/T(J)**2)*(1.+G1*DZ**2)/EXP(G1*DZ**2)
      DEL=P(I)-PC
      DELL=DEL/P(I)
      ADELL=ABS(DELL)
      IF(ADELL.LE.0.0005) GO TO 30
      IF(DEL.LE.0.) GO TO 50
      XL=DZ
      GO TO 40
   50 XU=DZ
      GO TO 40
   30 RETURN
      END
```

COPUTER PROGRAM FOR CALCULATING MIXING PARAMETER A12 FOR

BINARY SOLUTION

```
C           SOLUBILITY CORRELATION FOR BINARY  SOLUTION
      DIMENSIONTT(200),FFO2(200),VB(200),X2(200),VVM(200),FF(200),
     1 H(200),G(200),D(200),TITLE(20),PP(200),Q(200),W(200),DAV(200),
     2 FCC(5),FC(200,5),ERR(200,5),AVAER(5),U(200),AVPE(5)
100     FORMAT(8F10.4)
101     FORMAT(20A4)
200     FORMAT(1X,///,1X,20A4//////)
201     FORMAT(1X,7E14.7)
202     FORMAT(1X,////)
203     FORMAT(1X,5(1X,E14.7,5X)/)
204     FORMAT(1X,//1X,18HAVE ABS PCT ERROR=,F8.3,10X,14HAVE PCT ERROR=,F
     1 8.3)
205     FORMAT(1H1)
206     FORMAT(1X,////,1X,F10.5,8X,F10.5,8X,F10.5)
 207    FORMAT(19X,32H********************* MODEL NO. -,I1,21H-**********
     1*********,////)
208     FORMAT(1X,////,4(1X,F10.5,7X))
210    FORMAT(3X,10HTEMP DEG F,13X,5HP-PSI,14X,7HF/X-ATM,12X,12HF/X-CALC-
     1ATM,7X,7HPCT ERR///)
       R=1.9872
4      CONTINUE
       SUM1=0.
       SUM2=0.
       SUMER1=0.
       SUMER2=0.
       SHP=0.
       S1=0.
       S2=0.
       READ(5,101)(TITLE(I),I=1,20)
C      V1 AND V2 ARE LIQUID VOLUMES OF SOLVENT-1 AND SOLUTE-2
C      D1 AND D2 ARE SOLUBILITY PARAMETERS OF SOLVENT-1 AND SOLUTE-2
       READ(5,100)V1,V2,D1,D2
C
C      THE VARIABLES ON EACH DATA CARD ARE-SYST TEMP,STANDARD LIQUID
C      FUGACITY OF SOLUTE,LIQUID PARTIAL VOLUME OF SOLUTE,SYST PRESS,
C      LIQUID MOLAR VOLUME OF SOLUTION,LIQUID FUGACITY OF SOLUTE AT SYST
C      TEMP AND PRESS
C      WHEN 6TH FIELD (SOLUTION VOLUME) IS 3EFT BLANK, THE IDEAL
C      SOLUTION VOLUME WILL BE CALCULATED
C
C      LAST DATA CARD SHOULD BE BLANK
       DO 10 I=1,5000
       READ(5,100)TT(I),FFO2(I),VB(I),PP(I),X2(I),VVM(I),FF(I)
50     N=I
10     CONTINUE
60     CONTINUE
       WRITE(6,200)(TITLE(I),I=1,20)
       WRITE(6,201) V1,V2,D1,D2
      WRITE(6,201)(TT(I),FFO2(I),VB(I),PP(I),X2(I),VVM(I),FF(I) ,I=1,N)
       DO 20 I=1,N
       IF(VVM(I).EQ.0.) GO TO 25
       T=(TT(I)+459.6)/1.8
       VM=VVM(I)*28320./453.59
```

```
      GO TO 27
 25   VM=V2*X2(I)+V1*(1.-X2(I))
 27   VF2=X2(I)*V2/VM
      VF1=1.-VF2
      VBAR=VB(I)
      FO2=FFO2(I)
      P=PP(I)
      F=FF(I)
      H(I)=ALOG(F/FO2)
      G(I)=ALOG(V1/VM)-VF2*(1.-V2/V1)+VBAR*P/(1.8*T*10.731)
      D(I)=V2*(VF1**2-1.)/(R*T)
      U(I)=VBAR*P/(1.8*T*10.731)
      SUM1=SUM1+H(I)*D(I)-G(I)*D(I)
      SUM2=SUM2+D(I)**2
      SHP=SHP+H(I)*D(I)-U(I)*D(I)
 20   CONTINUE
      A12=SUM1/SUM2
      ASHP=SHP/SUM2
      WRITE(6,208)A12,ASHP
      WRITE(6,202)
      AL12=(D1**2+D2**2-A12)/(2.*D1*D2)
      AA=AL12*D1*D2
      WRITE(6,206) A12,AL12,AA
      XASHP=(D2**2+D2**2-ASHP)/(2.*D1*D2)
      AE=XASHP*D1*D2
      WRITE(6,206) ASHP,XASHP,AE
      DO 30 I=1,N
      AC1=D(I)*A12+G(I)
      AC2=D(I)*ASHP+U(I)
      T=(TT(I)+459.6)/1.8
      FCC(1)=EXP(AC1)
      FCC(2)=EXP(AC2)
      DO 44 K=1,2
      FC(I,K)=FCC(K)
      FF(I)=EXP(H(I))
      ERR(I,K)=(FF(I)-FC(I,K))/FFC(I,K)*100.
 44   CONTINUE
      SUMER1=SUMER1+ABS(ERR(I,1))
      SUMER2=SUMER2+ABS(ERR(I,2))
      S1=S1+ERR(I,1)
      S2=S2+ERR(I,2)
 30   CONTINUE
      XN=N
      AVAER(1)=SUMER1/XN
      AVAER(2)=SUMER2/XN
      AVPE(1)=S1/XN
      AVPE(2)=S2/XN
      DO 15 K=1,2
      WRITE(6,202)
      WRITE(6,207) K
      WRITE(6,204) AVAER(K),AVPE(K)
      WRITE(6,202)
      WRITE(6,210)
      DO 15 I=1,N
      WRITE(6,203) TT(I),PP(I),FF(I),FC(I,K),ERR(I,K)
 15   CONTINUE
      WRITE(6,205)
      GO TO 4
      END
```

COPUTER PROGRAM FOR CORRELATING TERNARY SOLUTION DATA

```
C           SOLUBILITY CORRELATION FOR TERNARY SOLUTION
      DIMENSIONTT(200),FFO2(200),VB(200),X1(200),VVM(200),FF(200),
     1 H(200),G(200),D(200),TITLE(20),PP(200),Q(200),W(200),DAV(200),
     2 FCC(5),FC(200,5),ERR(200,5),AVAER(5),U(200),AVPE(5),YM(200),YSH(2
     3 00),YSHP(200),YSHFH(200),POY(200)
100     FORMAT(8F10.4)
101     FORMAT(20A4)
200     FORMAT(1X,///,1X,20A4//////)
201     FORMAT(1X,7E14.7)
202     FORMAT(1X,////)
203     FORMAT(1X,5(1X,E14.7,5X)/)
204     FORMAT(1X,//1X,18HAVE ABS PCT ERROR=,F8.3,10X,14HAVE PCT ERROR=,F
     1 8.3)
205     FORMAT(1H1)
 207    FORMAT(19X,32H********************* MODEL NO. -,I1,21H-***********
     1*********,////)
208     FORMAT(1X,////,4(1X,F10.5,7X))
210    FORMAT(3X,10HTEMP DEG F,13X,5HP-PSI,14X,7HF/X-ATM,12X,12HF/X-CALC-
     1ATM,7X,7HPCT ERR///)
       R=1.9872
4      CONTINUE
       SUM1=0.
       SUM2=0.
       SUMER1=0.
       SUMER2=0.
       SHP=0.
       S1=0.
       S2=0.
C
C      1-CARRIER GAS,2-SOLUTE AT INFINITE DILUTION,3-SOLVENT
C      V=LIQUIDE VOLUME
C      D=SOLUBILITY PARAMETER
C      AA=A13 FROM BINARY DATA
C      AE=A13 FROM BINARY DATA,FLORY-HUGGINS TERM DELETED
       READ(5,101)(TITLE(I),I=1,20)
       READ(5,100) V1,V2,V3,D1,D2,D3
       READ(5,100) AA,AE
C
C      THE VARIABLES ON EACH DATA CARD ARE-SYST TEMP,STANDARD LIQUID
C      FUGACITY OF SOLUTE,LIQUID PARTIAL VOLUME OF SOLUTE,SYST PRESS,
C      LIQUID MOLAR VOLUME OF SOLUTION,LIQUID FUGACITY OF SOLUTE AT SYST
C      TEMP AND PRESS
C      WHEN 6TH FIELD (SOLUTION VOLUME) IS 3EFT BLANK, THE IDEAL
C      SOLUTION VOLUME WILL BE CALCULATED
C
C      LAST DATA CARD SHOULD BE BLANK
       DO 10 I=1,5000
       READ(5,100)TT(I),FFO2(I),VB(I),PP(I),X1(I),VVM(I),FF(I)
       IF(PP(I))50,60,50
50     N=I
10     CONTINUE
60     CONTINUE
       WRITE(6,200)(TITLE(I),I=1,20)
      WRITE(6,201) V1,V2,V3,D1,D2,D3
      WRITE(6,201)(TT(I),FFO2(I),VB(I),PP(I),X1(I),VVM(I),FF(I) ,I=1,N)
```

```
      DO 20 I=1,N
      T=(TT(I)+459.6)/1.8
      IF(VVM(I).EQ.0.) GO TO 25
      VM=VVM(I)*28320./453.59
      GO TO 27
 25   VM=X1(I)*V1+(1.-X1(I))*V3
 27   VF1=X1(I)*V1/VM
      VF3=1.-VF1
      VBAR=VB(I)
      FO2=FFO2(I)
      P=PP(I)
      F=FF(I)
      BF=V2/V1-V2/V3
      H(I)=ALOG(F/FO2)
      G(I)=V2/(R*T)*(VF1**2*D1**2+D3**2*(VF3**2-1.)+2.*VF1*VF3*AA )
     1 +ALOG(V3/VM)-VF1*BF          +VBAR*P/(1.8*T*10.731)
      D(I)=2.*V2/(R*T)*VF1
      U(I)=V2/(R*T)*(VF1**2*D1**2+D3**2*(VF3**2-1.)+2.*VF1*VF3*AE )+VBA
     1 R*PP(I)/(1.8*T*10.731)
      SUM1=SUM1+H(I)*D(I)-G(I)*D(I)
      SUM2=SUM2+D(I)**2
      SHP=SHP+H(I)*D(I)-U(I)*D(I)
20    CONTINUE
      AM=SUM1/SUM2
      ASHP=SHP/SUM2
      WRITE(6,208) AM,ASHP
      WRITE(6,202)
      DO 30 I=1,N
      AC1=D(I)*AM+G(I)
      AC2=D(I)*ASHP+U(I)
      FCC(1)=EXP(AC1)
      FCC(2)=EXP(AC2)
      FF(I)=EXP(H(I))
      DO 44 K=1,2
      FC(I,K)=FCC(K)
      ERR(I,K)=(FF(I)-FC(I,K))/FFC(I,K)*100.
 44   CONTINUE
      SUMER1=SUMER1+ABS(ERR(I,1))
      SUMER2=SUMER2+ABS(ERR(I,2))
      S1=S1+ERR(I,1)
      S2=S2+ERR(I,2)
30    CONTINUE
      XN=N
      AVAER(1)=SUMER1/XN
      AVAER(2)=SUMER2/XN
      AVPE(1)=S1/XN
      AVPE(2)=S2/XN
      DO 15 K=1,2
      WRITE(6,202)
      WRITE(6,207) K
      WRITE(6,204) AVAER(K),AVPE(K)
      WRITE(6,202)
      WRITE(6,210)
      DO 15 I=1,N
      WRITE(6,203) TT(I),PP(I),FF(I),FC(I,K),ERR(I,K)
15    CONTINUE
      WRITE(6,205)
      CALL AIS(D,G,Q,U,W,H ,XN,N,TT,PP)
      WRITE(6,205)
      GO TO 4
      END
```

```
C       SUBROUTINE AIS CALCULATES COEFFICIENT FOR EACH SYST. CONDITION
        SUBROUTINE AIS(D,G,Q,U,W,H ,XN,N,TT,PP)
        DIMENSION D(200),G(200),Q(200),U(200),W(200),YM(200),YSH(200),
     1 YSHP(200),YSHFH(200), H(200) ,TT(200),PP(200)
 208    FORMAT (1X,////,4(1X,F10.5,7X))
 211    FORMAT(1X,6(1X,E14.7,5X)/)
        SS1=0.
        SS2=0.
        A1=0.
        A2=0.
        DO 10 I=1,N
        YM(I)=( H(I)-G(I))/D(I)
        YSHP(I)=( H(I)-U(I))/D(I)
        SS1=SS1+YM(I)
        SS2=SS2+YSH(I)
 10     CONTINUE
        AV1=SS1/XN
        AV2=SS2/XN
        DO 12 I=1,N
        A1=A1+(YM(I)-AV1)**2
        A2=A2+(YSH(I)-AV2)**2
 12     CONTINUE
        SIGM1=SQRT(A1/XN)
        SIGM2=SQRT(A2/XN)
        DO 16 I=1,N
 16     WRITE(6,211) TT(I),PP(I),YM(I),YSHP(I)
        WRITE(6,208) AV1,AV2
 15     WRITE(6,208) SIGM1,SIGM2
        RETURN
        END
```

APPENDIX I

ANALYSIS OF THE ACTIVITY COEFFICIENT BEHAVIOR

Figures 35 through 40 show unusual behavior of some of the activity coefficient isotherms. In certain systems there is a particular isotherm which, on visual inspection, appears inconsistent with the other isotherms. The inconsistencies in the 10°F isotherms for the CO_2-CH_4-n-C_{10}, C_2H_2-CH_4-n-C_{10} and the C_2H_8-CH_4-n-C_{10} systems and the 70°F isotherms for the N_2-CH_4-n-C_{10} system are easily detected from Figures 35, 39, 40 and 36 respectively, and are listed in Chapter VII.

The above observations are not based on any expected theoretical behavior, but are simply deviations from an expected regular change in activity coefficient with temperature. Eq. (3-88) shows that the experimental error in the activity coefficient is determined by a combination of the experimental errors in the measurement of the K-value and the system pressure and the error in the determination of the Henry's law constant. Therefore, based on propagation of experimental errors in measurements, random scatter in the activity coefficients of a few percent could be expected. However, the unexpected behavior of certain isotherms is of a systematic nature rather than of a random nature.

The errors in system pressures were very small and are discounted as a cause for the inconsistencies mentioned above. The vapor fugacity coefficients determined by the modified B-W-R equation also could not explain the unexpected behavior in the four subject isotherms. The con-

clusion of this author is that the unexpected behavior, if incorrect, must be attributed to systematic experimental errors of unknown origin to the extent of a few percent in the K-values along the subject isotherms. The analysis of the inconsistent isotherms given below indicates that consistent errors in the K-values are the probable cause for the unexpected behavior of these isotherms.

Figure 11 suggests that the CO_2 K-values for the 10°F isotherm are lower than they should be inorder to be consistent with the other five isotherms. The deviations in these K-values are obviously not due to possible random experimental error since the 10°F isotherm is distinctly smooth. Furthermore, the comparison of the vapor phase fugacity coefficients for the CO_2-CH_4 mixture predicted by the modified B-W-R equation to that determined from the partial volume experiment shows that the predicted fugacity coefficients tend to be higher than the ones determined experimentally, thus the deviation in the predicted fugacity coefficient cannot explain the low activity coefficients of CO_2 at 10°F. Therefore, the low values of the CO_2 activity coefficients at 10°F shown in Figure 35 are attributed to the low CO_2 K-values for this isotherm.

A similar explanation is suggested for the low activity coefficients for N_2 at 70°F (Figure 36). Figure 18 shows that the K-values for this isotherm maybe somewhat low. Also in this case, the deviation in the K-values at 70°F are attributed to an experimental systematic error rather than a random error as is evident from the relatively smooth K-values curve at 70°F (Figure 12).

An analysis of the activity coefficients for C_3H_8 at 10°F provides a clear picture of how relatively small deviations in the K-values can result in a considerable deviation in the activity coefficients. Table

X shows that at 40°F the K-values of C_3H_8 obtained by this author are somewhat lower than those obtained by Koonce (50). The deviation increases with pressure, i.e. from 1.14% at 100 psia to 4.17% at 1000 psia. Further analysis shows that the Henry's law constant obtained from Koonce data at 40°F is close to that obtained in this work since the K-values become almost identical at low pressures. On the other hand, a comparison of K-value data at 10°F (interpolating Koonce's data) shows a different pattern. The K-value data obtained in this work are lower than Koonce's data up to a pressure of 400 psia but higher beyond this pressure with a maximum deviation of 5% at 1000 psia. Therefore, the Henry's law constant obtained from the 10°F data by this author will be lower from that obtained from Koonce's data by about 13% and consequently the activity coefficients obtained in this work will be higher by about 18% at pressures over 700 psia than those obtained from Koonce's data. This comparison shows clearly that a small systematic error of less than 5% in K-values could cause a considerable error in the resultant activity coefficients.

The activity coefficient data show that the effect of temperature on the non-ideality of the system studied is small, e.g., for most of the systems the change of the activity coefficient is about 10% or less over a range of 140°F. Therefore, a systematic error of 2 to 4% in the K-values at a certain isotherm which is rather usual in phase equilibrium measurements, can cause a displacement of the activity coefficient for this isotherm.

NOMENCLATURE

A - exchange energy density

A_o - B-W-R equation constant

a - cohesive energy density or B-W-R equation constant or Redlich-Kwong equation constant

B_o - B-W-R equation constant

b - B-W-R equation constant or Redlich-Kwong equation constant

C_o - B-W-R equation constant

c - B-W-R equation constant

e - electromotive force, differential pressure transducer output

f - fugacity or carrier gas flow rate

G - free energy

H - Hery's law constant or enthalpy

K - vapor-liquid equilibrium constant

k - pressure transducer coefficient

k_i - partition coefficient

k_{ij} - correction factor for binary interaction

l_{ij} - correction factor for binary interaction

P - pressure

R - gas constant

S - entropy

T - temperature

t_R - retention time

V - volume

$\bar{V}$ - partial molar volume

$\tilde{V}$ - molar volume of pure component

V_G - void volume in GLC column

V_L - volume of stationary liquid phase in the GLC column

v - volume

W_L - moles of stationary liquid phase in the GLC column

x - mole fraction in liquid phase

y - mole fraction in vapor phase

Z - compressibility factor

$\bar{Z}$ - partial compressibility factor

Z_G - compressibility factor of the carrier gas

Greek

α - B-W-R equation constant or empirical constant

α_{ij} - correction factor

β - empirical constant

γ - activity coefficient in liquid solution

δ - solubility parameter

μ - chemical potential

π - injection pressure

ρ - density

Φ - volume fraction

ψ - fugacity coefficient in vapor phase

Ω_a - dimensionless constant in Redlich-Kwong equation

Ω_b - dimensionless constant in Redlich-Kwong equation

ω - acentric factor

Subscripts

1 - methane or solvent in a binary solution

2 - solute

3 - n-decane

a - ambient conditions

c - critical conditions

FH - Flory-Huggins

i, j, k, ℓ - component in system

L - liquid phase

m - mixture

o - pressure independent

S - solvent, heaviest component in system

SH - Scatchard-Hildebrand

V - vapor phase

VP - vapor pressure

Superscripts

E - excess property

Id - ideal conditions

M - mixture

∞ - infinite dilution

o - pure state or standard state

* - unsymmetric convention or ideal state

' - reference state

VITA

Amos Yudovich

Candidate for the Degree of

Doctor of Philosophy

Thesis: PROPERTIES OF GAS MIXTURES AND LIQUID SOLUTIONS FROM INFINITE DILUTION STUDIES

Major Field: Chemical Engineering

Biographical:

Personal Data: Born in Tel Aviv, Israel, June 15, 1939, the son of J. Zehev and Rivka Yudovich.

Education: Attended elementary school in Haifa, Israel; graduated from high school in 1955; received the Bachelor of Science degree in Chemical Engineering from the Technion, Israel Institute of Technology, Haifa, Israel; received the Master of Science degree in Chemical Engineering from Oklahoma State University, Stillwater, Oklahoma, in 1966; completed requirements for the Doctor of Philosophy degree in May, 1969.

Professional Experience: Employed as a chemical engineer by Vita-Mayer Paper Mills Co., Milan, Italy, during the summer of 1959; employed as a process and development engineer by Alliance Tire and Rubber Co., Hadera, Israel; employed as a chemical engineer by Leonard Construction Co., Chicago, Illinois, during the summer of 1964.